Master Thesis

Validation of Dynamic Power System Models using Synchrophasor Measurements

T.L. den Boer

Technische Universiteit Delft

TU Delft

Master Thesis

Validation of Dynamic Power System Models using Synchrophasor Measurements

by

T.L. den Boer

to obtain the degree of Master of Science
at the Delft University of Technology,
to be defended publicly on Wednesday January 15, 2020 at 13:30.

Student number:	4210514	
University department:	Electrical Sustainable Energy	
Research group:	Intelligent Electrical Power Grids	
Company:	TenneT TSO B.V.	
Project duration:	May 2019 – December 2019	
Thesis committee:	Prof. ir. M. A. M. M. van der Meijden,	TU Delft, IEPG
	Dr. ir. J. L. Rueda Torres,	TU Delft, IEPG (supervisor)
	Dr. ir. B. Gholizad,	TU Delft, DCE&S
	Ir. J. A. Bos,	TenneT TSO B.V. (supervisor)

An electronic version of this thesis is available at `http://repository.tudelft.nl/`.

TU Delft

TenneT Taking power further

Cover photograph was taken by Chris Pennarts.

Preface

I am writing this preface as the final part of this thesis report while at the edge of 2019 and thereby the edge of this decennium. For me, the past decennium has been largely marked by my studies at the Delft University of Technology. I've set out for a bachelor's degree in Electrical Engineering back in 2012. And I am about to conclude with a master's degree in Electrical Power Engineering. I can look back on an interesting time, in which I've met some wonderful people.

This project was conducted in collaboration with the Dutch transmission system operator TenneT and set sail about 8 months ago with the goal of finding out how TenneT might approach the validation of their dynamic grid model. With the installation of Phasor Measurement Units in the Dutch power grid, a new view is offered at the dynamic behaviour occurring in the power system. With this, new possibilities open up for the validation of the dynamic grid model.

In this project, two simulation techniques were compared for the validation of dynamic grid models. Namely, System Wide Simulation and Hybrid Dynamic Simulation. System Wide Simulation has the potential to be used to gain some broad insights into the validity of the dynamic model. It can give can give indications on shortcomings of the model. For model calibration however, System Wide Simulation is not precise enough. Here Hybrid Dynamic Simulation can play a role. Hybrid Dynamic Simulation provides more accurate results that are required in a validation process. For Hybrid Dynamic Simulation however, Phasor Measurement Units need to be installed in specific locations.

I wish to express my gratitude towards the members of the thesis committee: Prof. ir. Mart van der Meijden, Dr. ir. Jose Rueda Torres, Dr. ir. Babak Gholizad and Ir. Jorrit Bos. For taking their time to evaluate my work and providing me with valuable feedback. Special thanks to Jorrit Bos, for guiding me along the way of this graduation project.

Finally, a word of thanks towards my sisters, for always having my back. My mother, for giving me a place to come home to. And my father, who continues to be a great mentor to me.

Tjerk Lenze den Boer
Utrecht, December 2019

Contents

1 Introduction

1.1. Introduction

Power system dynamics is the field of study that focuses on the dynamic behaviour of the power system. Dynamic behaviour occurs when the power system moves from one state of operation to another, or when a disturbance occurs in the power system. Control mechanisms are used to ensure that the power system remains in stable operation. When the dynamic behaviour of the power system becomes unstable, this could lead to partial or complete blackouts with potentially disastrous consequences.

Power system models

Generally speaking, models are utilized to study the behaviour of power systems. Because performing experiments using the actual power system would be highly impractical and could also directly affect the security of supply of the power system. In the 1940s through the 1960s, models were mainly physical analogues of the real power system. However, with the development of computer technology, mathematical models have become the standard for modelling power systems [23].

Models are however not perfect representations of a physical system. A model is a purposeful abstraction of reality. A model should be sufficiently accurate to capture the behaviour of interest but should not be overly complex. As this would for example negatively affect computation time.

Power systems modelling is generally a challenging task. One reason for this is the large size of interconnected power systems. Over time, regional and even national power systems have been connected to create vast interconnected power systems, such as the synchronous grid of Continental Europe. This power system stretches from Portugal in the south-west to Denmark in the north to Turkey in the south-east.

A second reason complicating the development of power system models is the fact that theres no single owner or responsible party for the power system. In vertically unbundled power systems, as are generally found in North America and Europe, generators are owned by private production companies whereas the transportation and distribution networks are owned by different private or public companies. The fact that no single party has full ownership over the power system makes it difficult to gather information on all components in the power system. Furthermore, certain power system components have long lifespans of 40 years or longer, which means that information may have been lost over time.

Power system models are therefore generally a best attempt given the information available and time available for the development of the model. An important question to ask for a given power system model is: Does the model provide a good enough prediction of the behaviour of the physical system? In other words, is the model valid?

Model validation

Recently, the validation of dynamic power system models has been receiving increasing attention in North America following two system break-ups in the Western Interconnection in the 1996. One of the key lessons learnt from these break-ups was the inadequacy of the models in reproducing the observed behaviour [15]. This makes it difficult to come up with proper mitigation methods to prevent such an event from happening again.

Following these events the Western Electricity Coordinating Council (WECC) developed guidelines for systematic testing and model validation of synchronous generators, excitation systems, power system stabilizers and turbine governors [36]. Furthermore, the North American Electric Reliability Corporation (NERC) has recently put forward a standard requiring the systematic validation of steady-state and dynamic models every 24 months [24].

[11] presented a general framework for the validation of dynamic power system models. Four stages are identified:

- Stage 1: Definition of Performance Indicators
- Stage 2: Establish Discrepancies
- Stage 3: Model Calibration
- Stage 4: Recommendations for model update

Stage 1 and 2 can be seen as the validation part; evaluating whether the model is good enough and identifying where the model might be improved. Stage 3 and 4 are concerned with the model (parameter) calibration; determining how the model can be improved.

Many different approaches exist for the validation of power system models. Traditionally, model validation and parameter identification or calibration for generators was performed by staged testing. With this method, planned manoeuvres of the generator are performed while the generator operates in island mode. These manoeuvres can include the rejection of small amounts of active or reactive power, or voltage reference steps. The response of the generator is then measured and the measurements are used to identify or calibrate the model parameters. This process is usually performed during the commissioning of generation equipment.

A newer method described in [27] is the use of on-line disturbance measurements for the validation of the models, where the system response to a disturbance is used to identify or calibrate model parameters. The benefit of using on-line measurements is that the production unit does not need to be taken out of service. Taking a production unit out of service is costly as it would mean a loss in revenue. Another benefit of the use of on-line measurements is that the behaviour of the generator can be observed under operating conditions. With off-line testing the generator is not loaded or loaded very lightly. The generator behaviour might be different under loaded conditions.

A simulation technique called *Hybrid Dynamic Simulation* has been increasingly used, and has shown good results for model validation using on-line disturbance measurements. With this approach, disturbance measurements are directly played into a running simulation. This method requires measurements to be taken at specific locations, in order to cover a boundary of a subsystem. The behaviour of the subsystem can then be compared with the measurements taken at the boundary.

Yet another approach to model validation using disturbance measurements is to simulate the entire model, whilst trying to replicate a recorded disturbance in the simulation. This *System Wide Simulation* approach does not require measurement devices to be set up in specific locations. Furthermore, global phenomena might be validated when simulating the entire system model.

TenneT TSO

This thesis project was proposed by, and was conducted in collaboration with, the Dutch transmission system operator TenneT. TenneT has a dynamic grid model that is currently being used for rotor angle and (short term) voltage stability studies. TenneT has set a goal to further develop and improve the dynamic grid model in order to increase robustness and performance and to improve quality and functionality. Part of this, is the development of a process for the validation of the dynamic model. This has been the focus of this thesis project.

1.2. Research goal

TenneT currently does not have measurement devices set up in the required locations to completely cover the boundaries of a subnetwork in order to create an isolated subsystem for the Hybrid Dynamic Simulation approach. The Dutch power grid is highly meshed, which means that many measurement points could be required in order to create isolated subsystems. Furthermore, the required locations for Hybrid Dynamic Simulation might be at odds with locations required for other goals, such as maximizing observability of

dynamics in the power system. If not given priority, it could take a while before enough measurement devices are installed in the required locations for Hybrid Dynamic Simulation to be used for model validation. For this reason the question arose, whether model validation could be performed using the method of System Wide Simulation, with measurement devices that are already present, or not specifically installed for model validation. The goal of this project is to research if and how the TenneT Dynamic Model can be validated using wide area PMU measurements.

1.3. Research questions

Based on the research goal and the initial literature review, the following research questions were formulated:

- What type of disturbances are suitable for model validation?
  - Which disturbances will cause dynamic behaviour in the power system?
  - Can asymmetrical disturbances be simulated in a positive sequence simulation tool?
- How can the measurement and simulation results be compared?
  - Which signals are suitable for the comparison of measurement and simulation results?
  - Which methods are available for the comparison of measurement and simulation results?
- How does model validation using System Wide Simulation compare to validation using Hybrid Dynamic Simulation?
  - How can both methods be implemented for validation of the Dutch power grid?
  - Is either one better suitable for model validation?

1.4. Document outline

Chapter 2 will introduce some background theory on power system dynamics and stability, dynamic models, model validation, Phasor Measurement Units and relevant information about the Dutch power system model. Chapter 3 will outline a process for the model validation approach using System Wide Simulation. Chapter 4 will outline a process for the model validation approach using Hybrid Dynamic Simulation. Both approaches are then applied to 3 study cases. In Chapter 5 both validation methods are tested on actual recordings of disturbances and the two approaches are compared. Lastly, the conclusions from the research are summarized in Chapter 6.

2

Theoretical background

2.1. Power System Dynamics and Stability

Power System Dynamics is a field of study that aims for the understanding of the dynamic behaviour of power systems and the resulting stability of the power system. It investigates control mechanisms that can improve the stability of the power system. Power system stability was defined by a joint IEEE/Cigre task force [17] as follows:

> *"Power system stability is the ability of an electric power system, for a given initial operating condition, to regain a state of operating equilibrium after being subjected to a physical disturbance, with most system variables bounded so that practically the entire system remains intact."*

The same task force proposed the classification of power system stability as shown in Figure 2.1. The following sections will briefly discuss the different classifications of power system stability.

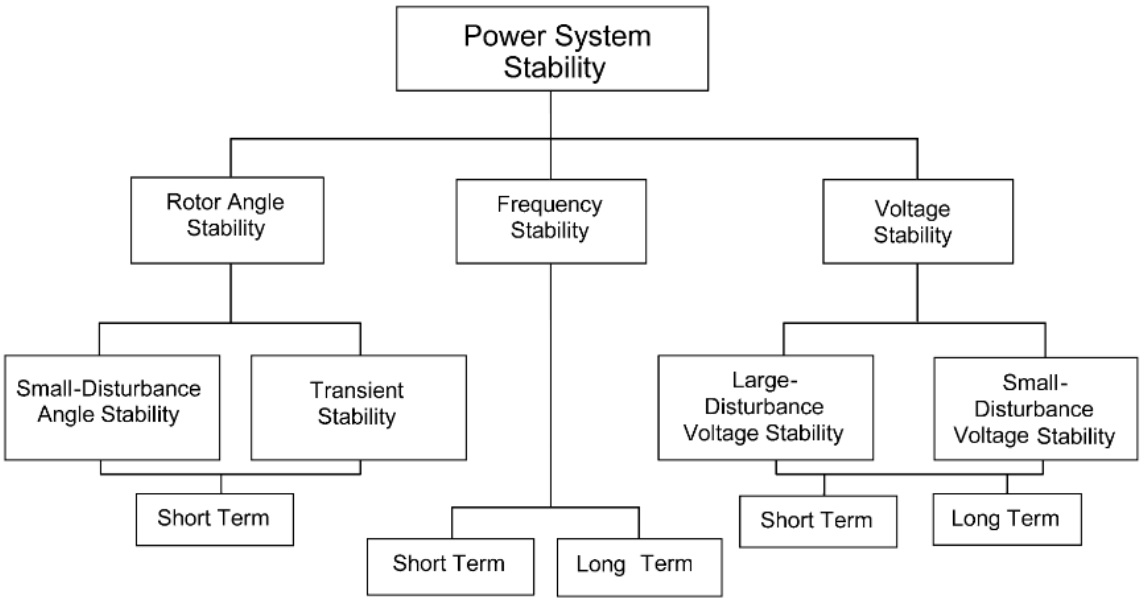

Figure 2.1: Classification of power system stability [17]

2.1.1. Rotor angle stability

Rotor angle stability refers to the ability of electrical machines, predominantly generators, to remain in synchronism with the power grid during and after a disturbance. In an interconnected power system with two or more synchronous machines, the machine voltages and currents must have the same frequency for power to be exchanged. During a disturbance, like a short circuit, some generators might speed up or slow down with respect to the synchronous speed. This will cause the rotor angle to increase or decrease. If the voltage angle difference between the internal generator voltage and the grid voltage becomes too large, the generator will lose synchronism and will start spinning uncontrollably. The generator will then have to be shut down. Control mechanisms might help the generator to remain in synchronism with the grid, but the most important mitigation is to clear a short circuit before a generator loses synchronism.

Rotor angle stability can be further divided in transient stability, as discussed above, and small-disturbance angle stability. Small-disturbances are continuously present in a power system as changes in load, generation or changes in the system topology (e.g. line switching). Under certain conditions small disturbances can excite oscillation modes, where power oscillates between (groups of) synchronous generators. An example are the oscillation modes observed in the interconnected power grid of continental Europe [8]. When poorly damped, these power oscillations might grow and in a worst case, cause generators to loose synchronism.

2.1.2. Voltage stability

Voltage stability refers to the ability of a power system to maintain a steady voltage at all nodes in the system following a disturbance. Voltage drops as active and reactive power flows through a power grid. Nodal voltage can be controlled by injecting (or absorbing) reactive power in a node, either by a synchronous generator or other devices such as series/shunt compensators or STATCOMs. Loss of a generator can affect the reactive power available to support the voltage. Also, a change in the loading of a power line will affect the reactive power consumption of the power line.

Voltage stability is further divided in large-disturbance voltage stability; maintaining voltage stability after a disturbance like loss of generation, short circuits or loss of a power line. And small-disturbance voltage stability; maintaining voltage stability after small disturbances such as incremental changes in system loading.

2.1.3. Frequency stability

Frequency stability refers to the ability of a power system to maintain a steady frequency following a system disturbance. Frequency falls when electricity consumption exceeds electricity production, and frequency rises when electricity production exceeds electricity consumption. Electricity consumption continuously varies, and production equipment is controlled to adjust to the variations in demand. Following a large disturbance however, a production unit or a large load, might be disconnected from the power grid. The remaining generators then need to be able to quickly adjust to this sudden change in order to prevent the frequency from changing too much. If the frequency either becomes too high or too low, extreme measures might have to be taken such as load shedding, where some of the electricity consumers are disconnected.

2.2. Dynamic Models

A power system model will generally be built from three types of model elements:

1. Network elements, e.g. transmission lines, cables, transformers, reactive power compensators.
2. Generation elements, e.g. synchronous generators, wind turbines, solar cells.
3. Load elements, e.g. synchronous machines, residential loads.

In a power flow model, or static model, these elements will remain constant. Using the network model, and the active and reactive power injected and absorbed at the nodes of the network, a power flow calculation can be performed. The result of the power flow calculation will tell the nodal voltages and and branch currents in the network. And thereby also the active and reactive power flows through the network.

In dynamic power system models, certain model elements have been expanded with equations describing their dynamic behaviour. These can include dynamic model for generation elements, such as generator models, exciter models, governor model, wind turbine models. Dynamic models for load elements, such as load models and synchronous machine models. And dynamic models for certain network elements, such as transformers with dynamic tap changing, circuit breaker models, and models for FACTS devices.

A dynamic simulation always starts out from a stable initial operation point. For this operating point a power flow calculation is performed to determine the nodal voltages and branch currents in the network. Next, the dynamic model is advanced with a discrete time-steps. During the simulation, the dynamic model might be perturbed by a disturbance in order to evaluate the response of the dynamic model to the disturbance. If the model accurately reflects the dynamic behaviour of the actual power system, the simulation will show how the actual system will respond to the disturbance. Based on these simulations, important information can be collected for power system planning and operation.

2.3. TenneT Dynamic Model

The TenneT Dynamic Model is a dynamic model that is used for dynamic studies at the Dutch transmission system operator TenneT. These studies mainly focus on transient rotor-angle stability and short term voltage stability. The transmission planning and analysis software PSS/E is used to run dynamic simulations with the model. The TenneT Dynamic Model is currently built up from the following components.

1. The ENTSO-E Dynamic Study Model (DSM). This is a simplified dynamic model of the interconnected power system of Continental Europe. Simplifications include: Reduction of parallel lines, reduction of coupled busbars, the use of standard dynamic models and a limitation for the use of dynamic models to generators with a maximum active power of at least 250 MW [30].

2. A detailed power flow model of the Dutch power grid. This power flow model is more detailed than its representation in the ENTSO-E DSM. The representation of the Dutch power grid in the ENTSO-E DSM was cut from the model, and replaced by the detailed power flow model of the Dutch power grid. The detailed power flow model of the Dutch power grid that was used during this project, was based on the KCD2018 model for the year 2018.[1]

3. Dynamic models for all synchronous generators in the Netherlands, including generator models, exciter model, governor models, power system stabilizer models and under excitation limiter models. The model parameters were based on surveys filled out by the operators of the power generation plants in the Netherlands [4].

4. Dynamic models for the loads in the Dutch power grid based on the work done in [35].

The model is to be further expanded with dynamic models for wind power generation, solar power generation and HVDC interconnections. Currently these elements are included in the model as static negative loads.

2.4. Phasor Measurement Units

Phasor measurement units are measurement devices that measure time synchronized phasors, often referred to as synchrophasors, in accordance with the IEC/IEEE 60255-118-1 standard [1]. (Formerly IEEE C37.118 standard.) An AC waveform can be mathematically represented as follows:

$$x(t) = X_m \cos(\omega t + \phi) \tag{2.1}$$

Where X_m is the amplitude of the AC wave, ω is the angular frequency which is related to an ordinary frequency as $\omega = 2\pi \cdot f$, and ϕ is the phase of the waveform. As the frequency of the AC wave is constant in a power system, the AC waveform can be represented by just its amplitude and phase angle in phasor notation[2]:

$$\mathbf{X} = X_m \angle \phi \tag{2.2}$$

A phasor measurement unit will measure time synchronized phasor quantities with respect to a constant cosine waveform at nominal frequency. Figure 2.2 shows this for a three voltage waveforms. Figure 2.2a shows the waveforms that are measured. The constant cosine waveform is shown as the black dotted lined. The figure further shows three voltage waveforms: a, b and c. The voltage amplitudes are shown as V_a, V_b and V_c. And the phase angles, measured with respect to the constant cosine, are shown as θ_a, θ_b and θ_c. Figure 2.2b

[1] The base model was adjusted to incorporate the temporary connection EOS-EEM-MEE.

[2] Instead of the amplitude X_m, the phasor magnitude will usually represent the RMS value of the AC waveform, $\frac{X_m}{\sqrt{2}}$, as many calculations can directly be performed using RMS quantities. Equation 2.2 then becomes $\mathbf{X} = \frac{X_m}{\sqrt{2}} \angle \phi$.

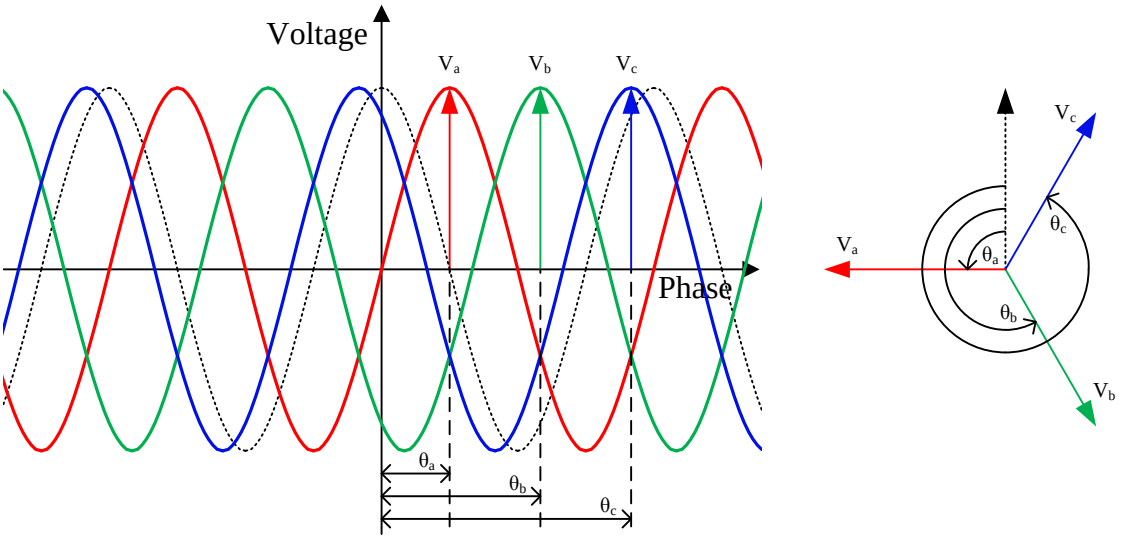

(a) Three-phase voltage waveforms

(b) Phasor diagram

Figure 2.2

shows a phasor diagram of the waveforms, where the amplidutes are represented as the phasor magnitudes, and the phase angles are shown with respect to the black phasor representing the constant cosine.

The main difference between PMUs and the older SCADA measurement systems is the resolution of the measurements. Traditional SCADA systems have a sample rate of 2-4 seconds per sample. PMUs on the other hand have sample rates that go up to 50 or 60 Hz (depending on the AC frequency). PMUs are therefore able to measure dynamic behaviour while the SCADA system is not.

A Phasor Measurement Unit can measure frequency and phasor quantities for three-phase voltage and current signals. Using the phasor quantities, active power and reactive power can be calculated for the individual phases as well as symmetrical components of the three-phase voltage and three-phase current signals.

2.5. Phasor Measurement Units in the Dutch power grid

Currently, TenneT has 6 PMUs installed in the Dutch power grid. The PMUs have a sample frequency of 50 Hz. In other words, one sample per cycle of an AC wave. They are located at the following 380kV substation: Eemshaven, Crayestein and Borssele. (Appendix A shows a map of the Dutch power grid for context.) Each substation contains two PMUs, measuring the phase voltage and the phase current in two different circuits. (A circuit here refers to a set of three phase conductors carrying a three-phase current.) Figure 2.3a, 2.3b and 2.3c show a schematic representation of the PMU locations in the substations Eemshaven, Crayestein and Borssele respectively.

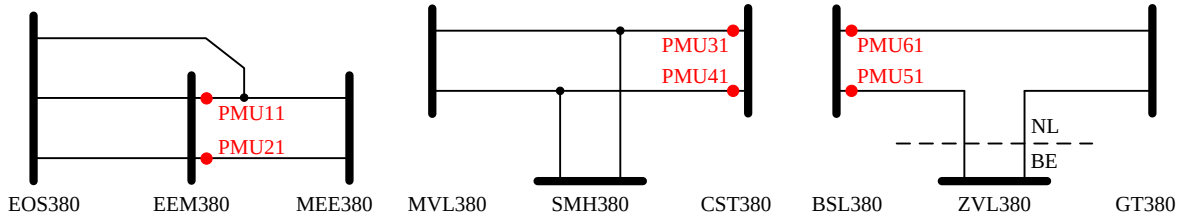

(a) PMUs at Eemshaven substation

(b) PMUs at Crayestein substation

(c) PMUs at Borssele substation

Figure 2.3: Single line diagrams showing the locations of the Phasor Measurement Units installed in the Dutch power grid.

Table 2.1 gives overview of the PMUs. As the data validity column in table 2.1 shows, the PMUs at the Crayestein substation are currently not operational. Both PMUs showed a very poor data validity and have therefore been turned off.

The other PMUs are more reliable, but still show periodic missing data. According to the supplier of PhasorPoint (see Section 2.7), the percentage of invalid data should generally not exceed 1% on average. Investigations should be conducted into poor performance of the PMU system, but the measurements that are captured by the functioning PMUs are nevertheless useable for the purpose of this thesis project.

Table 2.1: PMUs currently installed in the Dutch power grid. Data validity was calculated between 01-04-2019 and 01-07-2019.

Substation	ID	Measured circuit	Data validity
Eemshaven	PMU11	EEM-MEE380 W	95.16 %
	PMU21	EEM-MEE380 Z	95.66 %
Crayestein	PMU31	CST-MVL380 W	0 %
	PMU41	CST-MVL380 Z	0 %
Borssele	PMU51	BSL-ZVL380 G	95.09 %
	PMU61	BSL-GT380 Z	96.32 %

2.6. Model validation

As mentioned in the introduction, [11] presented a general framework for the validation of dynamic power system models, where four stages are identified:

- Stage 1: Definition of Performance Indicators
- Stage 2: Establish Discrepancies
- Stage 3: Model Calibration
- Stage 4: Recommendations for model update

However, in the literature, many different approaches to model validation can be distinguished. In [11] a distinction is made between component level model validation: Validation of a specific device, and system level model validation: validation of a whole system. To these, validation using Hybrid Dynamic Simulation should be added, as this technique is central in many validation approaches. Model validation using Hybrid Dynamic Simulation is performed on a subsystem or subnetwork of the complete model. If the subnetwork includes just one power plant, it can also be seen as component level model validation.

2.6.1. Component level model validation

The most thorough method of model validation would be to isolate single system components and test and validate them individually. Here, a component would generally refer to a generating unit. Testing of generators, where model parameters are derived, is often part of the commissioning phase. For synchronous generators, this is usually done using off-line staged testing. A wide variety of tests are used. These test can include: Enhanced sudden short circuit tests, Partial load rejection tests and Frequency response tests [16]. [26] presented a tool called Power Plant Parameter Derivation (PPPD) for the automated parameter derivation of synchronous generators including their control systems based on staged tests.

With the introduction of a new standard put forward by the North American Electric Reliability Corporation (NERC), which requires periodic validation of dynamic models, novel approaches to component level model validation are being developed. A downside of staged testing is that it involves a power plant to be taken out of service for the duration of the tests. Taking a production unit out of service will result in a loss of revenue. New approaches use on-line disturbance measurements as the basis for for model validation. [28] presented a method for model validation based on on-line disturbance measurements recorded by Digital Fault Recorder (DFR). Data was collected at the generator terminals and on the generator field. Parameter derivation was again performed using the PPPD tool mentioned above.

One thing to note here, is that the PPPD tool uses MATLAB for the simulation and derivation of the generator model parameters. The derived parameters can then be used in the simulation tool that is used for the

dynamic studies. Simulations with the same model parameters however, will not necessarily lead to precisely the same simulation results in different simulation tools. An example of this was demonstrated during the development of the ENTSO-E Dynamic Study Model. The ENTSO-E Dynamic Study Model was developed for different simulation tools. In order to ensure comparable results in different simulation tools, test simulations were performed with standard models in a small test system. While the simulation results generally showed good accordance between the different simulation tools, small deviations were observed especially during transients [6]. This might be problematic when model calibration is performed based on this transient behaviour. Model validation and calibration would therefore preferably be performed using the simulation tool that is also used for dynamic studies.

2.6.2. System level model validation

System level model validation, or model validation using System Wide Simulation, was demonstrated in [5] [18] [22] and [31]. With this approach, simulations are run using the entire system model. For [5], this entails the Brazilian interconnected power system, for [18] the Slovenian power system and for [22] the Western interconnection in the United States. [31] does not include information about the power system that is simulated, but it is stated that in terms of size, "the system can be considered to be on par with that of an interconnection, consisting of tens of thousands of buses".

In System Wide Simulation, a recorded event is replicated in the simulation. The simulation results can then be compared with the measurement results. For this, the state of the model should first be matched with the pre-event operating state of the system. This is because the pre-event operating state of the system has a big influence on the behaviour of the system during and after the event. In the research papers mentioned above, a (state estimator) snapshot from the Energy Management System (EMS) is used to adjust the model to the pre-disturbance operating state. Additionally, some fine-tuning might be performed based on other measurements like PMU measurements.

Events that can instigate dynamic behaviour in a power system are for example loss of generation, line switching and short circuits. While loss of generation would be easier to implement in a simulation as compared to a short circuit, loss of generation does not frequently occur. Short circuit occur more frequently. It is however more difficult to accurately simulate a short circuit, as the impedance of the short circuit, which determines the severity of the short circuit, is generally unknown. Line switching also occurs more frequently, however, switching normally does not produce a lot of dynamic behaviour in the system. So unless the switching occurs close to the measurement location, it will hardly be picked up in the measurements.

It should be noted lastly that model calibration was not described or implemented in the research papers mentioned above.

2.6.3. Subsystem level model validation using Hybrid Dynamic Simulation

The concept of Hybrid Dynamic Simulation was first introduced by [13] as a simulation technique to incorporate time domain measurements in a dynamic power simulations. It is 'hybrid' in the sense that is forms a bridge between the measurement world and the simulation world. The technique demonstrated in [13] uses a generator attached with an ideal phase shifting transformer at the bus where the measurement signal should be played back. This is shown in Figure 2.4. By adjusting the turns ratio n and the phase shift α of the transformer for every simulation step, the measured voltage magnitude and angle can be set based on the measurements. Model validation was identified as one of the potential use cases for this method. As well as post-event analysis, software validation and a means to simulate unmeasured signals.

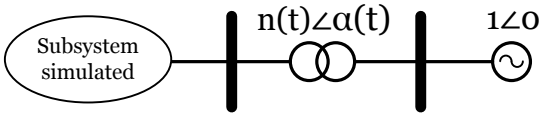

Figure 2.4: Initial approach to Hybrid Dynamic Simulation. Measured voltage magnitude and phase is played back into the simulation by adjusting the turns ratio and phase shift of an ideal phase shifting transformer.

Hybrid Dynamic Simulation has also been demonstrated using different simulation techniques. [19] used a large synchronous generator model in combination with a fast-responding exciter and governor to inject

recorded voltage and frequency signals into a dynamic simulation. By using the recorded signals as the exciter and governor set-points, the voltage and frequency at the generator terminal is forced to follow closely the recorded signals. More recently, simulation tools such as General Electric's PSLF/PSDS, Siemens PSS/E and Powertech Labs DSATools-TSAT have incorporated the capability of playing back signals in a dynamic simulation [14].

In the past few years, Hybrid Dynamic Simulation has shown promising results for model validation and calibration [10] [9] [25] [29] [12] [37] [20]. To perform model validation using Hybrid Dynamic Simulation, measurements need to be recorded at the boundary of the subnetwork. A recording of a system disturbance can then be played back at the boundary of the subnetwork. The response of the subnetwork can then be compared against the measurements at that were recorded at the boundary.

Figure 2.5 shows how such a process would work for a subnetwork with a wind power plant and a traditional power plant. The recorded voltage magnitude V and voltage phase δ are played back at the boundary of the subnetwork. The response of the subnetwork is shown in the active power P and reactive power Q exchanged at the boundary of the subnetwork. The simulated P and Q can be compared with the measured P and Q in order to evaluate the validity of the model. It should be noted that for this approach to work, all connections between the subnetwork and the external grid need to be measured. Otherwise the subnetwork cannot be isolated from the external network, and the P and Q cannot properly be compared. Also, the disturbance that is being played back at the boundary of the subnetwork needs to have originated outside of the subnetwork.

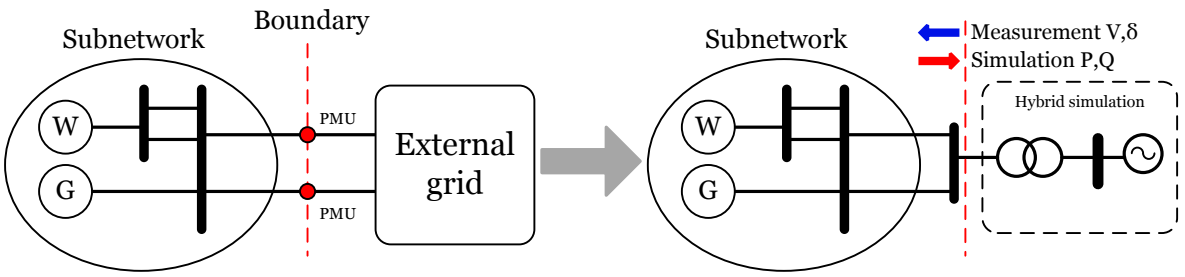

Figure 2.5: Model validation using Hybrid Dynamic Simulation for a subnetwork with a wind power plant (W) and a traditional power plant (G).

Figure 2.6 shows a simplified single line diagram the Dutch power grid near the Eemshaven. The figure further shows potential subnetworks for model validation using Hybrid Dynamic Simulation, including the required locations where PMUs should be installed. If the subnetwork encompasses just a single generation unit or plant, such as Subnetwork 1 or Subnetwork 2, the Hybrid Dynamic Simulation process would essentially be an alternative approach to component level model validation. In general, model validation is easier and more accurate with smaller subnetworks. However, smaller subnetworks will require more PMUs to be installed in the power system in order to cover all the subnetwork boundaries.

Figure 2.6 also shows the PMUs that are currently installed at Eemshaven. (Figure 2.6 does not include the temporary connection that was shown in Figure 2.3a.) From this it can be seen that currently, not enough PMUs are installed to perform Hybrid Dynamic Simulation with the Eemshaven subnetwork.

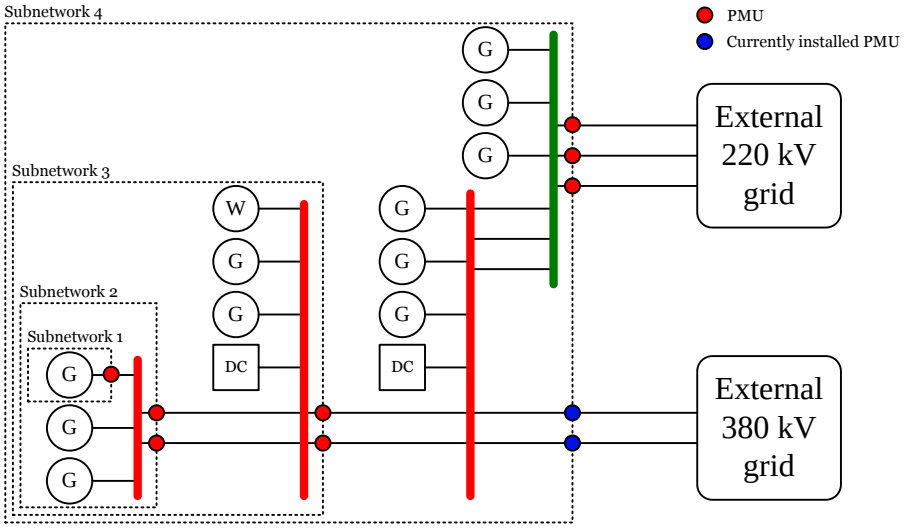

Figure 2.6: Simplified single-line diagram of the Eemshaven subnetwork. 380-kV bus shown as red and 220 kV bus shown as green. Transformers are not explicitly shown.

2.6.4. Comparing measurement and simulation results

The general framework for model validation proposed in [11], defines the definition of performance indicators and the establishment of discrepancies as stage 1 and stage 2 of the model validation process. Generally speaking, discrepancies are established through comparison of two signals: a measured signal and a simulated signal.

Signals of interest

For studies concerning electromechanical stability, variables such as frequency, bus voltages magnitude and voltage angle difference, branch active power and reactive power, generator speed and rotor angle, reflect the system behaviour. Generator speed and rotor angle however, cannot be measured using Phasor Measurement Units. The following signals can be measured or calculated using Phasor Measurement Units:

- **Frequency** - The European power grid is operated at a frequency of 50 Hz. The frequency is determined by the rotational speed of the generators in the power system. The frequency of the system is not constant but is constantly moving around 50 Hz. The change in system frequency is a measure of the balance in the power supply and power demand in the system. If demand exceeds supply, additional power is extracted from the rotational kinetic energy of the generators, which makes the generators slow down and the frequency fall. If supply exceeds demand, the additional power is absorbed by the generators which makes them speed up and the frequency rise. The transmission system operator is responsible for maintaining a steady frequency in the power grid.

- **Voltage magnitude** - Contrary to frequency, voltage magnitudes can vary greatly in a power system. Electrical energy distribution occurs at low and medium voltage, while electrical energy transmission occurs at high and extra high voltage. Voltage can be stepped up or down with the use of transformers. However, voltage magnitudes might also vary between nodes at the same voltage level.

  Voltage stability is generally an issue that is relevant for the transmission grid, and is thus mainly a concern at high and extra high voltage levels. As mentioned in section 2.1.2, the voltage can be controlled by injection or absorption of reactive power. Different component in the power grid will either produce or consume reactive power. A power line is generally an inductive component, which means that it consumes reactive power. (Although this depends on the loading of the line.) Cables on the other hand are capacitive components, which means that the produce reactive power. A synchronous generator can control its reactive power output by adjusting the field voltage.

- **Voltage angle difference** - By itself the voltage angle contains little information, as the voltage angle needs to be defined with respect to another angle. When considering the voltage angle difference between two nodes however, the voltage angle difference is related to the power flowing between the two

nodes. For a simple system with two nodes connected by a purely inductive branch, as shown in Figure 2.7a the power flowing from node 1 to node 2 is given by equation 2.3. With V_1, V_2 and δ defined as in Figure 2.7c. For a small angle difference, $\sin\delta \approx \delta$, which means the active power flow is strongly determined by the angle difference between two nodes. The angle difference between two distant nodes in a power grid gives an indication of the stress of the system [3]. If the voltage angle difference widens, this indicates that the system is loaded more heavily and is more heavily stressed. This is however a very general indicator, and says little about the behaviour of individual components in the system.

$$P = \frac{V_1 V_2}{X} \sin\delta \tag{2.3}$$

- **Active power** - Active power in an AC system is the resultant power of a voltage and a current oscillating in phase. It is the power that is consumed by resistive loads. Active power is produced by synchronous generators or renewable energy sources like solar panels or wind turbines. Figure 2.7b shows a simplified representation of a synchronous generator as a voltage source behind a reactance. The active power delivered by the generator follows the same equation as for the situation with two busses, described by equation 2.3. The output active power is therefore linked to the angle difference between the internal generator voltage and the grid voltage. As mentioned in 2.1.1, a generator might speed up or slow down following a system disturbance. If the generator speed changes with respect to the synchronous speed of the electrical grid, the voltage angle difference will change. Following equation 2.3, the active power delivered by the generator will change. An oscillation in the rotor angle with respect to the synchronous rotor angle, will cause an oscillation in the power delivered by the generator. The active power is therefore an indicator for the rotor angle stability.

- **Reactive power** - Reactive power in an AC system is the power that is the result of a voltage and a current oscillating 90 degrees out of phase. This means that reactive power is power that oscillates back and forth at twice the system frequency. As mentioned above, voltage and reactive power are related. For the simple system with two nodes connected by a purely inductive branch, as shown in Figure 2.7a the reactive power flowing from node 1 to node 2 is given by equation 2.4. Again, with V_1, V_2 and δ defined as in Figure 2.7c. The equation also holds true for the simplified representation of the synchronous generator in Figure 2.7b. For a small phase angle difference $\cos\delta \approx 0$. This means that the phase angle has little effect on the reactive power flow. Instead, the reactive power flow is determined by the difference in voltage magnitude. The opposite is also true, by injecting reactive power at node 1, the reactive power flow through the reactance will increase. This will cause the voltage at node 1 to rise with respect to the voltage at node 2.

$$Q = \frac{V_1^2 - V_1 V_2}{X} \cos\delta \tag{2.4}$$

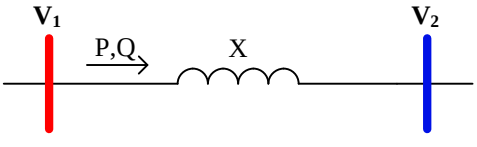

(a) Two buses connected by a reactance.

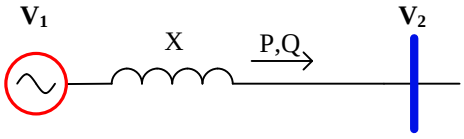

(b) Simplified representation of a generator as a voltage source behind a reactance.

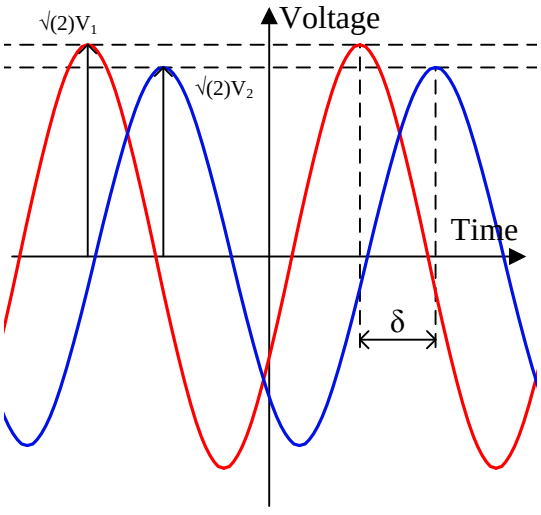

(c) Two voltage signals with different amplitudes and phases.

Figure 2.7

As the TenneT Dynamic Model is mainly used for rotor-angle stability and voltage stability assessments, the signals of interest are voltage magnitude, active power and reactive power. With Hybrid Dynamic Simulation, signal comparison is limited to active power and reactive power, as the frequency and voltage are used as playback signals in the simulation.

Comparison methods
Different methods are used to compare the measured and simulated signals. With the System Wide Simulation approach comparison is mainly done qualitatively. Though, in [5], comparison was done qualitatively and quantitatively:

- Qualitative comparison - The following qualitative metrics were used to evaluate the model performance:
  1. The model predicts system stability or instability.
  2. The model predicts the nature of the system response, such as oscillatory behaviour, lightly or heavily damped oscillations etc.
  3. The model predicts a similar range of variable excursions, with maximums and minimums occurring in comparable times.
- Quantitative comparison - Frequency and damping of electromechanical oscillations can also quantitatively be compared. Frequency and damping of an oscillating signal can be estimated using different techniques, such as Prony analysis, subspace methods and Fourier analysis.

The qualitative and quantitative metrics mentioned above are not suitable to be used in a model calibration process. They strongly depend on human judgement or interaction. This makes them difficult to implement in an automated parameter optimization process. In the Hybrid Dynamic Simulation approaches, where parameter optimization was performed, other quantitative metrics were used. Examples are the Sum of Squared Residuals [37] and the Root Mean Square Error [20].

As this project is focused on a comparison between the System Wide Simulation and the Hybrid Dynamic Simulation approach to model validation, signal comparison was limited to qualitative comparison, as it can be used in both approaches.

2.6.5. Parameter calibration

When discrepancies are established between the measurement and simulation results, the next step would be to identify how the model might be improved. The aim is to reduce the discrepancy between the measurement and simulation results.

Different techniques are used for the calibration of model parameters. The PPPD tool mentioned in Section 2.6.1 uses a non-linear recursive least-squeare algorithm to optimize the model parameters. As mentioned in Section 2.6.2, calibration of model parameters was not described with the System Wide Simulation approach to model validation. With Hybrid Dynamic Simulation, various techniques were used, such as an Ensemble Kalman filter algorithm in [12] or the Primal-Dual Interior Points method in [37]. No further investigation was done into different optimization techniques as it was not part of the scope of this project.

2.7. Software tools and data

This section gives a short description of the software tools and data that was used during this project.

PSS/E
As mentioned in section 2.3, simulations with the TenneT Dynamic Model are run in the transmission system planning and analysis software PSS/E (officially written as PSS®E). PSS/E is developed by Siemens PTI, and is used in over 145 countries around the world by transmission system enginieers, consultants, universities and research labs. PSS/E offers functionalities including: power flow calculations, dynamic simulations, short circuit calculations and contingency analysis.

PSS/E is used for its speed with which it can perform dynamic simulations. Speed is an important characteristic when simulating big models like the TenneT Dynamic Model, which includes models for the entire interconnected grid of continental Europe. A downside of the use of PSS/E is that it exclusively performs positive sequence dynamic simulation. This means that asymmetrical events cannot be simulated. The software does offer an option to calculate a symmetrical equivalent for asymmetrical events, however, this requires zero sequence model parameters to be included in the model, which currently are not.

Python
Python is an interpreted, general-purpose programming language. PSS/E has an interface for Python through the *psspy* API. Python was used to control PSS/E and scripts were written for the different simulations. Python was also used to calculate symmetrical components, active power and reactive power from the synchrophasor measurements.

PhasorPoint, synchrophasor measurements
PhasorPoint is a software tool developed by GE Grid Solutions that allows for synchrophasor based measurement and monitoring. PhasorPoint allows to view both real-time synchrophasor measurements as well as viewing historical measurement data. The raw synchrophasor measurements can be exported from PhasorPoint, and PhasorPoint has many options of generating alarms whenever abnormal behaviour is detected in the system. These alarms are based on settings specified by the user and are for example based on the rate of change of voltage angles. The software can however not create alarms retroactively based on historical measurement data when the settings are changed.

Disturbance reports
At TenneT, a disturbance report (Dutch: Storingsrapport) is written whenever a protection device in the transmission grid has been activated. An investigation is done into the event that caused the protection device to act, and the findings are logged. These reports are generally based on readouts from the protection devices and include information on the location of the disturbance and the time of the disturbance.

The information in the disturbance reports can then be used to as a starting point for finding measurements of dynamic behaviour in the PhasorPoint historical measurement database. They can also provide information about the nature of the disturbance.

Comtrade measurements and trip logs
Some protection devices save a measurement recording of an event that caused the protection device to trip. Additionally, protection devices will create a trip log whenever the device is activated. The disturbance report mentioned above, make use of these readouts. If available, these recordings can provide valuable information about the event. However, these recordings are often not stored and are therefore generally not available.

EMS snapshots
The EMS system uses SCADA measurements and state estimation techniques to estimate the power flows in the power grid. Every 15 minutes, a snapshot file is created which records the system state in the UCTE data exchange format [34]. The snapshot file includes the node and branches in the grid, as wel as the active and reactive power consumed and produced by loads and generators.

GEN eBase
The SCADA measurement including bus voltage and active and reactive power flows are also directly saved at 5 minute intervals in a database. The database can be accessed though the EBASE Energy Data Management software (until recently known as GEN eBase).

PQ meters
TenneT also has a network of PQ (power quality) measurement devices installed in the power grid. The PQ meters record voltage dips and can give information about the depth and duration of voltage dips. Information from PQ meters weren't used during this project, due to unawareness of their availability until late in the project. The measurements might however be useful when analyzing and simulating short circuits.

3

Model validation using System Wide Simulation

In the System Wide Simulation (SWS) approach to model validation, a simulation is run on the entire dynamic model. For this the dynamic event and the system conditions during the event need to be mimicked in the model. The simulation results can then be compared to the measurement results. This chapter will discuss the steps required for model validation using the System Wide Simulation approach.

3.1. General workflow

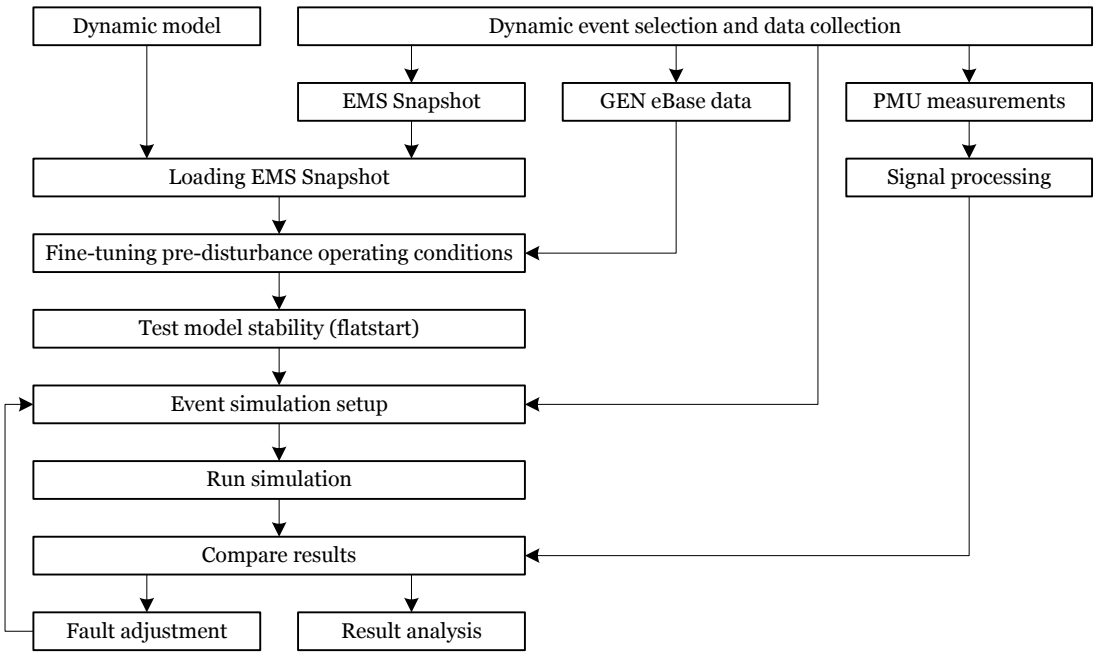

Figure 3.1: Flowchart for the model validation process using wide area measurements.

Figure 3.1 shows a flowchart for the model validation method using wide area measurements. The following steps are taken during the validation process:

1. First a dynamic event should be selected. For a dynamic event, information should be collected about the nature of the event and the system state before the event. Information about the state of the power

system before the event can be retrieved from an EMS snapshot and the GEN eBase measurements. The PMU measurements of the event need to be retrieved, and prepared for comparison with the simulation results.

2. Next, the information from the EMS snapshot can be loaded into the dynamic model. Section 3.2 will go into more detail about this process.

3. After loading the EMS snapshot, the model will not perfectly represent the initial conditions for the event. Especially nodal voltages and reactive power in the model will not correctly be loaded. Therefore, after loading the EMS snapshot the pre-disturbance operating conditions should be further adjusted. Here data from GEN eBase can be used as it provides more accurate information about the state of the power system. Section 3.3 will go into more detail about the adjusttment of the initial conditions.

4. After fine-tuning the pre-disturbance operating conditions, the stability of the model should be evaluated. Without any disturbance, the model should maintain operation in steady state. This is tested in a *flatstart* simulation. A simulation is run for 60 seconds without disturbances. If the model maintains stable operation during the simulation, the model is ready for the event simulation.

5. Next the event simulation should be set up based on the information collected about the event. This information includes for example the fault type, the duration of a fault and the operation of protective relays. This information should then be translated into commands given to the simulator. In case the event that is being simulated includes a fault, a process of fault adjustment is applied. The exact nature of a fault is generally unknown, and the fault should be approximated based on the measurements during the fault. This is an iterative process. Also, as PSS/E only simulates bus faults, the model might need to be altered when a branch fault needs to be simulated. A branch fault can be simulated by introducing a bus at the branch location where the fault occurred. Section 3.4 will go into more detail about the fault simulation.

6. With the event simulation correctly set up, the simulation can be run. Afterwards, the simulation result can be compared with the PMU measurements, and further analysis can follow for conclusions about the model validity.

3.2. Loading EMS snapshot

An important step into the process of model validation based on wide area measurements is to setup the dynamic model according to the system conditions during the event that is to be simulated. Every 15 minutes the Energy Management System (EMS) saves a snapshot of the operating condition of the power system in UCTE format [34]. For every node in the power grid, these snapshots contain information on the power and reactive power that is injected or extracted at that node. A script is available to load the EMS snapshot into the dynamic model [2]. The following steps are taken:

1. The UCTE snapshot is converted into a PSS/E model.

2. From the snapshot model, the active and reactive power consumption and generation information is extracted for all loads and generators.

3. All loads in the Dutch part of the dynamic model are removed, all generators in the Dutch part of the dynamic model are put out of service.

4. New loads are introduced in the dynamic model based on the load information from the snapshot model.

5. The generators in the dynamic model are dispatched based on the information from the snapshot model.

6. HVDC power flows in the dynamic model are setup according to the power flow in the snapshot model.

7. The total cross border power flow in the dynamic model is matched with the power flow in the snapshot model by scaling all loads outside of the Dutch power grid.

8. The power exchanges with Belgium and Germany in the dynamic model are matched with the exchanges in the snapshot model by scaling the loads in France and Germany.

9. Lastly, the cross border power flows for the individual tie-lines in the dynamic model are matched with the power flows in the snapshot model by adjusting the Phase Shifting Transformers available at certain tie-lines.

It should be noted that after loading the EMS snapshot, the dynamic model will not perfectly match the system conditions in the EMS snapshot. The active and reactive power consumption by loads in the Dutch power grid should correctly match the snapshot. Also the power dispatch of the generator should match the snapshot. The reactive power dispatch of the generators however, can significantly deviate from the snapshot. The reactive power dispatches of the generators are adjusted from their set-points in order to solve the power flow calculations during the EMS-loading process. The reactive power dispatch information will therefore not be retained. Furthermore, information on the nodal voltages is not part of the EMS snapshot. The nodal voltages will therefore also not be correctly represented in the model.

3.3. Fine-tuning pre-disturbance operating conditions

As mentioned in the previous section, when loading an EMS snapshot, the reactive power and node voltages will not accurately be represented in the dynamic model. Normally, the generators in the model are set up to control the voltage level of the substation to which they are connected. The default voltage set-point for the substations is 1.05 pu. The generators will inject or absorb reactive power until the voltage set-points in the substations are met. This process alters the reactive power dispatch from the dispatch value in the EMS snapshot.

Generally, the Dutch Extra High Voltage grid is operated at a higher voltage level, than is the case in the model. The voltage levels in the model are affected by many parameters, such as the tap position of the transformers, the reactive power injected by the generators, the reactive power injected by shunt compensators and also the voltage levels at the borders of the Dutch network play an important role. It is difficult to coordinate all these parameters in the model to get the nodal voltages and reactive power dispatch of the generators to correctly represent the system state as it was in reality. Here lies an opportunity for future improvements of the model. During this project, this problem was not addressed.

Locally however, a trade-off can be made in the model between the generator reactive power, and the generator terminal voltage. If the terminal voltage is increased, the generator will start injecting more reactive power. If the terminal voltage is decreased, the generator will inject less reactive power, or even start absorbing reactive power.

Simulations were run in a Single Machine Infinite Bus test system in order to check how these parameters, terminal voltage or reactive power, affect the dynamic behaviour of the generator. Appendix B contains details about the test system. The simulations were run in PowerFactory, as it allows generators to be set in either constant voltage mode or constant reactive power mode.

Firstly, simulations were run with constant reactive power mode. With these simulations, the tap ratio of the machine transformer was adjusted so that the voltage at the terminal of the generator was varied, while the voltage at the high voltage side was kept at 1 pu. Table 3.1a shows the model parameters for the different tap ratios. In constant reactive power mode, the reactive power dispatch was kept at -12.8 Mvar.

Secondly, simulations were run with constant voltage mode. In this case the transformer tap ratio was left unchanged, so that the voltage at both the low and the high voltage side were kept at 1 pu. The reactive power dispatch of the generator was adjusted by introducing a reactive load alongside the generator. The reactive load was either set to absorb or inject reactive power. In order to keep the reactive power constant, the generator will absorb or produce the excess reactive power. Table 3.1b shows the model parameters for the different reactive loads. As can be seen in the table, the terminal voltage was kept at 1 pu, while the reactive power was varied.

For each simulation, the active power dispatch was set to 350 MW. Using these initial conditions, simulations were run. During the simulations, a bolted three-phase fault is introduced on one of the lines connecting the machine transformer to the infinite bus. The fault has a duration of 60 ms.

Figure 3.2a and Figure 3.2b show the generator active power in response to the three-phase faults, for the initial conditions with constant reactive power and constant voltage respectively. The figures show that the initial conditions have an effect on the dynamic response of the generator. The dynamic response of the generator is more impacted by the reactive power dispatch as compared to the terminal voltage. From the constant voltage mode, is can be seen that especially if the generator is absorbing reactive power, the dynamic response is affected.

Table 3.1: Model parameters used in order to test sensitivity of dynamic response to initial operating conditions.

(a) Constant reactive power

Tap ratio [%]	Terminal voltage [pu]	Reactive power [Mvar]
-5.0	0.950	-12.8
-2.5	0.975	-12.8
+0.0	1.000	-12.8
+2.5	1.025	-12.8
+5.0	1.050	-12.8

(b) Constant voltage

Reactive load [Mvar]	Terminal voltage [pu]	Reactive power [Mvar]
100	1.000	87.2
50	1.000	37.2
0	1.000	-12.8
-50	1.000	-62.8
-100	1.000	-112.8

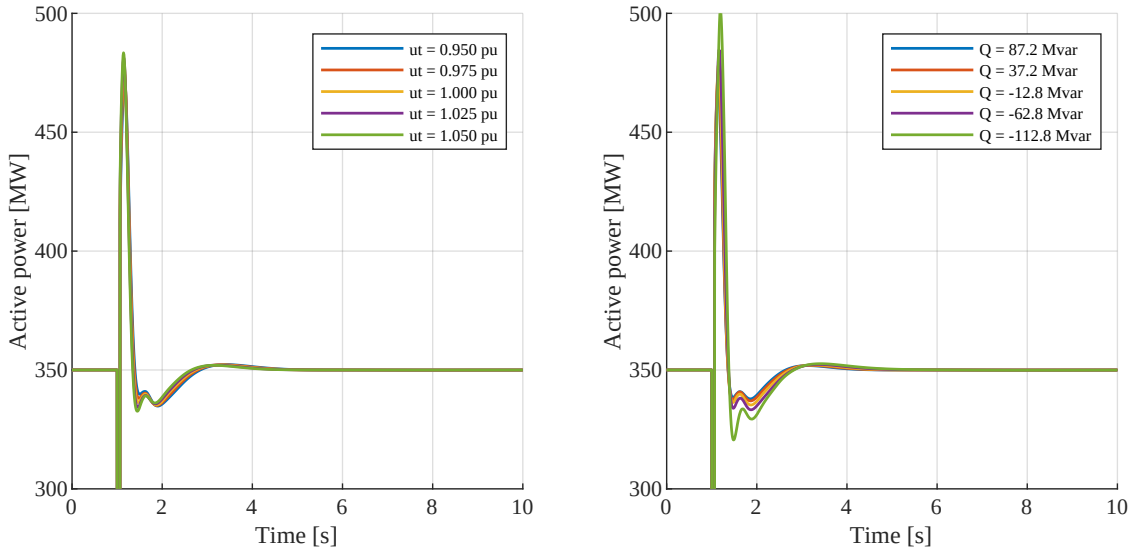

(a) Constant reactive power

(b) Constant voltage

Figure 3.2: Dynamic responses for different initial operating conditions.

Based on the results it was concluded that the pre-disturbance operating conditions of the generators should be adjusted to reasonably represent the conditions in reality. Correctly representing the reactive power dispatch is preferred over correctly representing the terminal voltage levels, especially when the generator is absorbing reactive power. As long as the terminal voltage levels are kept within reasonable limits, the effects on the dynamic behaviour will be acceptable. Measurements on the active and reactive power, as well as the voltages at the substations can be retrieved from GEN eBase.

3.4. Simulating faults and fault clearing

If the event that is to be simulated includes a fault occurring in the network, the fault should be simulated in the model. PSS/E offers limited capabilities of fault simulation. A three-phase fault is simulated in PSS/E by placing a shunt impedance at the faulted bus [32]. For the impedance, both the resistance and the reactance can be specified. The impedance can be specified as an admittance in MVA, an admittance in siemens (Ω^{-1}) or an impedance in ohms. By varying these variables, the severity of the fault can be adjusted.

PSS/E also offers an option to simulate a branch fault, but this is simulated as bus fault at one of the ends of the branch. (Depending on how the branch is addressed.) If a branch fault is required at a specific location on a branch, the branch could be split, introducing a new node along the branch. The branch fault can then be simulated by applying a bus fault at the newly created node.

When asymmetrical bus or branch fault need to be simulated, PSS/E offers a process for calculating and applying an equivalent positive-sequence fault. These processes however, require the model to contain zero-sequence parameters. Currently, the TenneT Dynamic Model does not contain zero-sequence parameters.

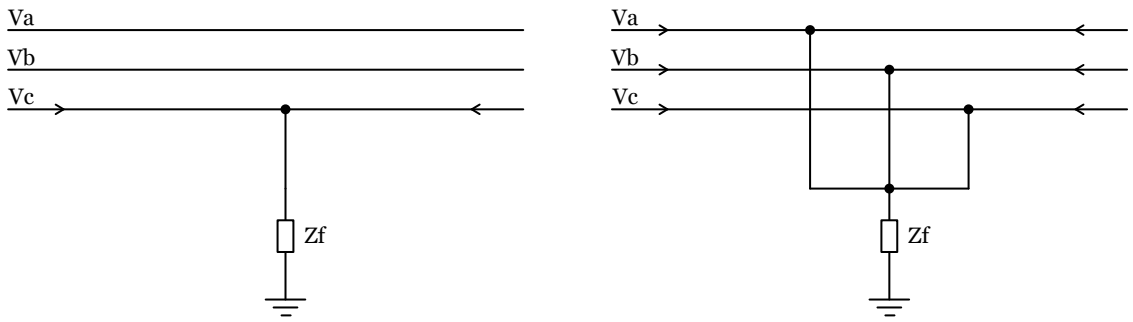

(a) Single-phase fault

(b) Three-phase fault

Figure 3.3: Schematic representations of single-phase faults and three-phase faults. The fault impedance is indicated as Zf.

Bolted three-phase faults, with zero fault impedance, are often used in simulations for stability analysis, as a three-phase fault is the most severe fault and thus represents a worst case scenario. If stability is maintained after a three-phase fault, stability will also be maintained after a single-phase fault or any other type of fault. As will be seen in section 5.2 and section 5.4 however, faults occurring in the power systems are usually not symmetrical three-phase faults. In fact, less than 5% of fault will affect three phases at once, while 70 to 80% of faults tend to be single-phase to ground faults [7]. Also, in reality a fault rarely has a zero fault impedance. When a flash-over occurs the arc usually has some level of impedance. Also the high voltage tower, or tree to which the arc flashes over will represent some amount of impedance. As the TenneT Dynamic Model is not capable of simulating these asymmetrical faults, an alternative method is needed to properly simulate the real-life faults that occurred during a disturbance. A method that is proposed here uses the standard symmetrical bus fault, where the fault impedance is tuned in such a way so that the system responds similarly as it has to the recorded asymmetrical fault. Additionally a similar approach is introduced to model situations where unbalanced line tripping occurs.

Simulating asymmetrical faults

During a fault, a short circuit path will be created between lines, or between a line and ground. This will result in a (large) fault current and a drop in the voltage. In case of a zero-impedance fault, the voltage would drop to zero. The fault will cause the (electrical) output power of the surrounding generators to change rapidly. As the (mechanical) input power of the generators cannot change as fast, the imbalance between the input power and the output power will cause the generator to slow down or speed up with respect to the synchronous speed.

Figure 3.3a shows a schematic representation of a single-phase to ground fault, and Figure 3.3b shows a three-phase to ground fault. As mentioned, most faults tend to be single-phase to ground faults. PSS/E however is only able to simulate three-phase faults. While a single-phase fault will be less severe than a three-phase fault, the fault impedance also has an effect on the severity of the fault. A higher fault impedance will result in a smaller voltage drop, and smaller fault currents. The fault will thus be less severe. This lead to the idea that a single-phase fault might be simulated as a three-phase fault with a higher fault impedance.

In order to see if this method works, simulations have been run in test systems in Digsilent PowerFactory, as PowerFactory can simulate both asymmetrical faults and symmetrical faults. Simulations were run in two test systems; a Single Machine Infinite Bus test system, and a test system was based on the 2 Area 4 Generator system as described in [21]. Details about the Single Machine Infinite Bus and the 2 Area 4 Generator test system is included in appendix B and C respectively.

The results for both test systems showed that it is possible to get a similar response from the test system to a single-phase fault and to a three-phase fault where the fault impedance was adjusted. Figure 3.4a and Figure 3.4b show the results that were obtained using the 2 Area 4 Generator test system. For the asymmetrical fault, a single-phase fault was introduced halfway along one of the lines between node 7 and node 8. The fault impedance for the single-phase fault had a resistance of 25 Ω and a fault reactance of 10 Ω. Next, a three-phase fault was introduced at the same location. The fault impedance for the three-phase fault was adjusted until the depths of the voltage and the power drop matched those during the single-phase fault. This was an

iterative process. A good match was obtained with a three-phase fault with a resistance of 90 Ω and a fault reactance of 130 Ω.

Figure 3.4a shows the deviation in terminal voltage of the four generators in the test system. The generator responses to the single-phase fault are shown in the coloured lines. Overlaid in the black dotted lines are the responses to the adjusted three-phase fault. The results for the three-phase fault show a very close match to the results for the single-phase fault. Similarly, Figure 3.4b shows the deviation in output power of the generators. Again the response to the single-phase fault is shown in colour, and the response to the adjusted three-phase fault is shown in black dotted lines. The deviation in output power also shows a very close match in the results.

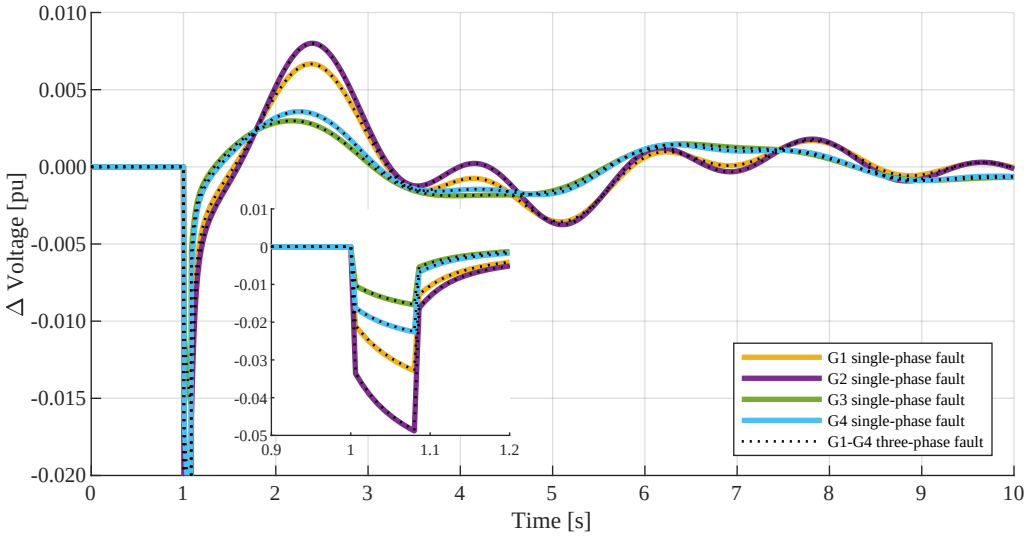

(a) Terminal voltage deviation

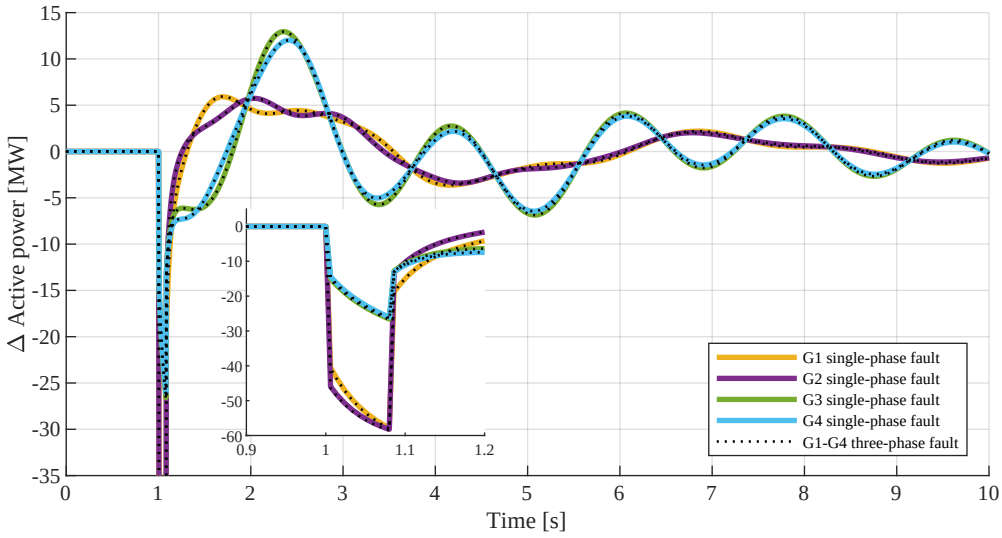

(b) Active power deviation

Figure 3.4: Terminal voltage deviation and active power deviation in response to a single-phase fault with fault impedance of $15 + 10j\Omega$, shown as coloured lines. And response to a three-phase fault with fault impedance of $90 + 130j\Omega$, shown as black dotted lines.

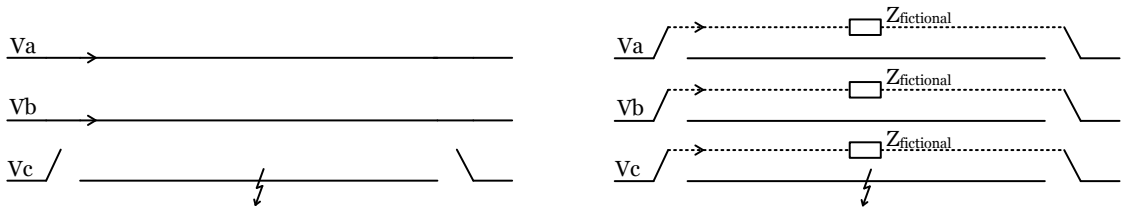

(a) Single-phase tripping

(b) Three-phase tripping with fictional line

Figure 3.5: Schematic representations of single-phase tripping and three-phase tripping with a secondary fictional line.

Simulating asymmetrical line tripping

Depending on the protection configuration, a fault might be cleared by tripping all phases, or only the phases that are faulted. When only the faulted phase is tripped, as was seen in event 3 (section 5.4), the power can flow through the other phases uninterrupted, this is beneficial for the system stability. Tripping a single phase however, results in asymmetrical currents and voltages, which cannot be simulated in PSS/E. A somewhat similar method to the three-phase fault adjustment is proposed for situations with asymmetrical fault clearing or line tripping.

Instead of tripping the three phases, the impedance of the lines is increased in order to account for a portion of power being able to flow through the phases that are unaffected by the fault clearance. In a simulation, this would be realized by having a secondary fictional line (three phases) with a higher impedance than the original, connected in parallel. When a single phase would trip, the original line will be taken out of service, while the fictional line is put into service. This then reverses when the fault is cleared. Again the impedance of the fictional line should be adjusted so that the response of the three-phase line tripping matches the response of single-phase line tripping.

This method was again tested in the Single Machine Infinite Bus test system and the 2 Area 4 Generator test system. In both cases the results showed that a similar response can be obtained by single-phase tripping and three-phase tripping where a fictional, higher impedance line is introduced. Figure 3.6a and Figure 3.6b show the results that were obtained using the 2 Area 4 Generator test system. During the simulation, a single phase of one of the lines between node 7 and node 8 was tripped. After 300 ms, the phase was put back into service. The lines between node 7 and 8 have positive sequence resistance of 5.819 Ω and a positive sequence reactance of 58.19 Ω. (Further details about the line parameters are included in appendix C.) The fictional line that was introduced to mimic the behaviour of a single phase tripping has a positive sequence resistance of 12.1 Ω and a positive sequence reactance of 121 Ω. These values were determined in an iterative process. During this process the focus was on matching the active power in both cases, as this resulted in a better overall match as compared to matching based on the voltage did. All other line parameter of the fictional line were kept equal to the original line.

Figure 3.6a shows the terminal voltage deviations at the terminals of the 4 generators in the test system. The generator responses to the single-phase line tripping are shown in the coloured lines. Overlaid in the black dotted lines are the responses to a three-phase line tripping with the introduction of the fictional line. The results for the three-phase line tripping show a very close match to the results for the single line tripping. Similarly, Figure 3.6b shows the deviation in output power of the generators. Again the response of the generator to the single-phase tripping is shown in colour and the response to the three-phase tripping is shown in the black dotted lines. The deviation in output power also shows a very close match in the results.

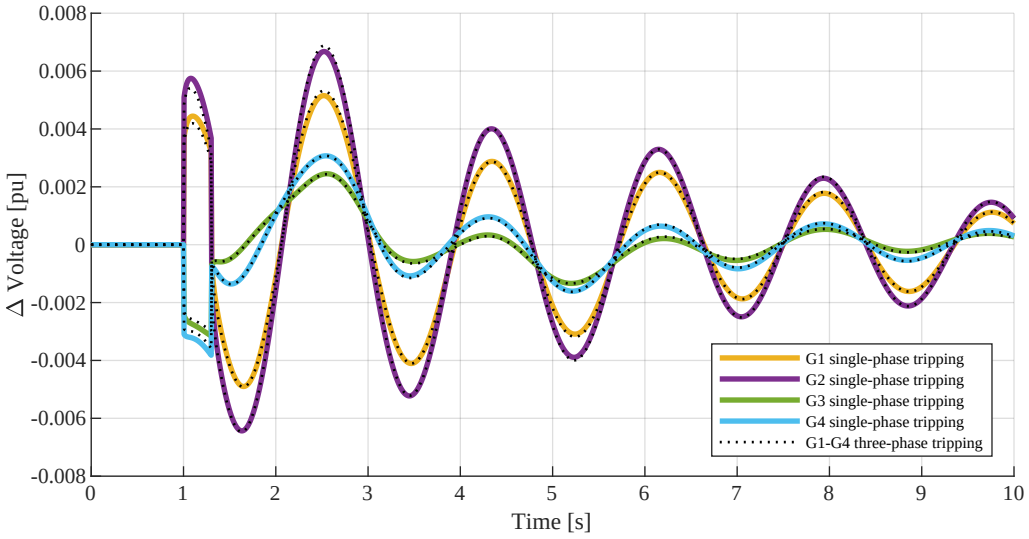

(a) Terminal voltage deviation

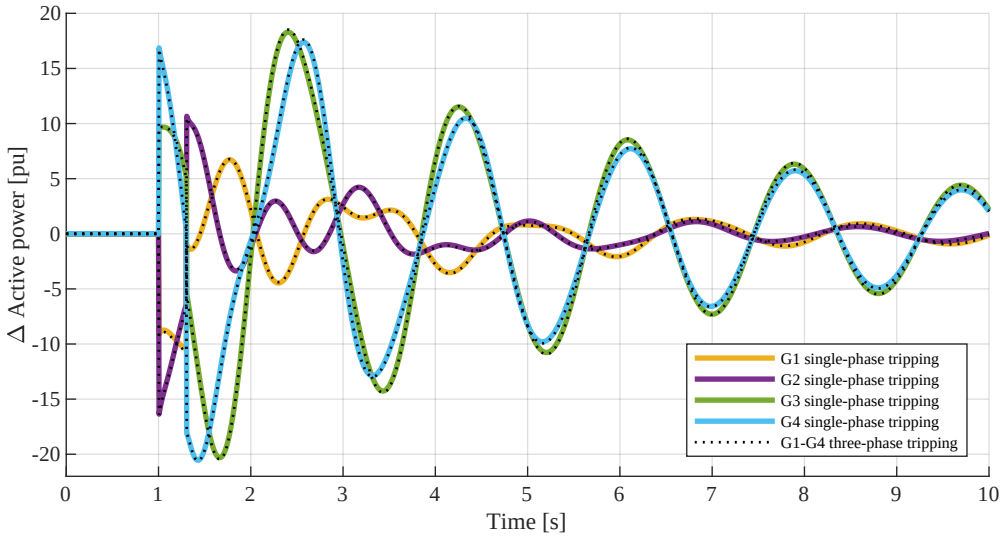

(b) Active power deviation

Figure 3.6: Terminal voltage deviation and active power deviation in response to single-phase line tripping, and three-phase line tripping compensated by a parallel higher impedance fictional line. The responses to single-phase tripping are shown as the coloured lines. And responses to three-phase tripping are shown as the black dotted lines.

Conclusion
Based on the results discussed in the previous paragraphs, it was concluded that the simulated single-phase faults and single-phase line tripping can be represented by a three-phase faults and three-phase line tripping. So if the simulated single-phase fault correctly represents an actual single-phase fault, this means that an actual single-phase fault can be accurately replicated in a simulation using three-phase disturbance. There are a few things to note with this approach:

- The approach of adjusting the fault impedance would not only be necessary in case of an unbalanced fault. Even for a balanced three-phase fault, the precise nature of the fault will generally be unknown. Fault adjustment would therefore also be necessary to match the fault impedance in case of a balanced fault.
- For this approach to be used, accurate measurements of the voltage drop and preferably also the current or power are required.
- The voltage drop during a fault is not only affected by the fault impedance. In order to check which other model parameters have an effect on the voltage drop, simulations were run in a single machine infinite grid model to evaluate the sensitivity of the voltage drop to other model parameters. Governor, exciter and power system stabilizer model parameters did not show any effect on the voltage drop during the fault. The only model parameters that seemed to have an effect on the voltage drop, other than the fault impedance, were the generator model sub-transient and transient reactances. These parameters however do seem to have a smaller impact on the voltage drop than the fault impedance has. Also, the generator model parameters are expected to be relatively accurate, as they are based on actual testing during the commissioning stage of the generator.

3.5. Comparing results

Section 2.6.4 listed different variables for the comparison of measurement and simulation result. Namely: Frequency, voltage magnitude, voltage angle difference, active power and reactive power.

The TenneT Dynamic Model is used for rotor-angle stability and voltage stability studies. The frequency behaviour depends on all generators and loads dispatched in the system. As the Dutch power grid is connected to the interconnected power grid of continental Europe, this does not only include the generators in the Netherlands. However, only for the Dutch generators the power dispatch is adjusted during initialization of a simulation. The frequency behaviour will therefore not correctly be represented, making this variable not suitable for comparison.

Something similar is true for the voltage angle difference. The voltage angle difference between two distant substations gives a general indication of the power flows between the substations. However, for distant substations, the phase angle difference might also be affected by power flows originating outside the Dutch power grid. Power flows from north to south Germany might partially flow through the Dutch power grid. This has an effect on the phase angle difference. The power flows in Germany are however not accurately adjusted in the initialization of the simulation.

This leaves voltage magnitude, active power and reactive power as variables for comparison. As mentioned before however, voltage levels and thereby also reactive power is generally not well represented in the model. Significant offsets might be present, making it difficult to directly compare the measurement and simulation results. A workaround is to compare the deviations of the signals from their initial value. This will remove the offset from both the measurement and the simulation results.

4

Model validation using Hybrid Dynamic Simulation

In the Hybrid Dynamic Simulation (HDS) approach to model validation, a simulation is run in a subnetwork of the dynamic model where a measurement is played back at the boundary of the subnetwork. This chapter will discuss the steps required model validation using the Hybrid Dynamic Simulation approach.

4.1. Hybrid Dynamic Simulation in PSS/E

Recently, the power system simulation software PSS/E has incorporated a specific model that can be used for measurement playback during dynamic simulation [33]. The model PLBVFU1 can play back a measured voltage, a measured frequency or both.

The PLBFVU1 model acts as a generator model and should be attached to a machine in the power flow model. Exciter and governor models should be omitted for the machine. The generator is modelled as a voltage source behind a source impedance. Figure 4.1a and Figure 4.1b show the block diagrams for the voltage magnitude and voltage angle of the internal voltage source of the playback generator. The measured signals are played back as the internal voltage magnitude and angle of the playback generator. The voltage angle is obtained by integrating the frequency measurement, as is seen in Figure 4.1b by block s2. The input signals can also be filtered using a simple first order filter (block s0 and s1). Filtering will create a time delay however, that should be taken into account when the results are compared in a model validation process.

In case the PLBFVU1 model is used to play back a signal measured at the generator terminals or at a substation, the generator MVA should be set to a very high value (e.g. 10,000 MVA) and the source impedance should be set to a low value (e.g. 0.01 pu). This should minimize the voltage drop across the source impedance, thus ensuring that the generator output voltage equals the generator internal voltage.

The measurement signals should be included in a comma separated file with the following structure:

Time [s], Voltage [V or pu], Frequency [Hz or pu]

When the simulation time step is smaller than the measurements sample time, the PLBVFU1 model will automatically calculate the intermediate measurement values by linear interpolation.

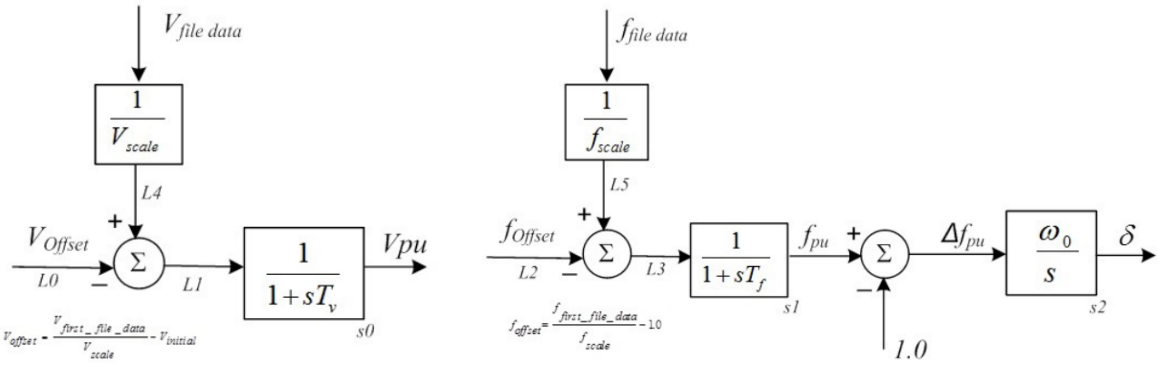

(a) Voltage magnitude

(b) Voltage angle (frequency)

Figure 4.1: PLBVFU1 block diagrams [33]

4.2. General workflow

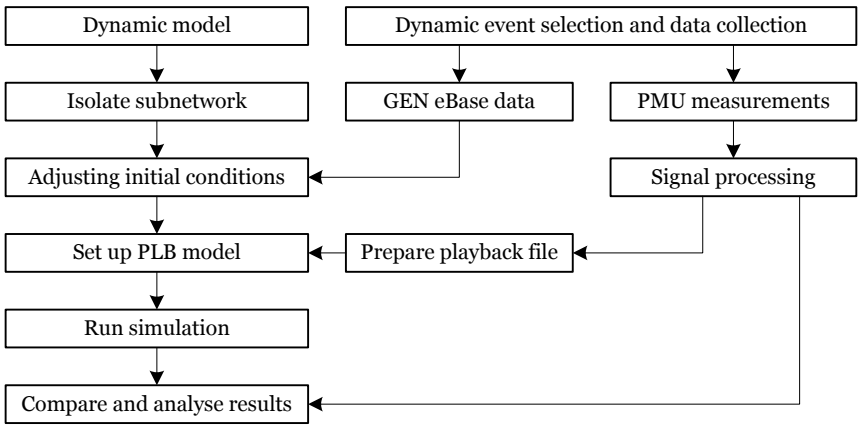

Figure 4.2: Flowchart for the model validation process using hybrid dynamic simulation.

Figure 4.2 shows a flowchart for the model validation method using hybrid dynamic simulation. The following steps are taken during the validation process:

1. The model validation approach again starts out with the selection of a dynamic event. For this event, the PMU measurements should be collected.
2. Next, the subnetwork of interest should be isolated from the rest of the dynamic model, and the playback generator model should be set up at the boundaries of the subnetwork.
3. then, the initial conditions of the sub-network should be adjusted to represent the pre-disturbance system state. For this purpose, GEN eBase data can be used.
4. Next, a playback file should be prepared from the measurements.
5. When everything is set up correctly, the simulation can be run. Afterwards, the simulation results can be compared with the PMU measurements, and further analysis can follow for conclusions about the model validity.

4.3. Isolating the Zeeland subnetwork

While the Phasor Measurement Units are currently not installed in the right locations to create a boundary required for Hybrid Dynamic Simulation, an attempt could be made for the Zeeland subnetwork. Figure

4.3 shows a schematical overview of the Zeeland subnetwork. The figure shows that there's measurements missing in the 150 kV grid to have all boundaries of the subnetwork covered with measurements. If we assume however that the power flowing across the 150 kV border has a negligible effect on the dynamical behaviour of the subnetork, we can cutoff the subnetwork at the boundary and attach a static load at the boundary to represent the power flowing through the 150 kV grid.

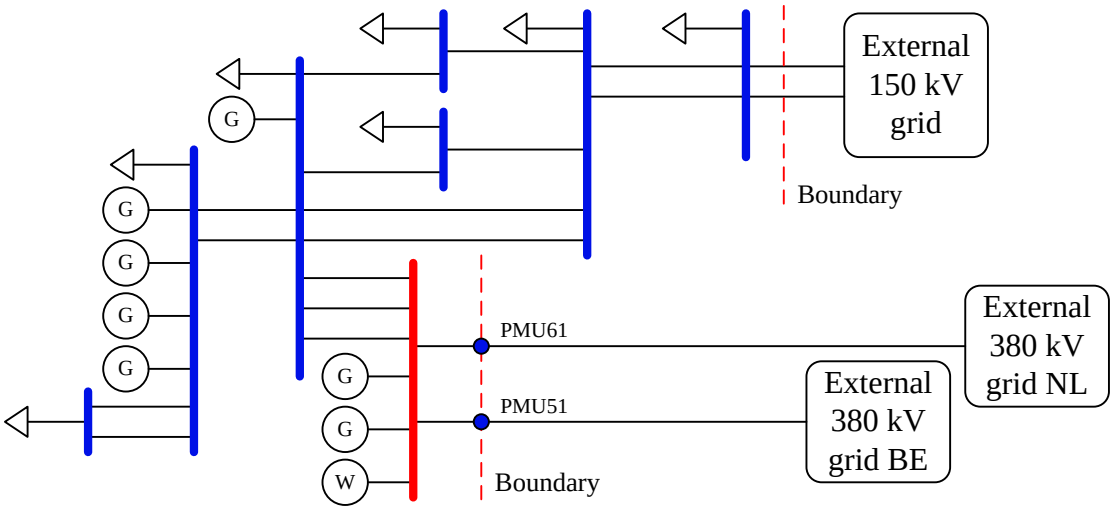

Figure 4.3: Simplified single line diagram of the Zeeland subnetwork. 380 kV buses are shown in red and 150 kV buses ar shown in blue. Transformers are not explicitly shown. The diagram shows the currently instally PMUs and also shows potential boundaries of the subnetwork in order for it to be isolated.

Figure 4.4 shows the isolated Zeeland subnetwork with the playback generator at the boundary. The boundary in the 150 kV grid is represented as a static load as no measurements are available at that location. As the voltage measurements taken by PMU51 and PMU61 measure approximately the same voltage, they cannot be played back individually. Therefore, a single playback generator is attached at the location of the measurement. This also means that the power flows measured by PMU51 and PMU61 cannot separately be compared with the simulation results. The measurement first need to be summed before they can be compared with the Hybrid Dynamic Simulation result.

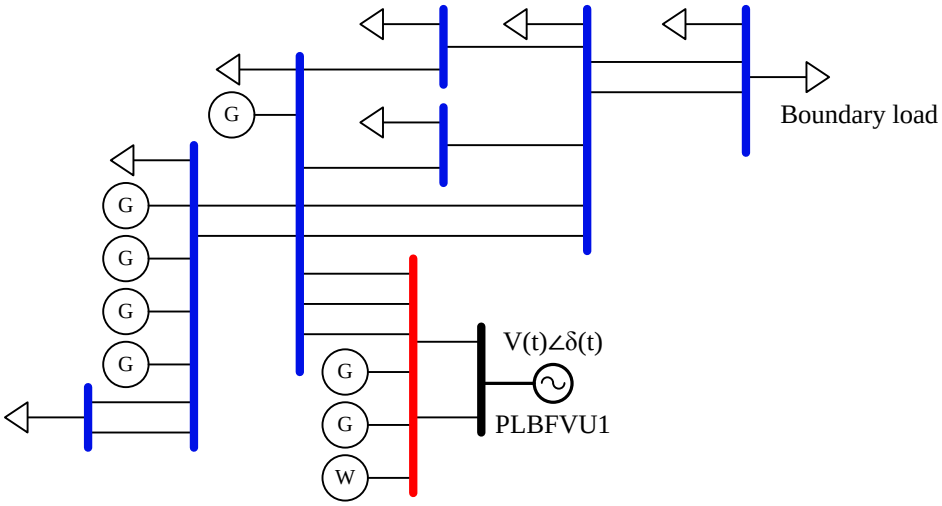

Figure 4.4: Isolated Zeeland subnetwork with playback generator attached at the boundary. 150 kV power flow is represented as a static boundary load.

4.4. Comparing results

Section 2.6.4 listed different potential variables for the comparison of measurement and simulation result. Namely: Frequency, voltage magnitude, voltage angle difference, active power and reactive power. For Hybrid Dynamic Simulation, the frequency and voltage are played into the simulation. Therefore, the simulated frequency and voltage should exactly match the measured frequency and voltage. They do not offer any useful comparison. Voltage angle difference is also not a suitable variable for comparison, as Hybrid Dynamic Simulation focuses on a subnetwork where only one phase angle is measured. An angle difference can therefore not be calculated. This leaves active power and reactive power as variables for comparison.

5

Model validation case studies

Both validation using System Wide Simulation and validation using Hybrid Dynamic Simulation start out with the recording of a disturbance event. In order to test the validation approaches, they were applied to actual disturbances that were recorded between April 2019 and July 2019.

5.1. Selecting disturbance events

Disturbances that are major causes dynamic behaviour in the power system are short circuits, a sudden power unbalance caused by loss of generation or loss of an HVDC interconnector and topological changes such as line switching. This is however not an exhaustive list.

- Single-phase short circuits occur on a relatively frequent basis, and can relatively easily be identified as disturbance reports are written whenever the protection equipment has tripped. Short circuits are however more difficult to simulate accurately. The exact nature of the fault is generally unknown. From the synchrophasor measurements and the disturbance report can usually be determined what type of short circuit has occurred (e.g. single-phase, phase-to-phase etc.). But usually no information is available about the fault impedance. The fault impedance in the simulation should therefore be tuned so that the measured system response is matched.
- Loss of generation and loss of an HVDC interconnector will disturb the power balance in the power system, and will usually cause a significant dynamic response. The events are relatively easy to simulate and, as these events are symmetrical, they can be simulated in a positive sequence simulation tool. As opposed to loss of a generator, loss of an HVDC interconnector might be of short duration in case of a commutation fault.
- Topological changes such as line switching will change the impedance between different nodes and power flows in the power system. When the loading of lines is changed, their reactive power consumption will change, and voltage stability might be affected. Also the active power output of a generator is affected by the impedance between the generator and the load, and a sudden change in impedance can cause a power oscillation. Switching events are however minor events when looking at the system as a whole. The effects of the event are mostly local. In order for them to be useful for model validation, they therefore have to have occurred close to a measurement location. Otherwise it would be difficult to discern the system response from the background dynamics present in the power system.

28 disturbance events occurring between April 2019 and July 2019 were reviewed as potential study cases to test the validation methods. Firstly, the PhasorPoint alarm history was used to find events, but it turned out that the alarms are currently not set up selectively enough to be able to identify potential disturbances that might be used for model validation. Too many alarms are currently created, most of which show no substantial disturbance of the power system.

Alternatively, disturbance reports were used as a basis for finding disturbance events. Based on the disturbance reports, the measurement data was sought out in PhasorPoint in order to review whether the disturbance is large enough to be of any interest for model validation.

As mentioned, 28 disturbances were reviewed. From these a selection of 3 events was made as study cases to test the validation processes. Multiple criteria were kept in mind when selecting these events. These include the impact the event showed in the measurements. For fault-events this is largely determined by the impedance between the fault location and the measurement point. Another criterion was the quality and availability of the measurement data during the event. And the available information on the cause of the event, which is necessary in order to properly simulate the event in the System Wide Simulation approach.

Two events concern a short circuit. One of which results in the loss of a generation unit. The other one, as it turned out, resulted in a commutation fault in the Norned HVDC link, shutting it down temporarily. The other event concerns line switching, and was found through the Phasorpoint alarms. The following sections will present the model validation approaches applied to the three events in order of their occurrence.

5.2. Event 1: 03/05/2019 SMH-MSEC380 short circuit

5.2.1. Event description and measurements

On Friday 03/05/2019 at approximately 07:46:29, a fault occurred in the cable connecting the MSEC power station to the substation Simonshaven. As a consequence of the fault, the cable, and thereby also the power station were disconnected from the power grid. This resulted in a loss of generation in the power system.

Figure 5.1a shows the positive sequence voltage magnitude measured during the event. The figure clearly shows a sharp drop in voltage during the fault. However, as the inset figure shows, the voltage drop has a very short duration. The voltage drop is picked up by just one sample. The next sample already shows a recovery in the voltage magnitude. The voltage drop is significantly deeper at Borssele (PMU51 and PMU61) as compared to the voltage drop at Eemshaven (PMU11 and PMU21). This indicates that the impedance between the fault location and the Borssele substation is smaller than the impedance between the fault location and the Eemshaven substation.

Figure 5.1b shows the active power measured during the event. The figure shows a large difference in the power measured by PMU11 and PMU21 at the Eemshaven substation. This is a result of the power flowing through the temporary connection EOS-EEM-MEE as discussed in section 2.5. Part of the power flowing through circuit EEM-MEE380-W bypasses PMU11. The figure further shows that from the Borssele substation approximately 700 MW is exported towards Belgium, as measured by PMU51. While approximately 370 MW is transported towards the rest of the Dutch power grid, as measured by PMU61.

Figure 5.1b shows that the power drops during the short circuit, and is followed by a power oscillation. The figure also shows that the power export to Belgium is reduced as a consequence of the loss of generation in the Dutch power grid.

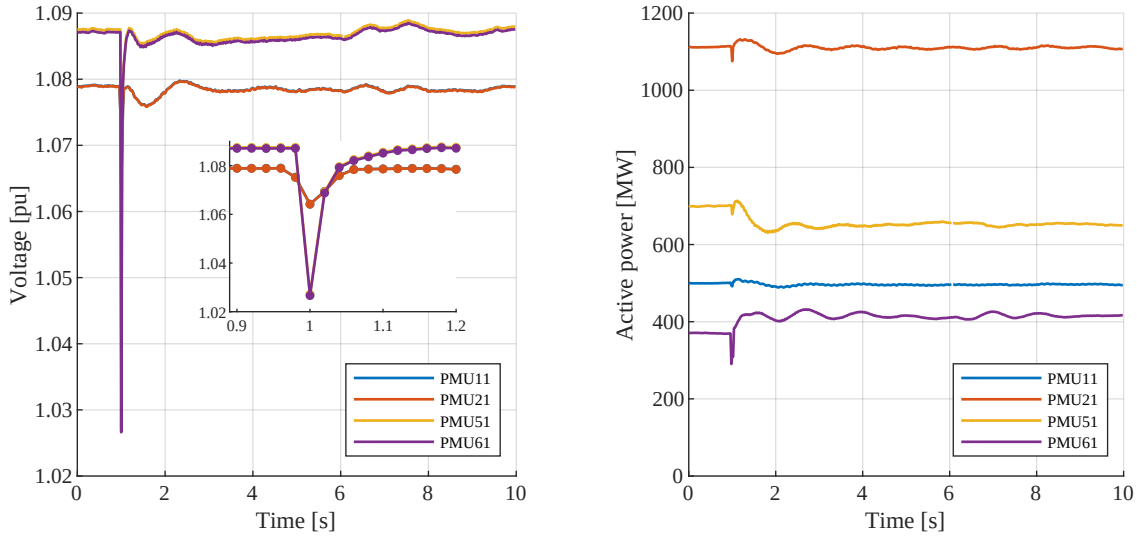

(a) Positive sequence voltage magnitude

(b) Active power

Figure 5.1: Measurements during event 1, SMH-MSEC380 short circuit, t_0 = 03/05/2019 07:46:28.

Figure 5.2a and Figure 5.2b show the measurements of the voltage magnitude and the current magnitude for the individual phases measured by PMU61 during the short circuit. The figures show that the voltage drop is largest for phase b, while the current spike is also largest for phase b. This indicates that the fault that occurred on the cable was a single-phase to ground fault in phase b. The figures also show that the protection equipment has isolated the fault very quickly. The voltage drop is only visible in a single measurement point. As the measurement frequency is 50Hz, the fault current seems to have persisted at most two cycles.

The disturbance report that was written following the fault confirmed the occurrence of a single-phase to ground fault. The disturbance report states a fault duration of 40 ms, which corresponds to two cycles. The fault was cleared by tripping all three phases, disconnecting the MSEC power station from the power grid, which was running at approximately 420 MW. The investigation of the fault also provided an approximate location of the fault, which can be used in the simulation of the fault.

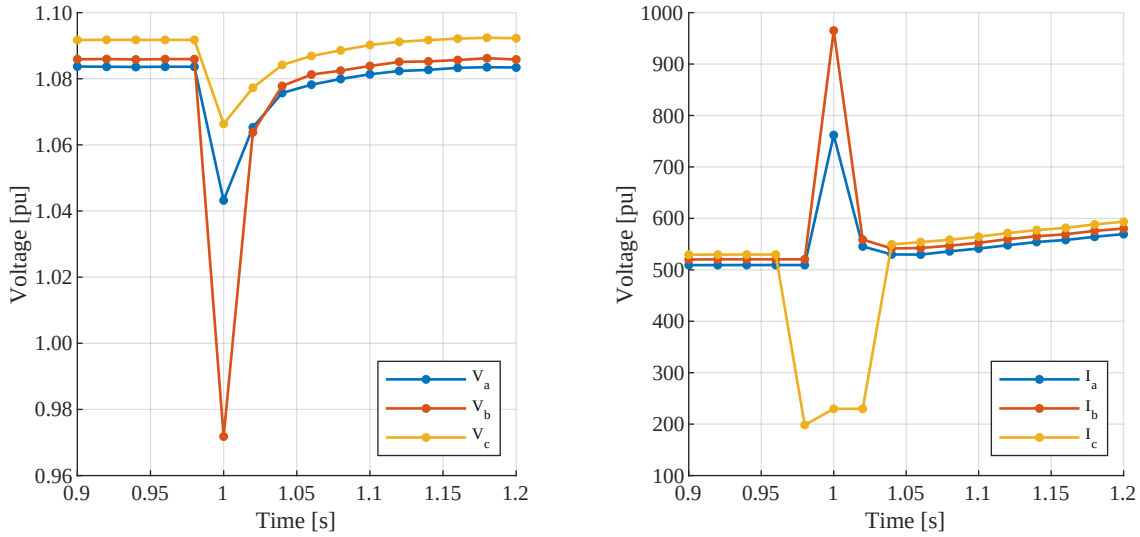

(a) Voltage magnitude

(b) Current magnitude

Figure 5.2: Three-phase measurements taken by PMU61 during event 1, SMH-MSEC380 short circuit, t_0 = 03/05/2019 07:46:28.

5.2.2. Validation using System Wide Simulation

After the EMS snapshot was successfully loaded into the dynamic model, manual adjustments were made to improve the match with the pre-disturbance operating conditions in the model. With these adjustments, the focus was on the generators located near the measurement points, Borssele and Eemshaven. Table 5.1 summarizes the adjustments that were made. The generator terminal voltages Ut were adjusted in order to better align the reactive power dispatch of the generators in the model with the measurement data from GEN eBase. Also, generator unit RWE2 had to be taken out of service manually, while the generating units TZE11G1 and TZE11G2 had to be put into service. These were not successfully loaded from the EMS snapshot.

Table 5.2 further shows how the adjustment of the initial conditions affect the voltages at the substations, and how the values deviate from the recorded values. As discussed in section 3.3, preference is given over correctly representing reactive power dispatch over correctly representing voltages.

After ensuring the stability of the model, the event simulation was set up. A bus was introduced in the fault branch SMH-MSEC at a the approximate distance of the fault. At this bus, a three-phase short circuit was applied. Table 5.3 shows the sequence of events for the simulation of event 1. The sequence of events was based on the information in section 5.2.1. Simulations were run to determine the impedance of the fault, as discussed in section 3.4. As the results will show, the voltage drop during the fault could not be matched exactly to both the voltage drops that were measured in Borssele and in Eemshaven. Therefore an impedance value was chosen that resulted in a compromise between both measurements. The fault impedance that was used was 0+33j Ω.

Table 5.1: Comparison of SWS model initial active and reactive power with GEN eBase measurements for event 1.

	GEN eBase		Model before adjustments			Model after adjustments		
Unit	P	Q	P	Q	Ut	P	Q	Ut
RWE1	789	10	439	56	0.967	789	30	0.955
RWE2	-	-	467	35	0.963	-	-	-
MAG1	481	-13	476	6	0.988	480	3	0.970
MAG3	357	0	338	33	0.990	355	18	0.970
EC3	356	-2	351	106	1.041	356	12	0.990
EC5	357	-7	351	108	1.041	357	-2	0.985
EC6	362	1	357	15	1.011	362	1	0.990
EC7	360	0	354	5	1.008	360	2	0.990
SL10	423	9	423	87	0.985	423	4	0.950
SL20	424	3	425	86	0.985	425	4	0.950
BS30	481	2	484	-118	0.964	484	10	1.000
TZE11G1	118	17	-	-	-	118	-1	1.053
TZE11G2	122	10	-	-	-	122	-2	1.053
TZE11S1	36	-2	36	4	1.027	36	10	1.032

Table 5.2: Comparison of SWS model initial voltages with GEN eBase measurements for event 1.

	GEN eBase	Model before adjustment	Model after adjustment
Substation	V [pu]	V [pu]	V [pu]
EOS380	1.085	1.050	1.031
EEM380	1.082	1.050	1.031
EEM220	1.062	1.050	1.025
BSL380	1.092	1.050	1.039
BSL150	1.042	1.053	1.053
TZN150	1.042	1.050	1.050

Table 5.3: Sequence of events for the simulation of event 1.

Simulation time	Event
0.00	Start simulation, PMU time is 07:46:28.
0.98	Apply fault at fault bus.
1.02	Trip three phases on branch SMH-MSEC.
1.02	Trip MSEC generator.
10	End simulation.

Validation results

Figure 5.3a and Figure 5.3b show a comparison between the simulation voltage and the voltage measurements at the Eemshaven substation and Borssele substation respectively. The graphs show the voltage deviation from the initial value and not the absolute voltage values. As the initial conditions of the model are not perfectly aligned with the measurements, the absolute simulation and measurement results can lie far apart. Comparing the voltage deviations is therefore more insightful.

The figures show, the voltage drop measured at Eemshaven was less deep as compared to the voltage drop that was simulated. Conversely, the voltage drop measured at the Borssele substation was deeper as compared to the voltage drop that was simulated. It was not possible to adjust the fault impedance in such a way to align the simulation with both measurements. Therefore, a compromise between both measurements was used.

The figures show a voltage drop which is the result of the short circuit. The measured voltage drop is deeper at Borssele as it is closer to the location of the short circuit. After the voltage drop, the voltage quickly stabilizes both in the measurement and the simulation.

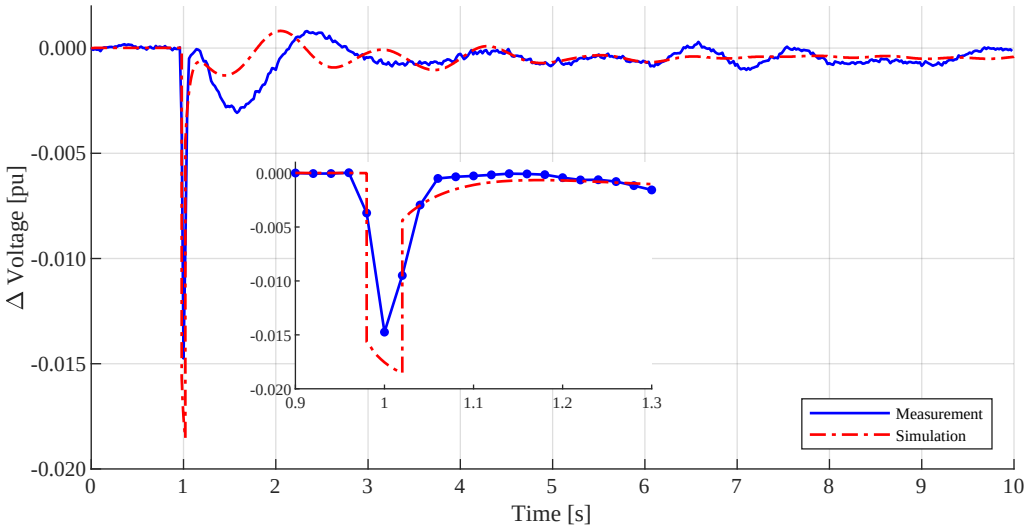

(a) PMU21: Eemshaven

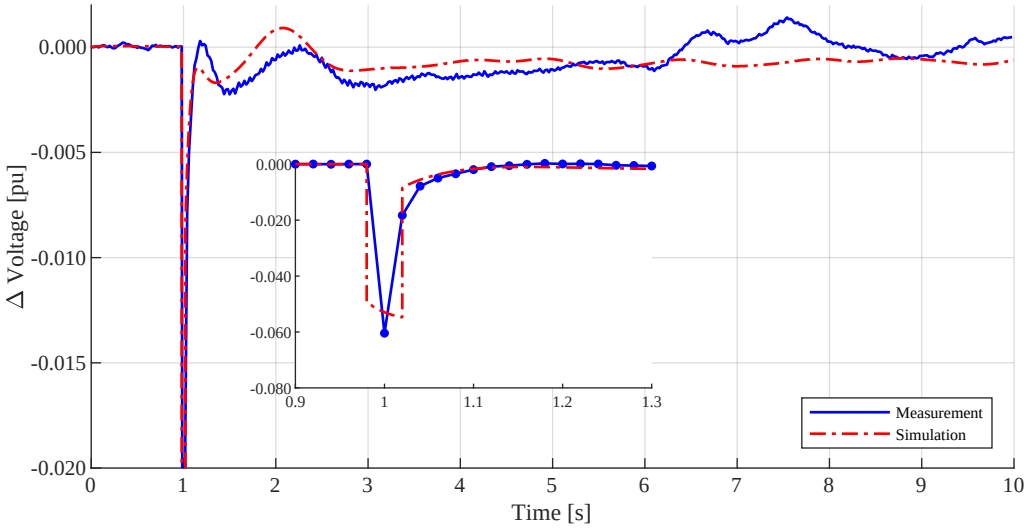

(b) PMU61: Borssele

Figure 5.3: Comparison of voltage measurement and SWS simulation results for event 1. The graphs show the deviation from the initial value.

Figure 5.4 shows comparisons for the active power measured and simulated. As with the voltage, the figure shows deviations from the initial value. The model correctly predicts a power oscillation at the Eemshaven substation following the event as can be seen in Figure 5.4a and Figure 5.4b. The figures show that the oscillations have a similar frequency. For Figure 5.4b however, the damping seems to be stronger in the model. In fact, in the measurement the oscillation seems to be growing after 6 seconds, while the oscillation in the model is almost completely damped.

Figure 5.4c and Figure 5.4d show the comparisons for the measurements taken at the Borssele substation. The model correctly predicts the reduction in power exported to Belgium directly after the fault. After the loss of the MSEC power station, about 40 MW that was being exported to Belgium, flows to the Dutch power grid instead. The model also shows a power oscillation at Borssele. However, the oscillation in the model seems to have a higher frequency and higher damping than was measured.

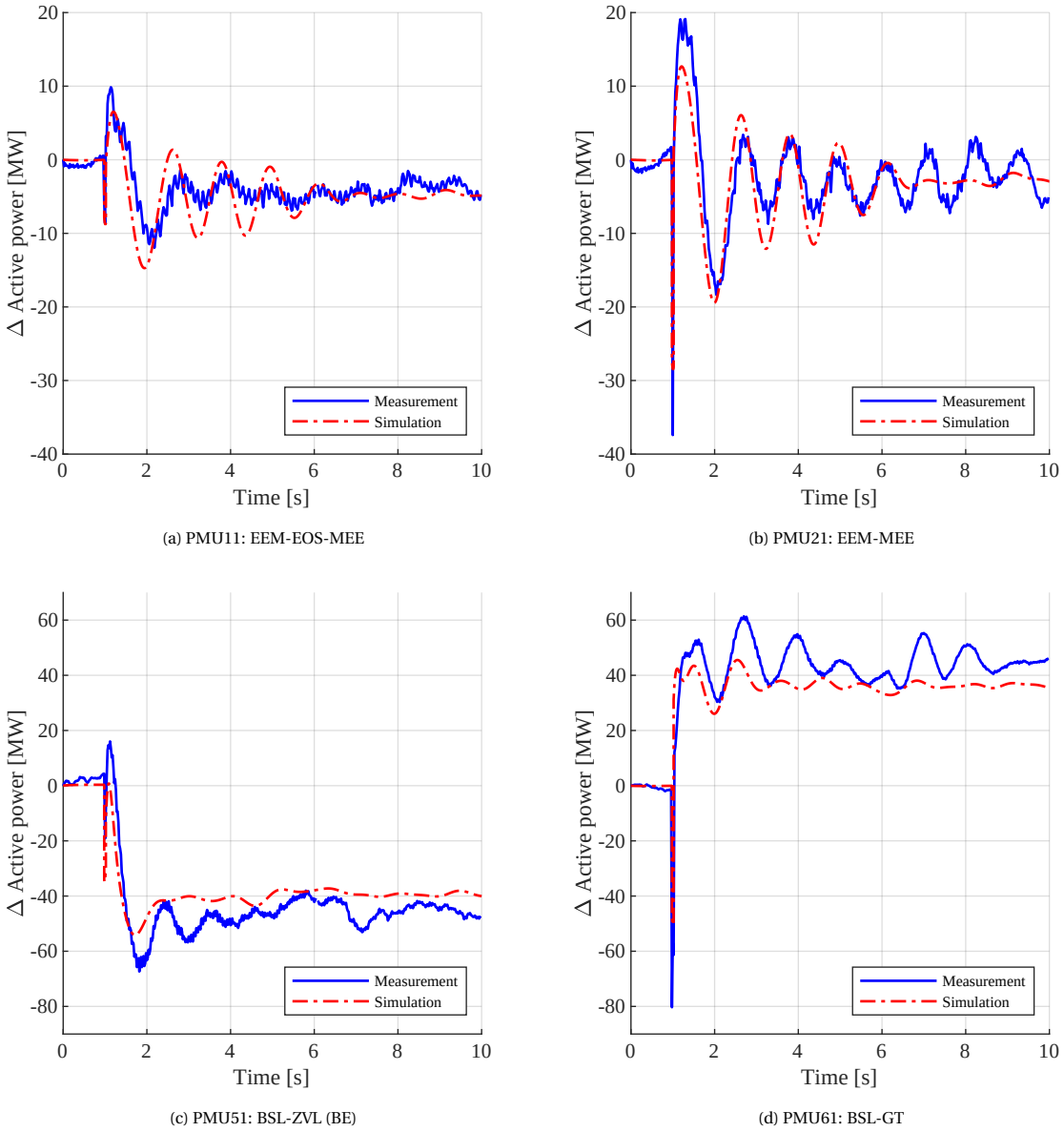

(a) PMU11: EEM-EOS-MEE

(b) PMU21: EEM-MEE

(c) PMU51: BSL-ZVL (BE)

(d) PMU61: BSL-GT

Figure 5.4: Comparison of active power measurement and SWS simulation results for event 1. The graphs show the deviation from the initial value.

Figure 5.5 shows the deviations in reactive power. The figures show a peak in reactive power during the short circuit. Figure 5.5c shows the peak downwards, as the figure shows the exported reactive power to Belgium. During the short circuit reactive power is drawn towards the Dutch power grid, which reduces the export.

The figures further show that measured reactive power show no clear pattern. The reactive power fluctuates more based on background phenomena as compared to the active power. This makes it difficult to compare the reactive power for small disturbances, when background phenomena might be dominant.

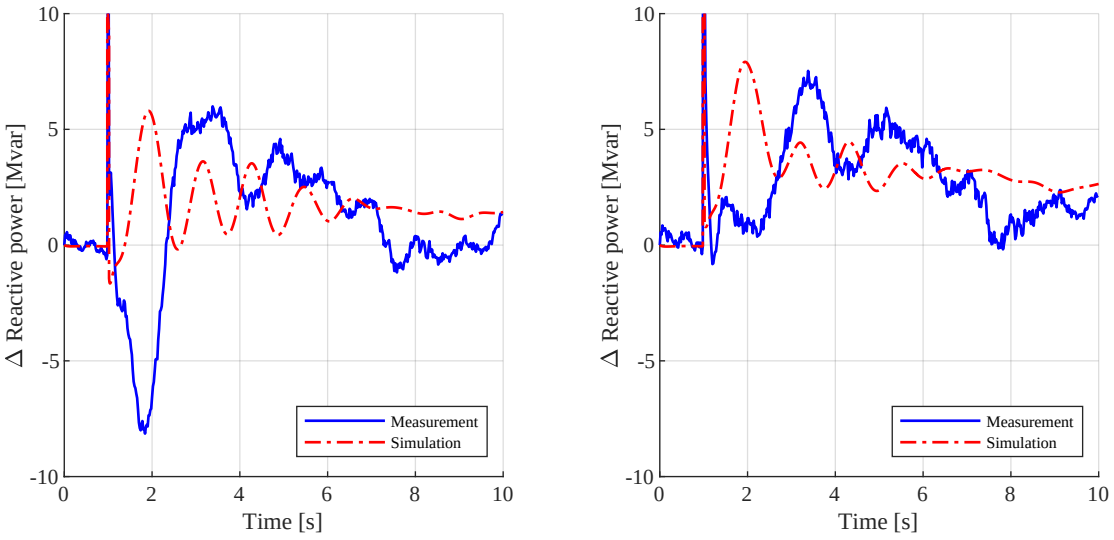

(a) PMU11: EEM-EOS-MEE

(b) PMU21: EEM-MEE

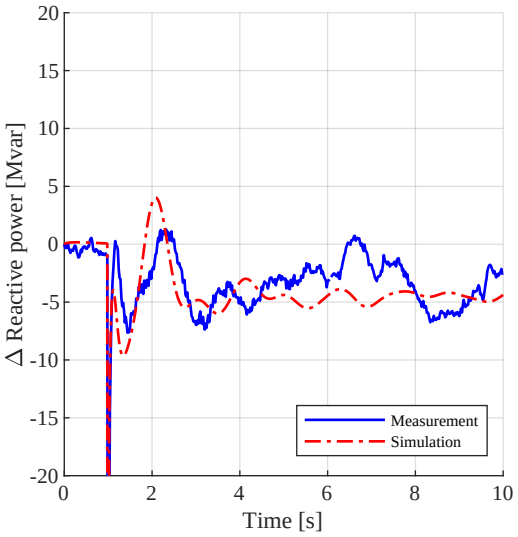

(c) PMU51: BSL-ZVL (BE)

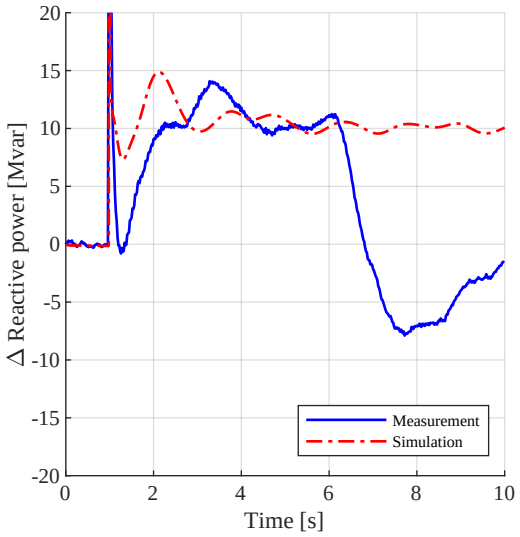

(d) PMU61: BSL-GT

Figure 5.5: Comparison of reactive power measurement and SWS simulation results for event 1. The graphs show the deviation from the initial value.

5.2.3. Validation using Hybrid Dynamic Simulation

In order to prepare the model for the Hybrid Dynamic Simulation, the Zeeland network was isolated from the rest of the model, as discussed in chapter 4. The loads and generators were setup according to the measurements from GEN eBase. A static load was added to the Rilland substation to represent the connection between the Zeeland 150 kV grid and the Brabant 150 kV grid. In total, 167 MW was flowing from the Rilland substation towards the Brabant 150 kV grid. With about 430 MW flowing from the Borssele substation through the 380 kV connection towards the rest of the Dutch power grid, the 150 kV flow accounts for approximately 28% of the total power flow from the Borssele substation towards the rest of the Dutch power grid.

Table 5.4 shows the measurements of the active and reactive power dispatch of the generators in the Zeeland subnetwork compared with the values in the model. Table 5.5 further shows comparisons of the voltages at selected substations. The initial conditions were adjusted by adjusting the transformer winding ratios, and by adjusting the generator terminal voltage. As the tables show, the initial conditions can approach the measured values more accurately in the subnetwork than was possible in the complete model as is used with System Wide Simulation.

Note that the voltage at the Borssele 380 substation was adjusted based on the PMU measurements, instead of the measurements from GEN eBase. The PMU measurements were used, because the simulation results are going to be compared with the PMU measurements.

Lastly, a static load was added to the model in parallel with the playback generator in order to precisely match the playback generator active and reactive power with the PMU measurements. This boundary load accounts for losses in the subnetwork and measurement inaccuracies of discrepancies between the GEN eBase measurements and the PMU measurements. The boundary load has an active and reactive power consumption of -10.6 MW and -8.5 Mvar.

With the subnetwork model setup and PLB file prepared, the Hybrid Dynamic Simulation was run.

Table 5.4: Comparison of HDS model active and reactive power with GEN eBase measurements for event 1.

	GEN eBase		Model		
Unit	P	Q	P	Q	Ut
SL10	423	9	423	9	0.994
SL20	424	3	424	2	0.992
BS30	481	2	480	3	1.003
TZE11G1	118	17	118	16	1.000
TZE11G2	122	10	122	9	1.000
TZE11S1	36	-2	36	-3	1.000

Table 5.5: Comparison of HDS model voltages with GEN eBase measurements for event 1.

	GEN eBase	Model
Substation	V [pu]	V [pu]
BSL380	1.092	1.087
BSL150	1.042	1.044
TZN150	1.042	1.042

Validation results

Figure 5.6a shows a comparison between the measured and simulated voltage at the Borselle substation. Figure 5.6b shows a comparison between the measured and simulated frequency at the Borselle substation. As these measurements are played into the simulation by the playback generator, the measurement and the simulation results show an accurate match. Figure 5.6b shows that simulated frequency is smoother than the measured frequency. This is possibly a result of the integration step as was shown in Figure 4.1b. An integration acts as a simple low pass filter. (The actual filters included PLBFVU1 model were not used in the Hybrid Dynamic Simulations.)

Figure 5.7 shows a comparison between the simulated and measured active power flowing from the Borssele substation. (For this, the individual power flows recorded by PMU51 and PMU61 were summed.) As the initial conditions in the Hybrid Dynamic Simulation can be represented more accurately as compared to the System Wide Simulation, it is possible to compare the actual measurement and simulation results instead of the deviation from the initial condition.

The figure shows that on average, the simulated power flow is higher than the measurement. This can be explained by the fact that the power transport flowing through the 150 kV grid was simplified using a static load. As Figure 5.4d has shown, after the event, more power starts flowing towards the dutch power grid. This

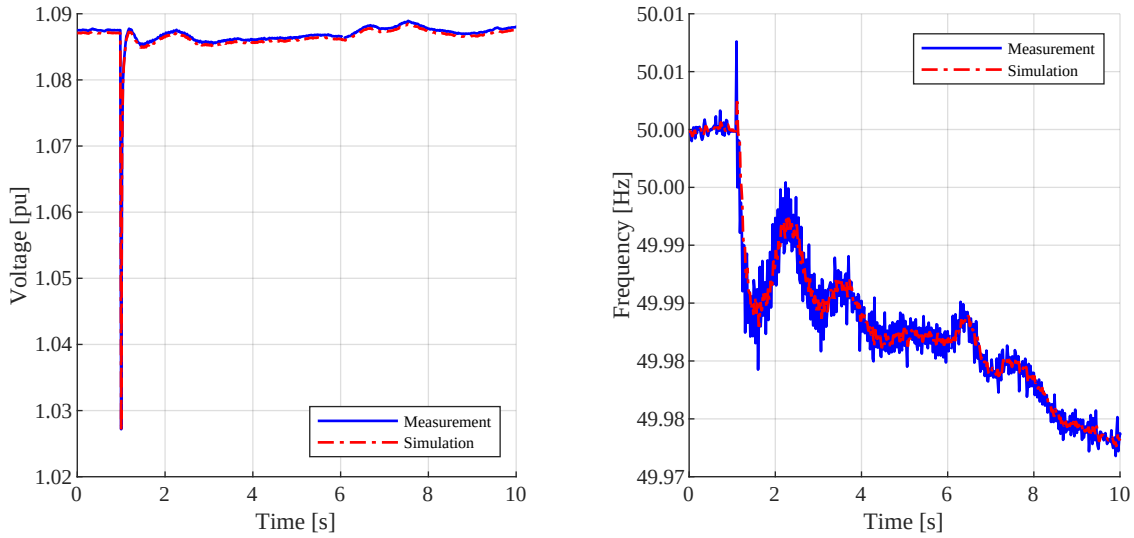

(a) Positive sequence voltage magnitude

(b) Frequency

Figure 5.6: Comparison of voltage and frequency measurement and HDS simulation results for event 1.

will have likely also resulted in a larger flow through the 150 kV grid. As this is not considered in the model with the static load representing the 150 kV flow, the simulated flow through the 380 kV grid is larger.

What stands out in the simulation result is the first swing in the power oscillation. The valley around 1.25 seconds is not present in the measurement. Subsequently, the oscillation in the simulation seems to have a similar frequency with the measurement, but is lagging behind the measurement.

Figure 5.8 shows the comparison for the reactive power. The figure shows that the simulation results follow the measurement results quite well. However, the oscillation present in the simulation results show a bigger amplitude as compared to the measurement results.

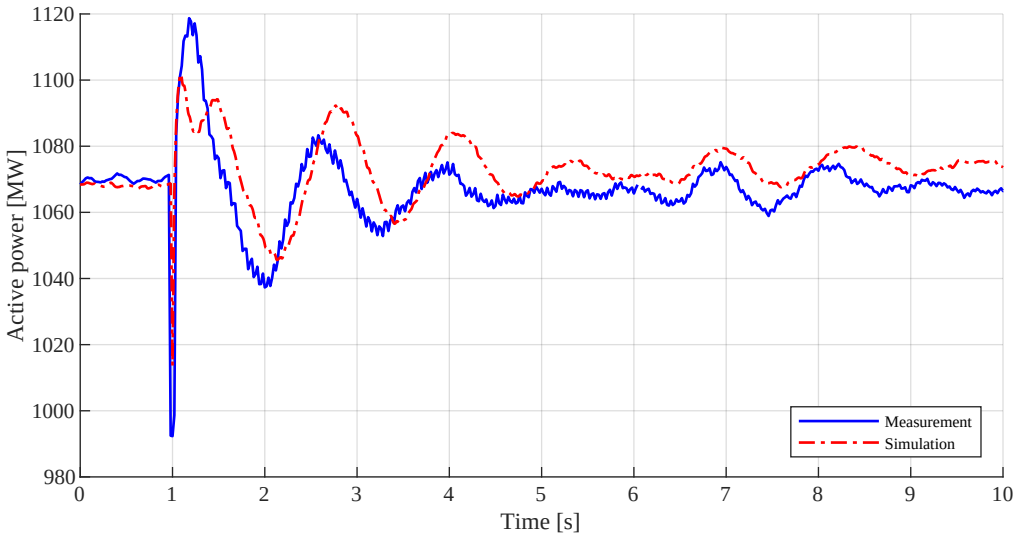

Figure 5.7: Comparison of active power measurement and HDS simulation result for event 1.

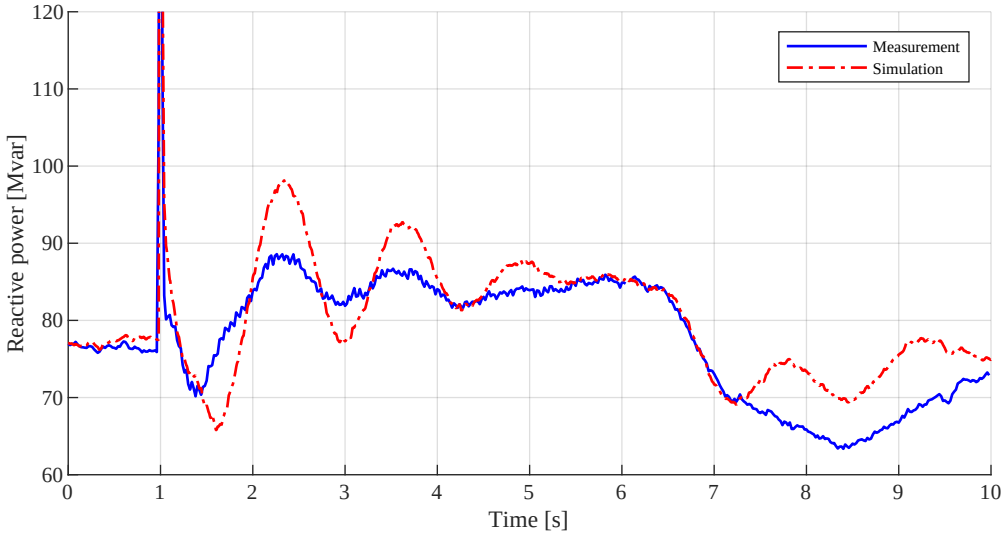

Figure 5.8: Comparison of reactive power measurement and HDS simulation result for event 1.

Figure 5.9 shows the contributions of the different power plants in the simulation to the power oscillation. The figure shows the deviation in active power from the initial value. The figure also includes the deviations in the measurement and simulation result that were shown in Figure 5.7. Deviations are used here so that the overall response of the subnetwork can be compared to the responses of the different generators.

From the figure can be concluded that the Sloe generators (SL10 and SL20) are responsible for the first swing in the power oscillation, that was not present in the measurement. This indicates that the models for the Sloe generators might be inaccurate.

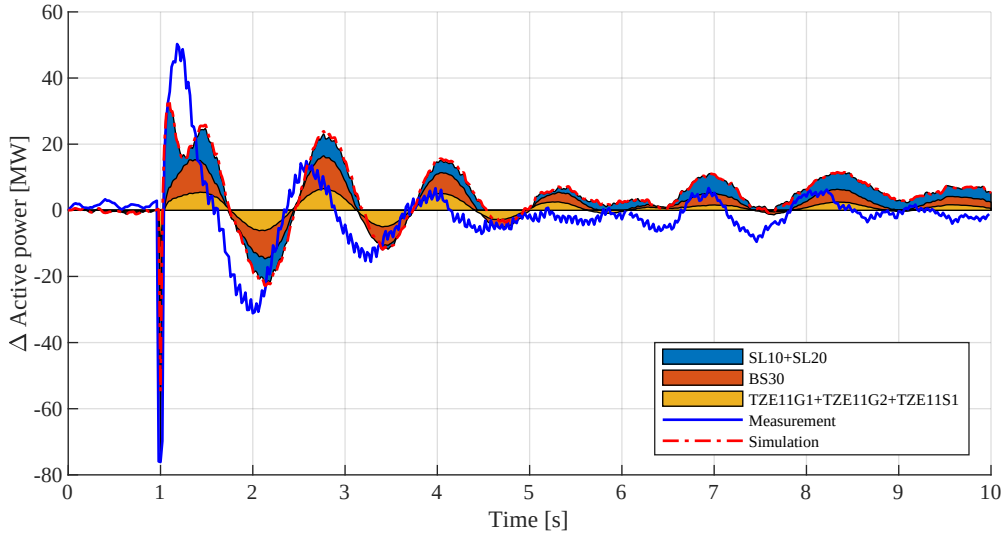

Figure 5.9: Comparison of active power measurement and HDS simulation result for event 1. Including contributions of the different generating units. Graphs show deviations from the initial value. Contributions were plotted by overlapping the graphs; *SL10+SL20* includes the contribution of all generators, *BS30* shows the response excluding SL10 and SL20, *TZE11G1+TZE11G2+TZE11S1* shows the respons excluding SL10, SL20 and BS30.

5.3. Event 2: 21/05/2019 EEM-MEE380 Line switching

5.3.1. Event description and measurements

On Tuesday 21/05/2019 around 18:02:44 the circuit EEM-MEE380-W was put into service after being out of service for approximately 6 hours. (For maintenance reasons possibly.) Figure 5.10a and Figure 5.10b show the measurements of the voltages and active power respectively.

Figure 5.10b clearly shows the effect of the switching action. Before the circuit is put into service, circuit EEM-MEE380-Z (measured by PMU21) carries all the power. When EEM-MEE380-W (measured by PMU11) is put into service the power flow is neatly divided over both circuits.

The fact that the power flowing in both circuits is approximately equal after the switching event, indicates that the temporary connection between Eemshaven-Oudeschip (EOS380) and the circuit EEM-MEE380-W as shown in Figure 2.3a was not in service at the time of the measurement. Otherwise part of the power flow from EOS380 would flow through the temporary connection and bypass PMU11. This would have resulted in a significant difference in power flow measured by PMU11 and PMU21. This effect was for example visible in the measurements of event 1, shown in Figure 5.1b.

The sudden reduction in impedance which is the result of activating the second circuit causes a damped oscillation in the power flowing from Eemshaven. The oscillation has an initial amplitude of approximately 50 MW and a frequency around 0.9 Hz. A power oscillation was also picked up by the PMUs located at the Borssele substation. However, with an amplitude of approximately 5 MW, the oscillation is hardly visible at the scale of Figure 5.1b.

The voltage measurements in Figure 5.10a show that the voltage magnitude at the Eemshaven substation is slightly increased after the switching event. Also an oscillation in voltage can be distinguished. The switching event however, hardly has an impact on the voltage at the Borssele substation.

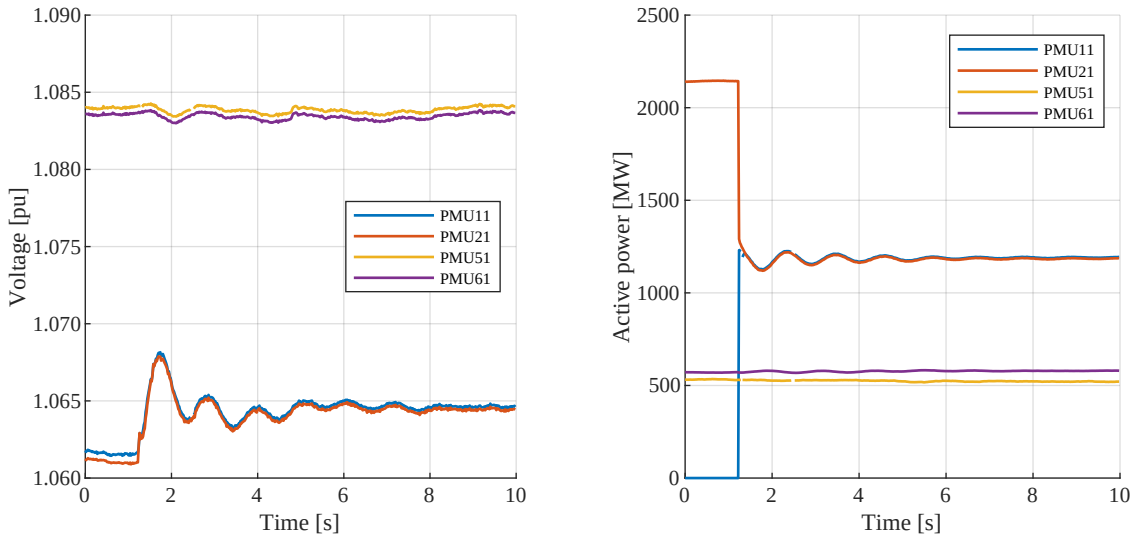

(a) Positive sequence voltage magnitude

(b) Active power

Figure 5.10: Measurements during event 2, EEM-MEE380-W line switching, t_0 = 21/05/2019 18:02:43.

5.3.2. Validation using System Wide Simulation

Again, the System Wide Simulation process was started by loading the EMS snapshot from 21-05-2019 18:00 into the dynamic model. For the adjustment of the initial conditions, most attention was given to the generators in Eemshaven, as the event was hardly picked up in the measurements taken at Borssele.

Table 5.6 shows a summary of the adjustments that were made for the initial conditions for the System Wide Simulation of event 2, compared to the measurement values that were retrieved from GEN eBase. The table shows quite a big difference in the active power dispatch loaded from the EMS snapshot (Model before adjustments) and the measurement values recorded in GEN eBase. It is unclear what had caused this discrepancy, but it highlights the importance of checking the model after loading the snapshot. The information from GEN eBase is considered to be more reliable as it includes the actual measurements.

The table also again shows that the snapshot loading process fails to activate the generating units TZE11G1 and TZE11G2, and to deactivate one of the RWE generating units. Manual adjustments were made to correct the active and reactive power dispatch.

Table 5.7 shows how the adjustment of the initial conditions affected the voltages at the substations.

After loading the snapshot, adjusting the initial conditions and testing for the stability of the model, the simulation of event 2 was relatively straightforward. 1.22 seconds into the simulation, circuit EEM-MEE380-W is put into service, and subsequently the simulation is ended after 10 seconds.

Table 5.6: Comparison of SWS model initial active and reactive power with GEN eBase measurements for event 2.

	GEN eBase		Model before adjustments			Model after adjustments		
Unit	P	Q	P	Q	Ut	P	Q	Ut
RWE1	-	-	358	104	0.976	-	-	-
RWE2	787	32	390	78	0.970	785	17	1.000
MAG2	477	10	411	42	0.995	477	1	0.970
MAG3	420	20	469	30	0.993	420	8	0.970
EC3	329	1	210	157	1.052	321	5	0.990
EC5	343	13	267	154	1.052	343	6	0.990
EC6	331	-6	219	52	1.018	331	4	0.990
EC7	342	10	241	35	1.014	342	3	0.990
SL10	415	-9	416	91	0.986	415	53	0.970
SL20	421	-15	421	90	0.986	421	52	0.970
BS30	479	2	479	-117	0.967	479	-3	1.000
TZE11G1	113	16	-	-	-	111	-18	1.015
TZE11G2	117	11	-	-	-	114	-18	1.014
TZE11S1	28	-6	32	-30	0.997	30	-8	1.016

Table 5.7: Comparison of SWS model initial voltages with GEN eBase measurements for event 2.

	GEN eBase	Model before adjustment	Model after adjustment
Substation	V [pu]	V [pu]	V [pu]
EOS380	1.066	1.050	1.032
EEM380	1.063	1.050	1.032
EEM220	1.015	1.050	1.029
BSL380	1.089	1.050	1.045
BSL150	1.044	1.055	1.057
TZN150	1.045	1.050	1.050

Validation results

Figure 5.11a and Figure 5.11b show comparisons of the positive sequence voltage measurements and the System Wide Simulation results. Figure 5.11a shows that the model correctly predicts an increase in the voltage magnitude at the Eemshaven substation, followed by a damped oscillation. However, the increase in the voltage magnitude in the simulation is more than twice as large as the voltage increase that was measured. In absolute terms, the voltage increase is quite small; settling at about 0.0033 pu in the measurement 0.0088 pu in the simulation. The difference in voltage deviation could be a consequence of the difference in initial conditions in voltage and reactive power.

Figure 5.11b shows that the voltage deviation measured at Borssele is hardly large enough to be distinguished from normal voltage deviations occurring in the system.

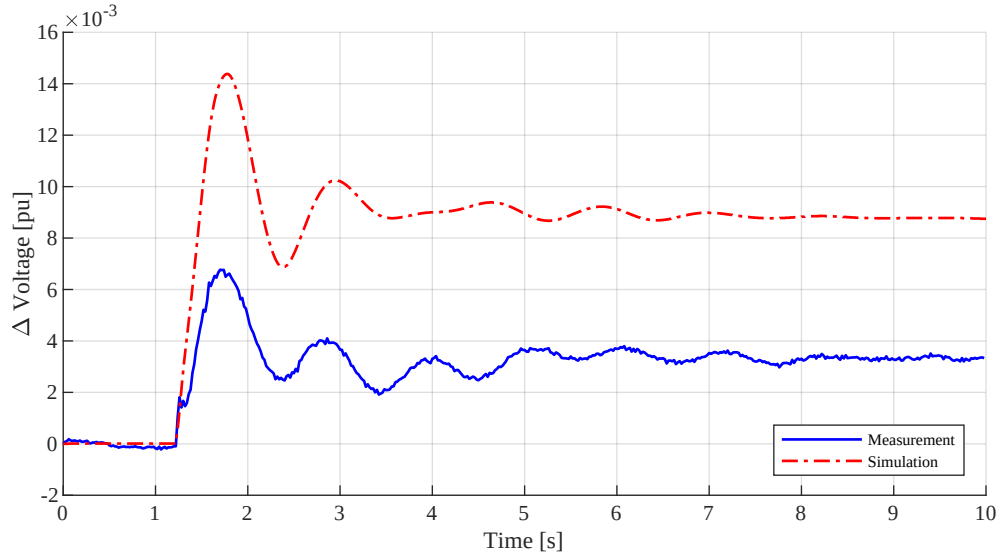

(a) PMU21: Eemshaven

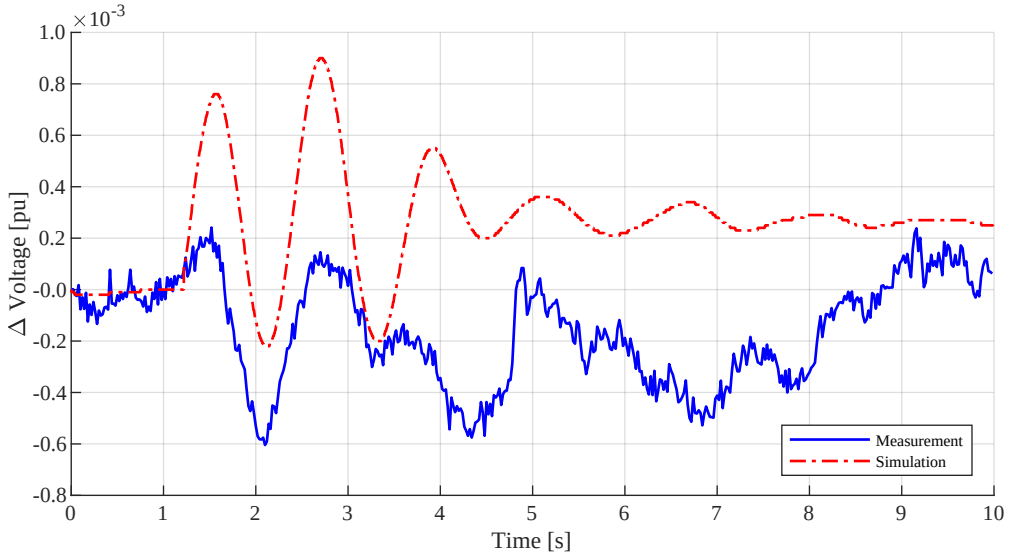

(b) PMU61: Borssele

Figure 5.11: Comparison of positive sequence voltage magnitude measurement and SWS simulation results for event 2. The graphs show the deviation from the initial value.

Figure 5.12 shows comparisons for the active power. Again, the figures show deviations from the initial value. Figure 5.12a and Figure 5.12b show that the model initially follows the measurement relatively well. The simulated oscillation has approximately the same frequency. 3 seconds into the simulation however, the oscillation flattens out and restarts in anti-phase with the measurement. Furthermore, the oscillation in the simulation shows a lot more damping as compared to the oscillation in the measurement.

The response measured by PMU51 in Figure 5.12c is largely obscured by background behaviour in the system. In Figure 5.12d however, the model shows a nice match with the measured behaviour, in terms of frequency and amplitude of the oscillation. The measurements further show that the active power flowing towards Belgium is reduced, while the power flowing towards the rest of the Dutch power grid increases. The reduction in the power export is most likely not a consequence of the line switching event, and is thus also not found in the simulation results.

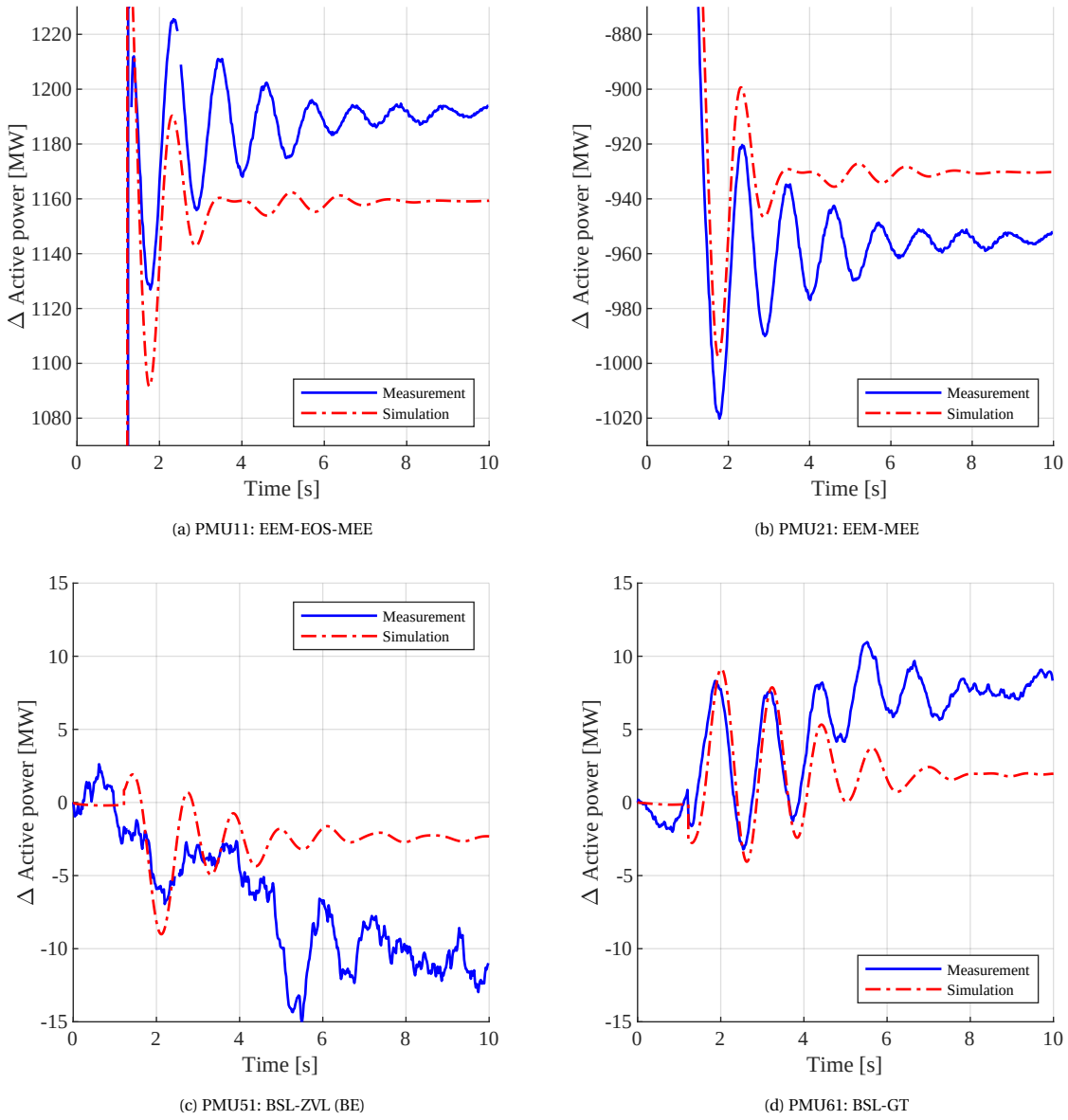

(a) PMU11: EEM-EOS-MEE

(b) PMU21: EEM-MEE

(c) PMU51: BSL-ZVL (BE)

(d) PMU61: BSL-GT

Figure 5.12: Comparison of active power measurement and SWS simulation results for event 2. The graphs show the deviation from the initial value.

Figure 5.13 shows comparisons for the reactive power. Figure 5.13a and Figure 5.13b show that the measured reactive power flow is reduced after the line switching event. This makes sense as the power lines will consume less reactive power if their loading is reduced. It is unclear why this effect was not observed in the simulation. Possibly again due to the difference in the pre-disturbance reactive power flow between the model and the situation in reality.

At the Borssele substation the effect of the disturbance is too small to be distinguished in the measurement results.

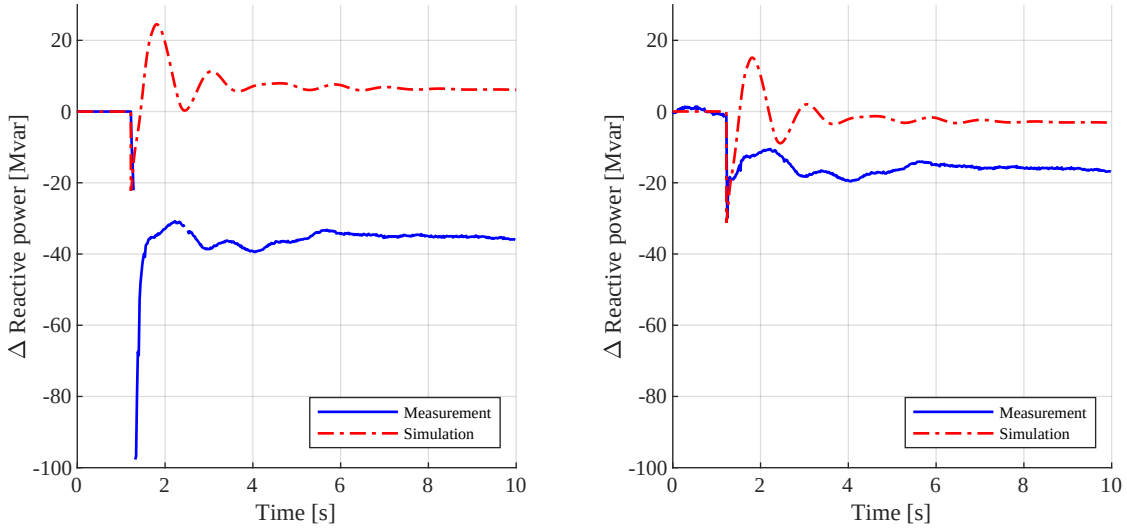

(a) PMU11: EEM-EOS-MEE

(b) PMU21: EEM-MEE

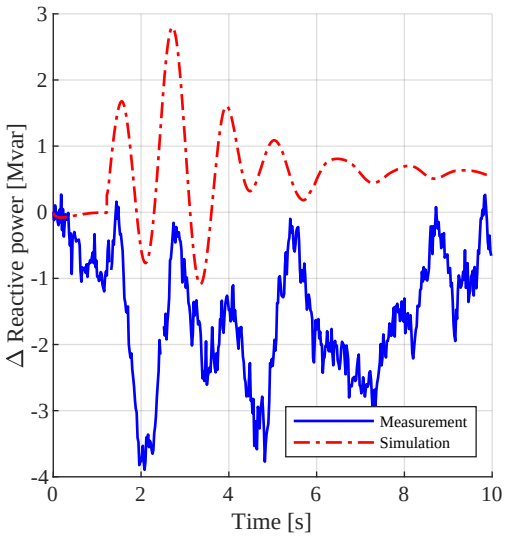

(c) PMU51: BSL-ZVL (BE)

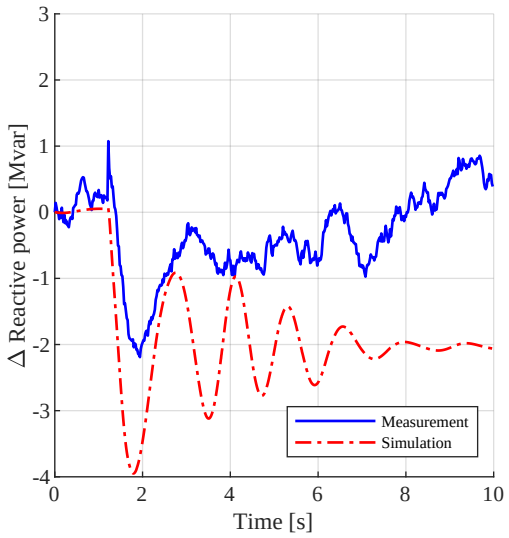

(d) PMU61: BSL-GT

Figure 5.13: Comparison of reactive power measurement and SWS simulation results for event 2. The graphs show the deviation from the initial value.

Figure 5.14 provides a closer look at the power oscillation at the Eemshaven substation in response to the switching event. The measurement and the simulation show the total power flowing from the Eemshaven substation towards the Meeden substation. The figure further shows the contributions of different generating units to the power oscillation. The generators show different oscillation frequencies. The interference between the individual power oscillations explains why the total oscillation flattens out and starts oscillating in anti-phase with the measurement at the 4 seconds mark.

The measurement result indicates that the generating units were oscillating in phase at the same frequency. However, with so many contributing generators, it is difficult to draw a definitive conclusion. The figure does reinforce the idea that the damping is higher in the model as compared to the system in reality. The Norned HVDC link might have also played a role in the power oscillation, as well as the wind farm Gemini. In the model, both are currently (still) modelled as a static load, and do therefore not contribute to the power oscillation.

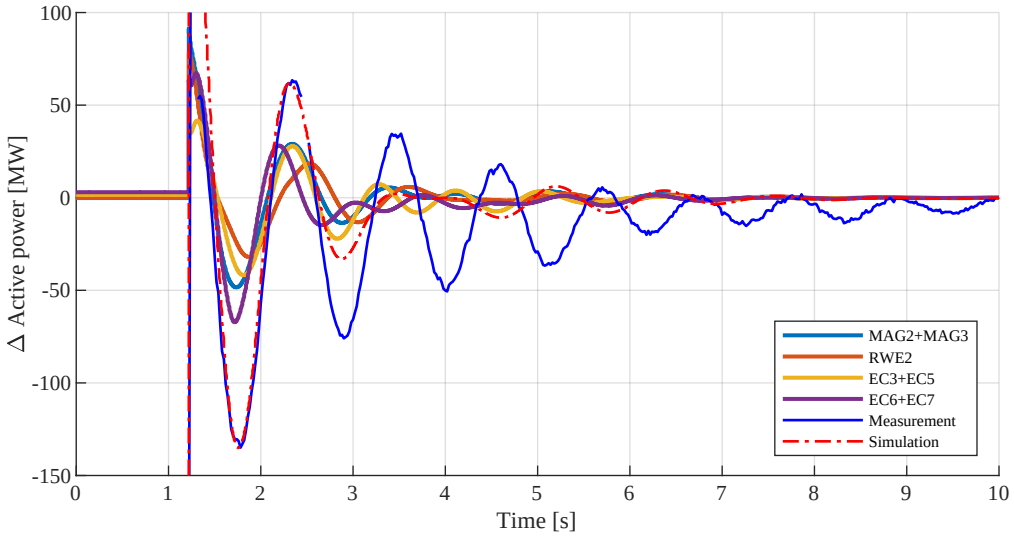

Figure 5.14: Power oscillation measurement at Eemshaven substation in response to event 2, compared with the System Wide Simulation results. Measurement and simulation show the total power flow from the Eemshaven substation towards the Meeden substation. Generator power obtained from simulation results, where generators with a similar behaviour are summed. All graphs are offset in order to have a final value of 0.

5.3.3. Validation using Hybrid Dynamic Simulation

As the event did not have a significant impact on the voltage nor frequency measurements at Borssele, this event was not suitable for Hybrid Dynamic Simulation in the Zeeland subnetwork.

5.4. Event 3: 18-06-2019 ZYV-VVL220 Short circuit

5.4.1. Event description and measurements

On Tuesday 18/06/2019 a single-phase fault occurred on the circuit ZYV-VVL220-Z. The fault was cleared by the protection system by interrupting only the faulted phase conductor. After the fault was cleared the conductor was taken into service again by the automatic recloser, after which normal operation was resumed without any permanent changes to the network topology.

Figure 5.15a shows the positive sequence voltage magnitude measured during the event. The figure shows a sharp drop in voltage during the fault measured at the Eemshaven substation (PMU11 and PMU21). A voltage drop is also visible in the measurements at the Borssele substation (PMU51 and PMU61) though much smaller than the voltage drop at Eemshaven. At the Eemshaven substation, the voltage drop is immediately followed by a voltage spike with a duration of approximately 0.4 seconds.

Figure 5.15b shows the active power measured during the event. The measurements taken by PMU11 and PMU51 show a large amount of data loss. The figure shows a large difference in the power measured by PMU11 and PMU21. This again is a result of the power flowing through the temporary connection EOS-EEM-MEE as discussed in section 2.5. The figure further shows that the power exported to Belgium from the Borssele substation is approximately 0, while there's approximately 150 MW flowing from the Borssele substation towards the rest of the Dutch power grid. Little power is produced at the Borssele substation. As the event occurred early in the morning, demand for electricity was likely not very high.

The fault occurring on the circuit ZYV-VVL220-Z is picked up by the PMU's at substation Eemshaven as a sharp drop in voltage as well as a drop in the power flowing towards Meeden. During the fault, part of the power that was flowing towards Meeden is instead now flowing into the 220kV grid towards the fault. After the fault has been cleared an oscillation can be seen in the power flowing from the Eemshaven substation.

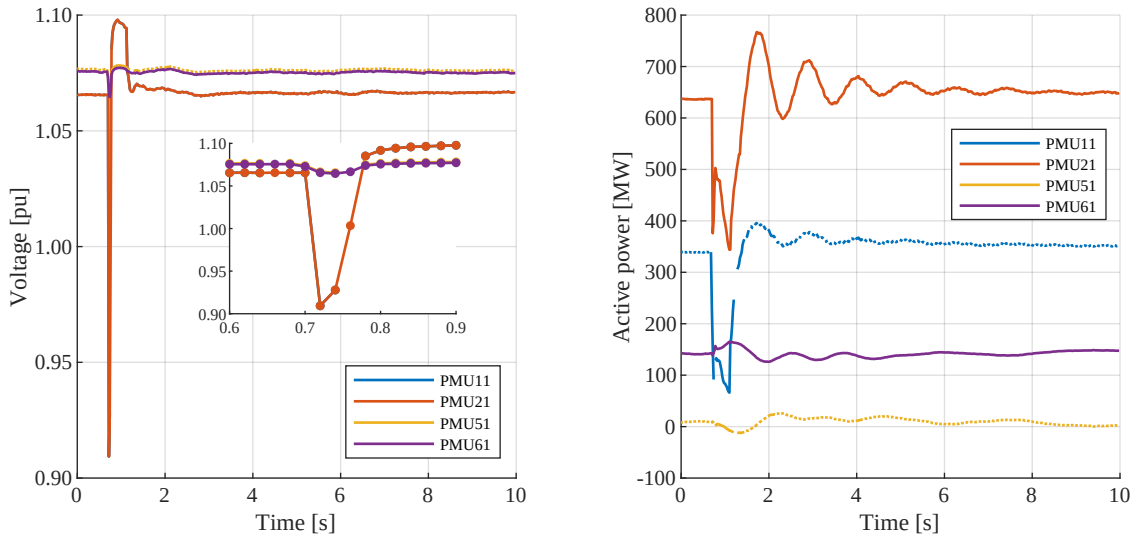

(a) Positive sequence voltage magnitude

(b) Active power

Figure 5.15: Measurements during event 3, ZYV-VVL220 short circuit. (Note that there's data missing in the measurements from PMU11 and PMU51, which explains the interruptions in the graphs.) T_0 = 18/06/2019 04:27:16.

Figure 5.16a and Figure 5.16b show the current measured by the protection equipment in substation Vierverlaten (VVL220) and substation Zeyerveen (ZYV220) respectively. And Figure 5.16c and Figure 5.16d show the measured voltages. Note that as opposed to the PMU measurements, these measurements do not represent RMS values but instead are the instantaneous values. The measurements are taken at a higher sample-rate of 999 Hz.

From the figures it can be seen that the fault was a single-phase to ground fault on phase c. The current shoots up during the fault, while the voltage drops. The figures further show that the fault is cleared after 3.5 cycles, corresponding to 70 milliseconds. The fault was cleared by only tripping the circuit-breakers for phase c, allowing phase a and b to stay in operation. The figures also show that the fault location was close to the Vierverlaten substation, as the fault current is approximately 5 times as large as compared to the fault current measured at the Zeyerveen substation.

From the trip logs that were extracted from the protection equipment in substations Vierverlaten and Zeyerveen, can be read that an automatic reclosing command was given 775 milliseconds (VVL220) and 794 milliseconds (ZYV220) after detection of the fault.

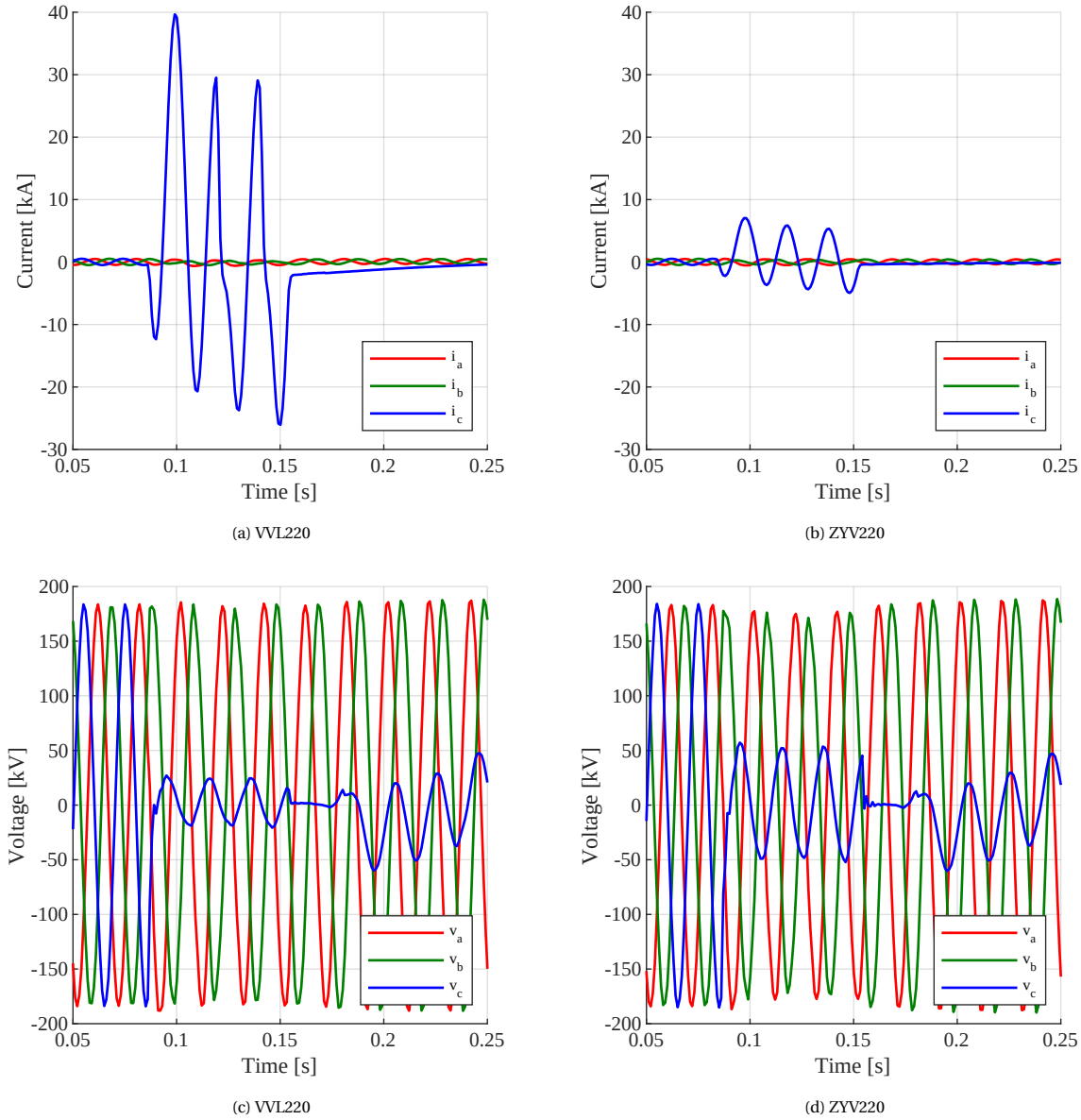

(a) VVL220

(b) ZYV220

(c) VVL220

(d) ZYV220

Figure 5.16: Instantaneous current and voltage during the ZYV-VVL220 short circuit measured by the protection equipment in substations Vierverlaten (VVL220) and Zeyerveen (ZYV220). The time axis is relative to the start of the measurements and not synchronized.

5.4.2. Validation using System Wide Simulation

As with the previous events, an EMS snapshot was loaded into the model, after which adjustments were made based on the measurement data in GEN eBase. The EMS snapshot at time 04:30 was used and for the GEN eBase data, an average was taken between the measurements at 04:25 and 04:30.

Table 5.8 shows a summary of the adjustments that were made for the initial conditions of the System Wide Simulation of event 3. The table shows less generators as compared to the previous events. As mentioned before, event 3 took place early in the morning, when energy consumption is generally low in the Netherlands. Therefore, less production units were in operation during the fault. Table 5.9 again shows the effect of the manual adjustments on the voltages at selected substations.

After ensuring the stability of the model, the event simulation was setup. A bus was introduced on the ZYV-VVL branch at the approximate location of the fault. At this bus a three-phase short circuit was applied to mimic the branch fault that had occurred in reality. Simulations were run in order to determine the fault impedance of the short circuit. The initial simulations however, showed quite significantly different behaviour in the model than was observed in the measurements. The model was unable to explain the voltage peak right after the fault, nor the power drop after the fault.

Further investigation pointed out that the Norned HVDC link connected at Eemshaven had likely experienced a commutation fault due to the voltage imbalance during the short circuit. This caused a momentarily collapse of the HVDC link interrupting the power flow and explaining the power drop that was observed. Furthermore, as the HVDC link consumes reactive power in operation, a sudden excess of reactive power was present at Eemshaven during the collapse of the HVDC link. This explains the voltage peak that was observed. The collapse of the Norned cable highlights a shortcoming of the dynamic model. Due to the simplicity with which Norned is currently modelled, the model cannot predict the momentary collapse of the HVDC link.

Table 5.10 shows the sequence of events for the simulation of event 3. The sequence of events was based on the information in section 5.4.1 and the findings about the Norned commutation fault. While a method was introduced in section 3.4 for the simulation of asymmetrical line switching, no apparent difference was observed in the simulation results for symmetrical or asymmetrical switching. Therefore the simpler symmetrical swithcing was used in the System Wide Simulation of event 3.

Simulations were further run to determine the impedance of the fault. As with the simulation of event 1, the voltage drop could not be matched for Eemshaven and Borssele simultaneously. Again, a fault impedance value was chosen that resulted in a compromise between both measurements. The fault impedance that was used was 0+10j Ω. The commutation fault in the Norned HVDC link, currently still modelled as an negative load, was simulated by temporarily taking the negative load out of service.

Table 5.8: Comparison of SWS model initial active and reactive power with GEN eBase measurements for event 3.

	GEN eBase		Model before adjustments			Model after adjustments		
Unit	P	Q	P	Q	Ut	P	Q	Ut
RWE1	547	4	465	156	0.987	547	2	0.970
RWE2	382	0	465	114	0.979	382	15	0.970
EC3	330	-9	332	302	1.098	330	16	0.970
EC7	347	-8	339	33	1.016	346	-1	0.970
SL20	231	-150	230	108	0.985	230	-148	0.980
TZE11G1	111	17	-	-	-	111	8	1.073
TZE11G2	112	11	-	-	-	112	7	1.072
TZE11S1	28	-5	29	-57	0.976	29	17	1.037

Table 5.9: Comparison of SWS model initial voltages with GEN eBase measurements for event 3.

	GEN eBase	Model before adjustment	Model after adjustment
Substation	V [pu]	V [pu]	V [pu]
EOS380	1.072	1.050	1.011
EEM380	1.068	1.050	1.011
EEM220	1.024	1.050	1.005
BSL380	1.079	1.050	1.030
BSL150	1.045	1.059	1.049
TZN150	1.046	1.051	1.050

Table 5.10: Sequence of events for the simulation of event 3.

Simulation time	Event
0.00	Start simulation, PMU time is 04:27:16.
0.70	Apply fault at fault bus.
0.72	Disconnect Norned model.
0.77	Trip ZYV-VVL branch.
1.14	Reconnect Norned model.
1.45	Reclose ZYV-VVL branch.
10	End simulation.

Validation results

Figure 5.17a and Figure 5.17b show a comparison between the simulation results and the voltage measurements at the Eemshaven substation and the Borssele substation respectively. This time, the voltage drop measured at Eemshaven was deeper as compared to the simulation, while the voltage drop measured at Borssele was less deep as compared to the simulation. The opposite was true for the simulation of event 1. However, the short circuit for event 1 was electrically closer to Borssele, while the short circuit for event 3 was electrically closer to Eemshaven. In other words, the absolute voltage drop during event 1 was deepest measured at Borssele, while the absolute voltage drop during event 3 was deepest measured at Eemshaven. In both cases, if the fault adjustment would have adjusted for the deepest absolute voltage drop, the simulated voltage drop at the other substation would be far below the measured value. This indicates that a voltage drop propagates more strongly in the simulation, as compared to the propagation in reality. Further research is required for the cause of this observation.

Figure 5.17a further shows that the voltage peak in response to the Norned commutation fault is quite different in the simulation as compared to the measurement. A reason for this could be the simplicity with which the Norned link is currently modelled. The measured voltage peak rises and falls more instantly as compared to the voltage peak in the simulation.

At the Borssele substation, the simulated voltage peak quite closely matched the measured voltage peak, as shown in Figure 5.17b. However, the effect of event 3 on the voltage at Borssele is very small, and background effects also seem to play a large role in the measurements.

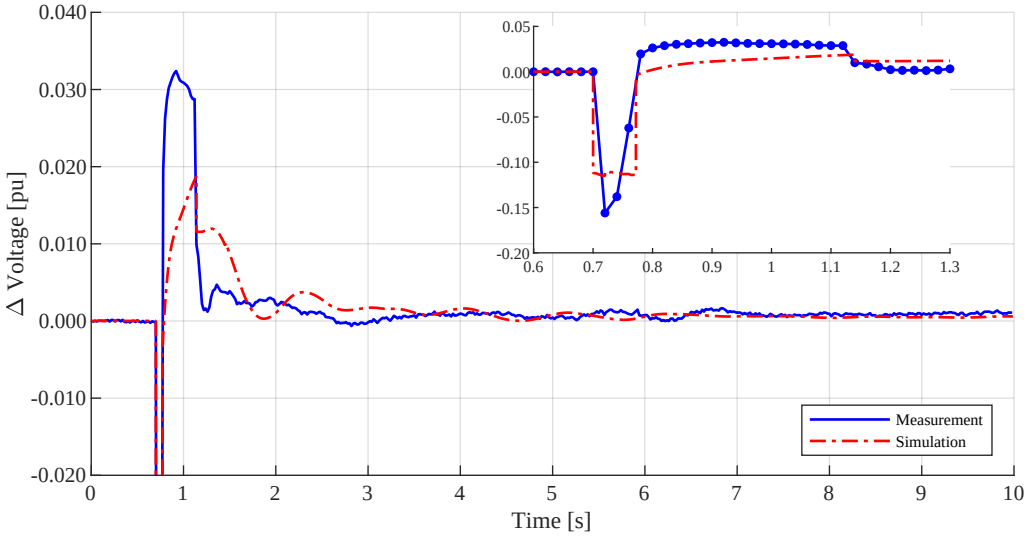

(a) PMU21: Eemshaven

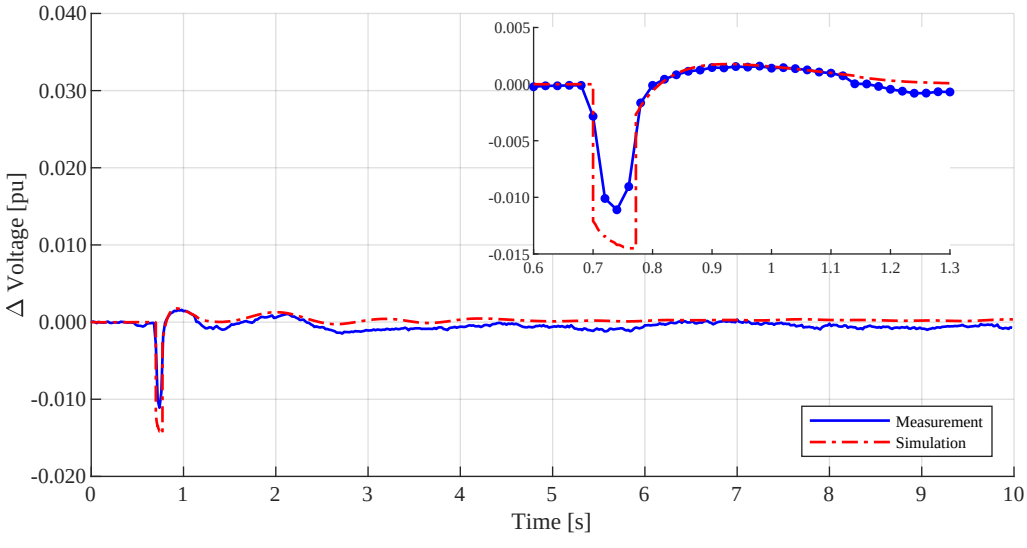

(b) PMU61: Borssele

Figure 5.17: Comparison of voltage measurement and SWS simulation results for event 3. The graphs show the deviation from the initial value.

Figure 5.18 shows comparisons for the active power measured and simulated. Figure 5.18a and Figure 5.18b show the results for PMU11 and PMU21 respectively. The figures show that the difference in oscillation amplitude between the measurement results is greater than the difference that is shown in the simulation result. It is unclear what causes this. The temporary connection EEM-EOS-MEE likely plays a role. However, the steady state power flow calculation showed a relatively accurate division of power flow. Figure 5.18a and Figure 5.18b further show that the oscillation frequency is higher in the model as compared with the measurement.

Figure 5.18c and Figure 5.18d show the results for PMU51 and PMU61 respectively. Again, the measurements are somewhat obscured by background phenomena. Figure 5.18d shows however that the initial oscillation frequency and amplitude are quite accurately predicted by the model.

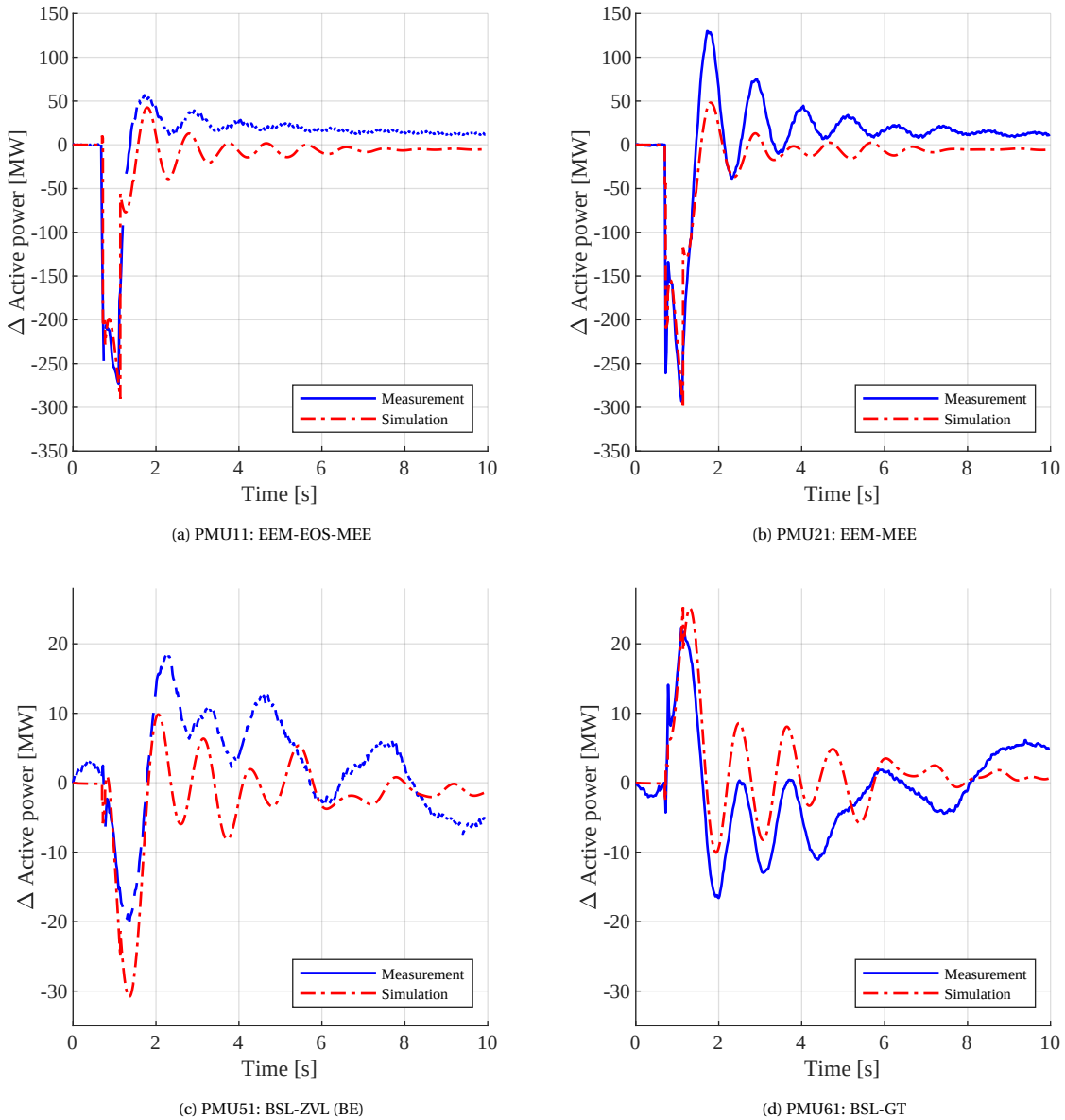

(a) PMU11: EEM-EOS-MEE

(b) PMU21: EEM-MEE

(c) PMU51: BSL-ZVL (BE)

(d) PMU61: BSL-GT

Figure 5.18: Comparison of active power measurement and SWS simulation results for event 3. The graphs show the deviation from the initial value.

Figure 5.19 shows the comparisons t=for the reactive power flows in response to the disturbance. Figure 5.19a and Figure 5.19b show the same effect that was observed in the voltage measurements at the Eemshaven substation. The tripping of the Norned HVDC interconnector results in a sudden abundance of reactive power. An additional 300 Mvar is suddenly flowing from the Eemshaven substation. This causes the peak that was observed in the voltage measurement. The simulation does not show this repsonse properly. The reason for this is that the Norned HVDC interconnector is currently not yet properly represented in the model. Here lies an opportunity for improvement in the model.

At the Borssele substation, the effect of the disturbance was again relatively small.

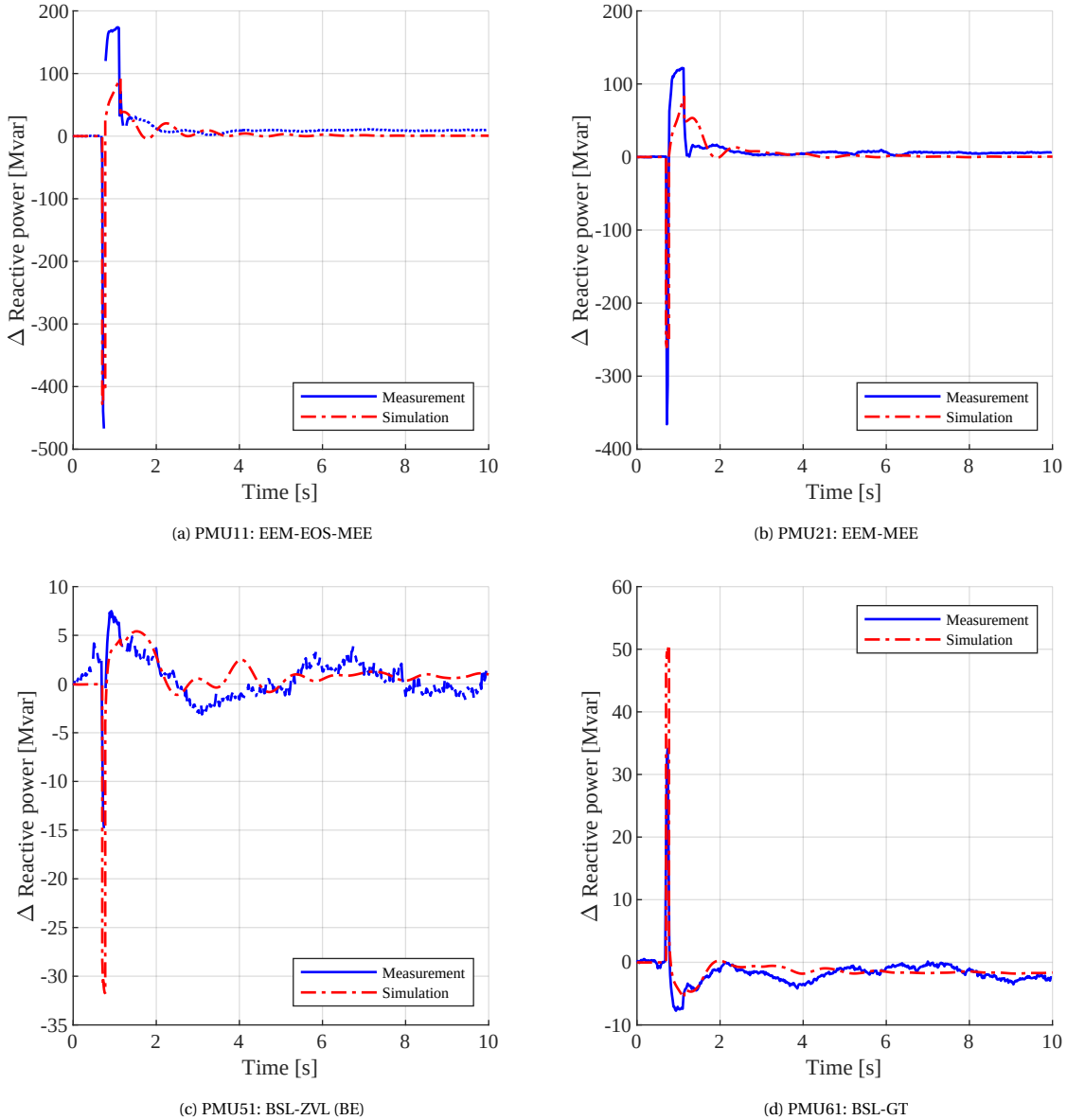

(a) PMU11: EEM-EOS-MEE

(b) PMU21: EEM-MEE

(c) PMU51: BSL-ZVL (BE)

(d) PMU61: BSL-GT

Figure 5.19: Comparison of reactive power measurement and SWS simulation results for event 3. The graphs show the deviation from the initial value.

5.4.3. Validation using Hybrid Dynamic Simulation

The first step in the Hybrid Dynamic Simulation process, is to isolate the Zeeland subnetwork from the rest of the model. This was already done for the simulation of event 1. The next step is to adjust the initial conditions in the subnetwork based on the measurement data in GEN eBase. Again, the reactive power dispatch of the generators were adjusted by adjusting the transformer winding ratios, and by adjusting the terminal voltage of the generators. Table 5.11 shows the adjustment results for the generators and Table 5.12 shows the voltage at selected substations. The voltage at BSL380 was adjusted based on the PMU measurement, not the GEN eBase measurement. Lastly a boundary load was attached in parallel with the Playback generator to precisely match the active and reactive power with the measurement. The boundary load consumes 1.9 MW and -50.6 Mvar.

With the subnetwork setup and PLB file prepared, a Hybrid Dynamic Simulation was run.

Table 5.11: Comparison of HDS model active and reactive power with GEN eBase measurements for event 3.

PQUt	GEN eBase		Model		
Unit	P	Q	P	Q	Ut
SL20	231	-150	231	-149	0.998
TZE11G1	111	17	111	14	1.037
TZE11G2	112	11	122	5	1.030
TZE11S1	28	-5	28	3	0.995

Table 5.12: Comparison of HDS model voltages with GEN eBase measurements for event 3.

	GEN eBase	Model
Substation	V [pu]	V [pu]
BSL380	1.079	1.076
BSL150	1.045	1.048
TZN150	1.046	1.047

Validation results

Figure 5.20a and Figure 5.20b show a comparison between the measured and simulated voltage and frequency at the Borssele substation. The figures show an offset between the measurement and the simulation result. Offsets in the playback measurements are removed as show in Figure 4.1a and Figure 4.1b. The offset do not affect the Hybrid Dynamic Simulation process.

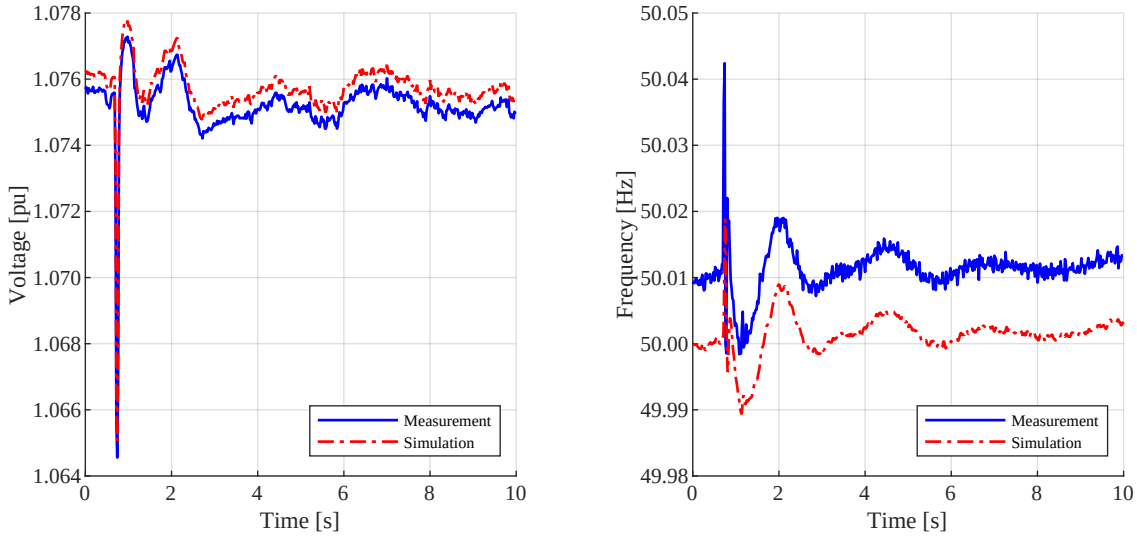

(a) Positive sequence voltage magnitude

(b) Frequency

Figure 5.20: Comparison of voltage and frequency measurement and HDS simulation results for event 3.

Figure 5.21 shows a comparison between the simulated and measured power flowing from the Borssele substation. While the power oscillation is relatively small, the simulation result shows a decent match with the measurement. As with the results for event 1 however, the simulation result seems to be lagging the measurement result. At this moment it is unclear whether the lag is caused by a model inaccuracy, or by the Hybrid Dynamic Simulation process.

Figure 5.22 shows the comparison for the reactive power flowing from the Borssele substation. The measured reactive power response is quite different from the simulated response. It should be noted however that the response that was measured is relatively small, while the reactive powerflow is usually not very stable. The response in the measurement might therefore largely be determined by background phenomena.

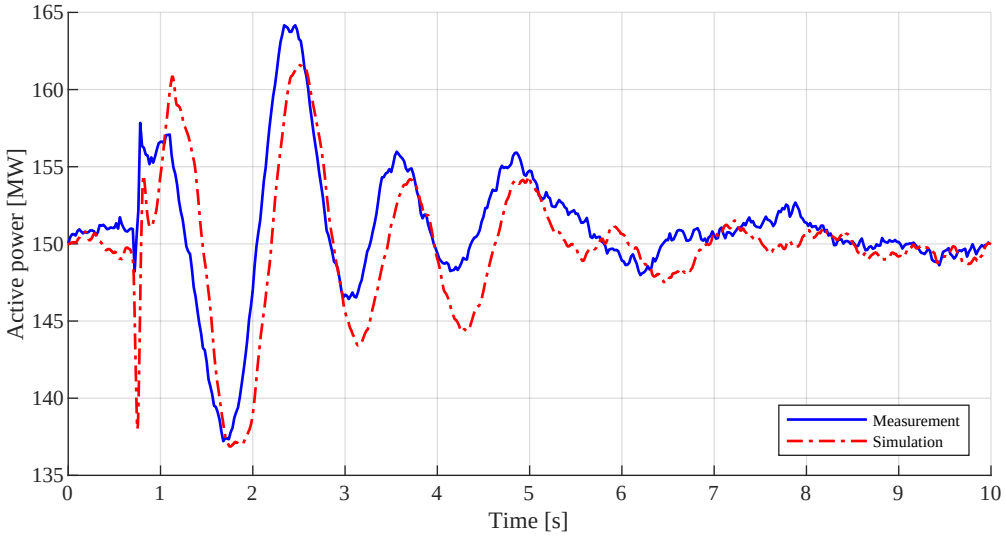

Figure 5.21: Comparison of active power measurement and HDS simulation result for event 3.

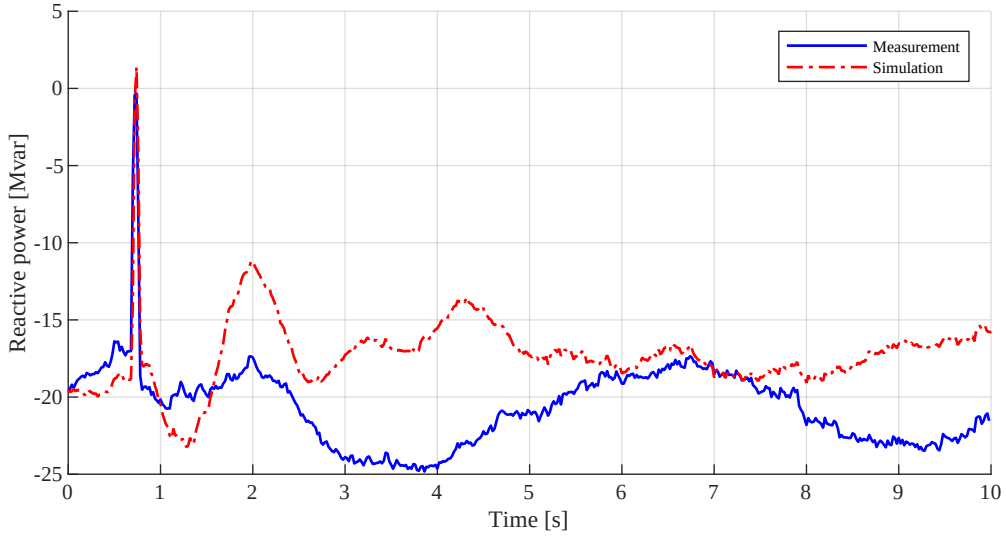

Figure 5.22: Comparison of reactive power measurement and HDS simulation result for event 3.

Figure 5.23 shows the contributions of the individual generators to the power oscillation. The Figure shows that the combined TZE generators have a larger contribution to the power oscillation than the SL20 generator, while the total power dispatch is similar. (See Table 5.11.) This could be explained by the fact that the TZE11G1 and TZE11G2 generators operate close to their maximum rated power which deteriorates their stability.

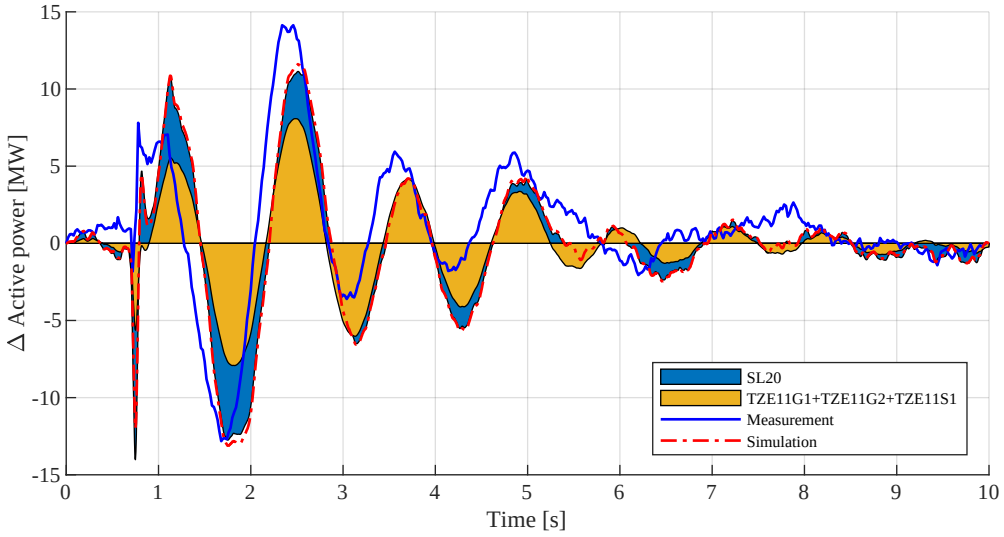

Figure 5.23: Comparison of active power measurement and HDS simulation result for event 3. Including contributions of the different generating units. Graphs show deviations from the initial value. Contributions were plotted by overlapping the graphs; *SL20* includes the contribution of all generators, *TZE11G1+TZE11G2+TZE11S1* shows the respons excluding SL20.

5.5. Comparing SWS and HDS simulation results

Figure 5.24 shows a comparison of the simulation results obtained with the System Wide Simulation method and the Hybrid Dynamic Simulation method. Figure 5.24a shows the comparison for event 1 and figure 5.24b shows the comparison for event 3. No comparison is made for event 2 as the Hybrid Dynamic Simulation method could not be performed for event 2. The figures show the power flowing from the Borssele substation. For the measurement and the System Wide Simulation, this result was obtained by summing the power flows in circuit BSL-GT380 and circuit BSL-ZVL380. The comparison is limited to the power flow at Borssele as this was the only location where Hybrid Dynamic Simulation could be performed. Figure 5.25 shows a more detailed comparison of the simulated behaviour of individual generators during event 1. Figure 5.25 only compares simulation results, as measurements are not available for the individual generators.

The figures show that higher damping is observed in the System Wide Simulation as compared to the Hybrid Dynamic Simulation. The damping in the Hybrid Dynamic Simulation seems to be more aligned with the damping that was observed in the measurements. Figure 5.24 consistently shows higher damping for the System Wide Simulation results. The fact that the damping seems relatively accurate in the Hybrid Dynamic Simulation approach indicates that the damping inaccuracy does not necessarily stem from the Zeeland subnetwork. Other parts of the dynamic model could be responsible.

From the figures it can further be concluded that both simulation methods lead to quite different simulation results. This raises the question which of the simulation methods leads to a more accurate result. Generally speaking, the results from the Hybrid Dynamic Simulation should be more trustworthy than the results from the System Wide Simulation. As the Hybrid Dynamic Simulation deals with a smaller subnetwork, pre-disturbance operating conditions can be better approached in the model. Furthermore less uncertainties are introduced by the simulation of the disturbance, as a recording of the disturbance is directly played back into the simulation.

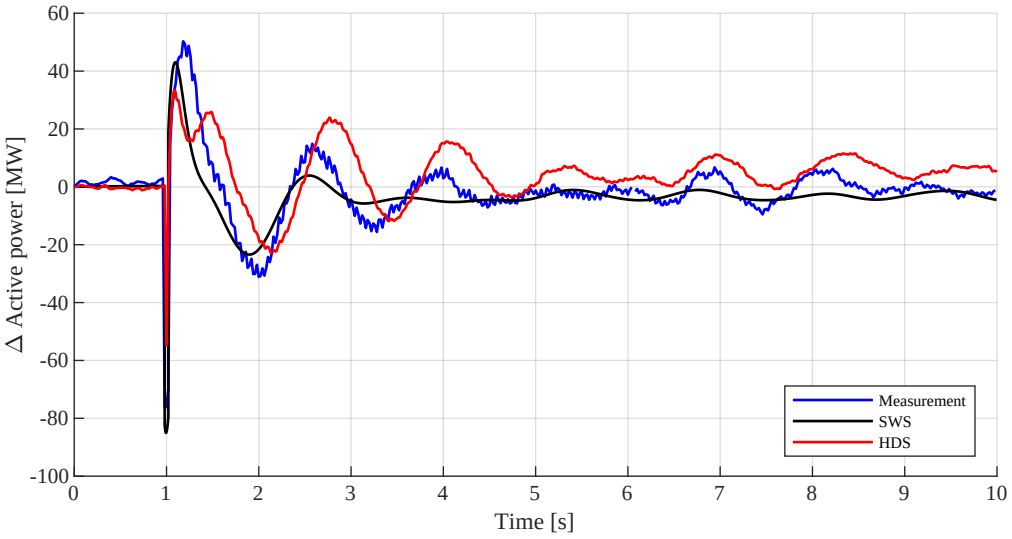

(a) Event 1

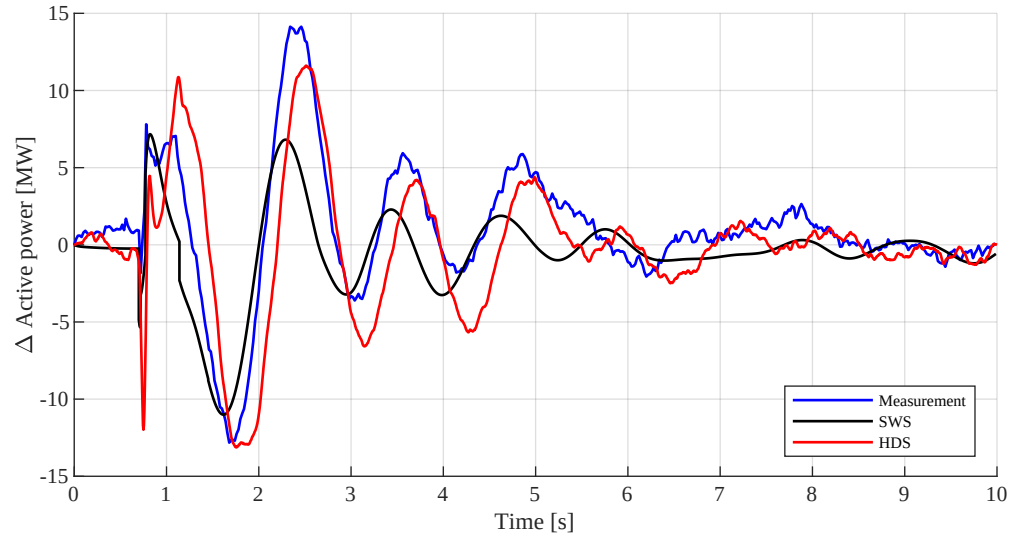

(b) Event 3

Figure 5.24: Comparison of the simulation results obtained with the System Wide Simulation method and the Hybrid Dynamic Simulation method. The graphs show the total power flowing from the Borssele substation. The graphs show the deviation from the initial value.

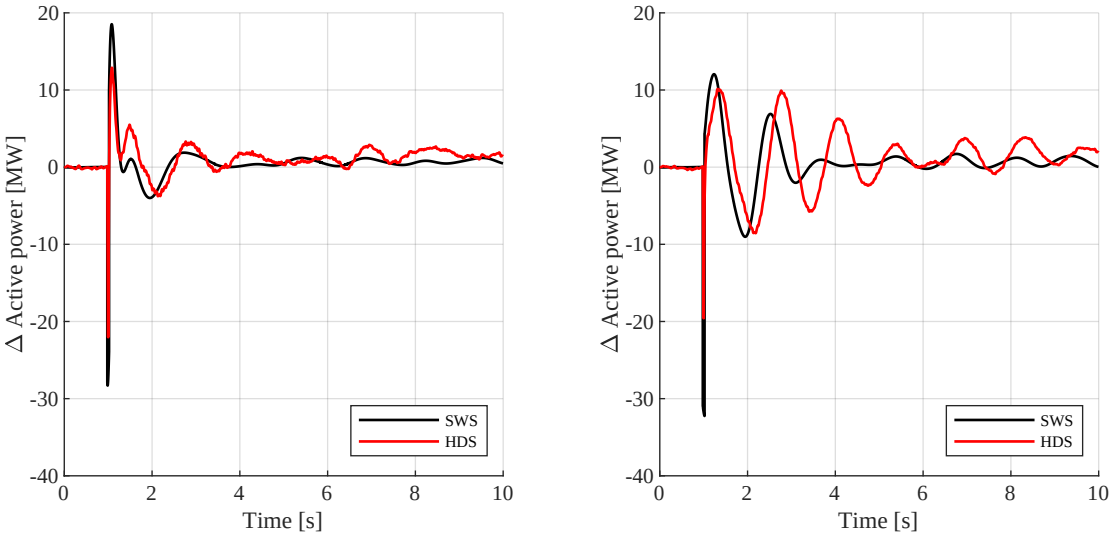

(a) SL10

(b) BS30

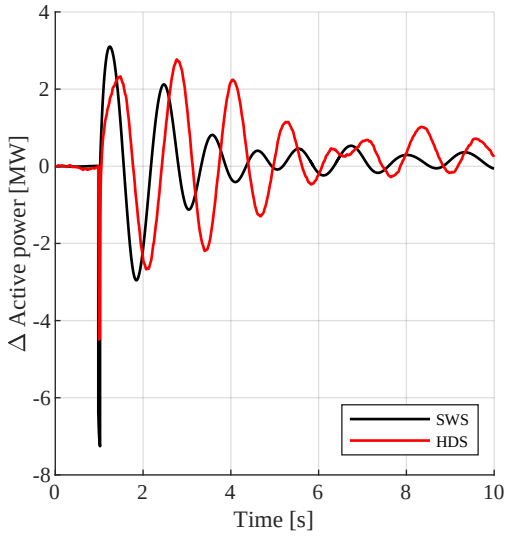

(c) TZE11G1

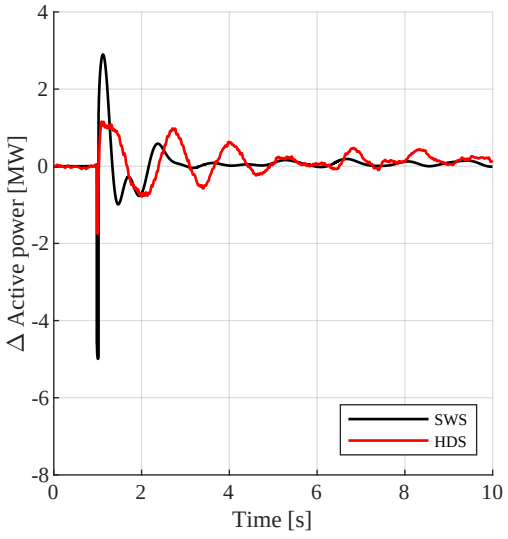

(d) TZE11S1

Figure 5.25: Detailed comparison of the simulated behaviour of individual generators during event 1, with the System Wide Simulation method (SWS) and the Hybrid Dynamic Simulation method (HDS). The graphs show the deviation from the initial value.

5.5.1. Sensitivity of Hybrid Dynamic Simulation to measurement inaccuracies.

Uncertainties that the Hybrid Dynamic Simulation process does suffer from, are uncertainties resulting from inaccurate measurements during fast phenomena like a short circuit. In order to gain some insight into the sensitivity of Hybrid Dynamic Simulation to measurement inaccuracies during a short circuit, simulations were run with altered measurement playback files. For this, the Hybrid Dynamic Simulation of event 3 was used as a base case. The playback file was altered for the measurement points during the measured fault, as these measurement points might not be accurate. Table 5.13 describes the alterations that were made in the playback files. Figure 5.26 shows the voltage and frequency signals in the altered playback files.

Table 5.13: Altered playback files for Hybrid Dynamic Simulation

Playback file	Variable	Description of the alteration
PLBFILE1	-	No alteration, original measurements used.
PLBFILE2	Voltage	Wider voltage drop during short circuit.
PLBFILE3	Voltage	Deeper voltage drop during short circuit.
PLBFILE4	Frequency	Larger frequency deviation during short circuit.
PLBFILE5	Frequency	No frequency deviation during short circuit.

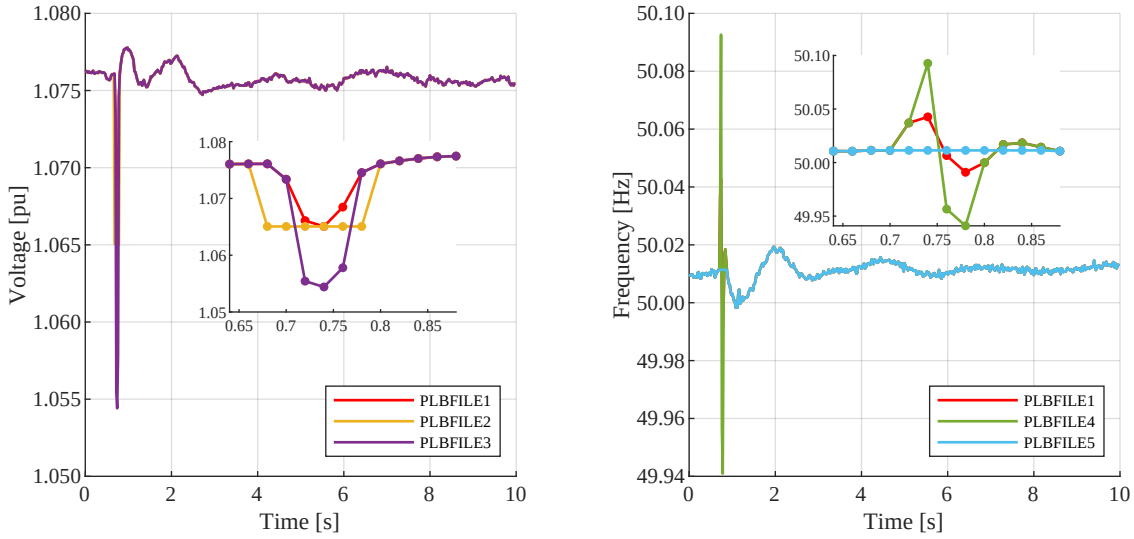

(a) Voltage alterations

(b) Frequency alterations

Figure 5.26: Voltage and frequency signals in altered playback files used to check Hybrid Dynamic Simulation sensitivity to measurement inaccuracies during a short circuit.

Figure 5.27 shows the simulated active power flowing from the Borssele substation for Hybrid Dynamic Simulations with the altered playback files. The measurements taken during event 3 are also included in the figure as a reference. The figure shows that the alterations in the playback file has a significant impact on the simulation during and shortly after the fault. While the general shape of the simulation result during the fault remains similar, the alteration affect the amplitude of the peaks and valleys during the fault. After the fault however, the different simulations are converging towards the same result.

Based on these results it can be concluded that potential measurement inaccuracies during fast phenomena like a short circuit with a short duration, will not greatly affect the overall Hybrid Dynamic Simulation results. Care should be taken when comparing measurements and simulation results during and shortly after the short circuit. However, after about two seconds, a fault measurement inaccuracy will hardly have an effect on the subsequent simulation. One thing to note is that this might not hold true when generators are operating close to their stability limit. In this case, the model response might be more sensitive to the severity of the short circuit that is played back.

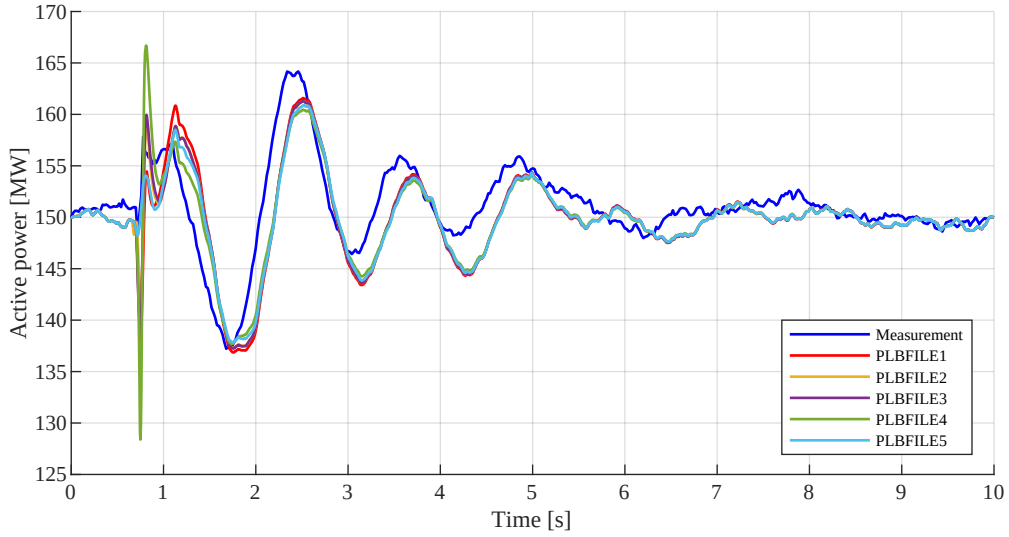

Figure 5.27: Active power flowing from the Borssele substation as simulated using Hybrid Dynamic Simulation with altered playback files. The measurement of event 3 is included for reference.

6

Conclusions and recommendations

6.1. Conclusions

The sections below summarize the answers to the three main research questions.

6.1.1. What type of disturbances are suitable for model validation?

Although not an exhaustive list, disturbances that will cause dynamic behaviour in the power system include short circuits, a sudden power unbalance caused by loss of generation or loss of an HVDC interconnector and topological changes such as line switching. Short circuits however, most often affect just a single phase. Single-phase faults cannot directly be simulated in PSS/E, the simulation tool that is used at TenneT for dynamic studies, as it exclusively performs positive sequence simulations.

A method was introduced for the simulation of single-phase faults and single-phase line tripping in a positive sequence simulation tool. It was demonstrated that the same simulation result can be obtained with a three-phase fault as with a single-phase fault. For this, the fault impedance of the three-phase fault was increased and tuned in such a way so that the positive sequence voltage drop during the three-phase fault matched the positive sequence voltage drop during the single-phase fault. This approach could be used to simulated a measured single-phase fault by adjusting the fault impedance a three-phase fault until the simulated positive sequence voltage drop matches the measured positive sequence voltage drop.

Similarly, the single-phase tripping can be simulated symmetrically by switching off the three phases whilst simultaneously switching on a fictional parallel line with an increased impedance. Again, the impedance of the fictional line was tuned in such a way so that the positive sequence voltage drops or peaks during the tripping match the results from the single-phase tripping.

The method for simulating a single-phase short circuit in a positive sequence simulation tool was put in practice with the System Wide Simulation of short circuit events. It was however found, that it was not possible to match the measured voltage drop in two (distant) locations simultaneously. It is unclear what the underlying cause for this is. A possible explanation is that the PMU measurement of the voltage drop is not accurate. As the short circuit is cleared very rapidly, the voltage drop may only be covered by one measurement point. Another explanation could be that the network model is inaccurate. Possibly due to inaccurate parameters, or a network topology that is different from the situation during the measurement.

While (single-phase) short circuits occur far more frequently than loss of generation or an HVDC interconnector, they are less suitable as disturbances for model validation using System Wide Simulation. It is difficult to accurately represent a short circuit in the simulation, while the system response in the System Wide Simulation is largely determined by the short circuit. For Hybrid Dynamic Simulation this was shown to be less of a problem. Inaccuracies in measurements during a short circuit were shown not to have a dominant effect on the overall response of the subsystem during the simulation.

Simulation of loss of generation or an HVDC interconnector is a lot more straightforward as compared to a short circuit, and should therefore lead to more accurate results. However, as they occur less frequently, they require more time for measurement data to be gathered. Or in other words, model validation can be performed less frequently.

A switching event can be suitable for System Wide Simulation, if the event occurred close to a measurement location. Otherwise the event will result in a relatively small system response, making it difficult to discern the system response from the background behaviour in the measurement.

It should be noted that a disturbance might not occur as a single event. As was shown with the case studies, loss of generation or tripping of an HVDC interconnector can be the result of a short circuit.

6.1.2. How can the measurement and simulation results be compared?

Frequency, voltage magnitude, voltage angle difference, active power and reactive power are signals that can be measured or calculated using PMUs and reflect the electromechanical behaviour of a power system. As the TenneT Dynamic Model is focused on rotor-angle stability and voltage stability, the frequency behaviour will not correctly be represented, and is thus not a relevant signal for comparison. Voltage angle difference between two distant substations gives a general indication of power flows in a system and the loading of the system. For comparison of measurement and simulation results it is however too general, containing little information about individual components.

Voltage magnitude, active power and reactive power signals are used for comparison between measurements and simulation results. Due to the strong connection between rotor-angle and active power output of a generator, the active power is a good indicator for rotor-angle stability. On the other hand, voltage magnitude and reactive power are important variables for voltage stability.

Measurement and simulation results can be compared both qualitatively and quantitatively. Qualitative comparison looks at similarities between the measured system response and the simulated system response. Broad conclusions about the validity of a model can be drawn based on qualitative comparison. For model parameter calibration however, quantitative comparison would required. This project was limited to qualitative comparison as the results from System Wide Simulation are not suitable for quantitative methods such as Root Mean Square Error.

6.1.3. How does model validation using System Wide Simulation compare to validation using Hybrid Dynamic Simulation?

Implementations for the System Wide Simulation method and the Hybrid Dynamic Simulation method were outlined in Chapter 3 and Chapter 4 respectively. With the System Wide Simulation approach, a simulation is performed with the complete dynamic model. In order to compare the measurement and simulation results, the measured disturbance must be reproduced in the simulation. For this, the pre-disturbance operating conditions of the system should be set up in the model. Then, the disturbance should be reproduced in the simulation.

Uncertainties are introduced in the simulation results when System Wide Simulation is performed. Generally speaking, two factors contribute to the simulation inaccuracy:

- Firstly, inaccuracies are introduced by poor representation of the pre-disturbance operating conditions of the power system in the model. Accurately setting up the initial conditions in a large model is a lengthy and complicated task. Trade-offs had to be made with a focus on active and reactive power dispatch of the generators. This at the expense of the voltage at the substations. Also, the adjustment of the initial conditions was limited to the generators near the PMU locations.

- Secondly, inaccuracies are introduced by poor representation of the disturbance in the simulation. As mentioned in Section 6.1.1, short circuits are are difficult to accurately represent in the simulation, while the response of the system is largely determined by the short circuit. The accuracy of the simulation of a short circuit might be improved if more measurement locations are introduced. Another option would be to avoid short circuits as disturbance events for System Wide Simulation and instead use disturbances like loss of generation, or line switching.

With System Wide Simulation, voltage magnitude, active power and reactive power measurements can be compared with the simulation results. However, as the initial conditions can be quite different in the measurements as compared to the simulation, the simulation results will often show a (large) offset with respect to the measurement results. This makes the results difficult to compare. In order to mitigate this problem, comparison was not done directly, but on the deviation of the results with respect to the initial value. Both results were first offset to zero before the were compared.

With the Hybrid Dynamic Simulation approach, part of the dynamic model is first isolated. At the boundary of the isolated subnetwork, a playback model is set up in order to play back measured voltage and frequency signals. Again the model should be adjusted to reflect the pre-dsturbance operating conditions.

Hybrid Dynamic Simulation suffers from similar inaccuracies as System Wide Simulation, however to a much lesser extent. As Hybrid Dynamic Simulation is performed in a (small) subnetwork, it is easier to accurately adjust the model to the pre-disturbance operating conditions. Accuracy of the initial conditions might be further improved by reducing the size of the subnetwork. This would also make a parameter calibration process easier.

Hybrid Dynamic Simulation also suffers less from poor representation of the disturbance in the simulation. For one, the measurement of the disturbance is directly played back at the boundary of the subnetwork. And, it was also demonstrated that an inaccuracy in the measurement of a short circuit does not have a dominant effect on the overall response of the subsystem in the simulation.

As the initial conditions in the subnetwork can be relatively accurately represented, the measurement and simulation results can be directly compared. There is no need to first offset the measurement and simulation results. For Hybrid Dynamic Simulation, active power and reactive power measurements can be compared with the simulation results. As the frequency and voltage measurements are played into the model, they offer no useful comparison.

Overall, the process of Hybrid Dynamic Simulation is a lot more straightforward than the process of System Wide Simulation. The results from Hybrid Dynamic Simulation will be more accurate than the results from System Wide Simulation.

Both approaches could be used complementary. The System Wide Simulation approach has potential to be used to gain some general insights into the model validity based on qualitative measures. The results will give an indication of shortcomings in the model. However, due to the uncertainties introduced with this approach, it is less suitable for model calibration. With System Wide Simulation it would be difficult to distinguish whether discrepancies are stemming from inaccuracies in the model or inaccuracies that are the result from the simulation approach.

For model calibration, Hybrid Dynamic Simulation, can be used. Hybrid Dynamic Simulation will result in more accurate results that might be used for quantitative comparison in a model parameter optimization process. For Hybrid Dynamic Simulation however, PMUs need to be installed in specific locations. Without the measurements at the right location, Hybrid dynamic Simulation cannot be performed. Results from model validation using System Wide Simulation can point out where the model needs improvement. This information can be used for the placement of PMUs for Hybrid Dynamic Simulation.

An important thing to bear in mind is that the events that were used to test the validation methods, did not always cause a large dynamic response in the model. This can make the comparison of measurement and simulation results difficult as it becomes harder to distinguish the response to the disturbance from the response to other background events occurring in the power system. The power system is constantly perturbed by large and small disturbances. Given more time, more measurement data can be collected, and disturbances might be recorded that are more suitable for model validation.

6.2. Recommendations

Below some recommendations are given for future research and improvement of the validation process.

- This project focused on the comparison of the System Wide Simulation approach to model validation and the Hybrid dynamic Simulation approach to model validation. Further research is required into the process of model calibration with Hybrid Dynamic Simulation. For this however, first additional PMUs need to be installed in the Dutch power grid. Questions might include:
  - Which quantitative comparison method is best used for model calibration using Hybrid Dynamic Simulation?
  - Which algorithms can be used in order to optimize the model parameters?
- System Wide Simulation might be improved with a better process for setting up the pre-disturbance operating conditions of the model. For this, it would be helpful if the dynamic model and the system operation model in the EMS show more accordance. Furthermore, in [18] it was mentioned that a more detailed EMS snapshot was used which includes exact topology data. Such a snapshot would be helpful

for accurately setting up the pre-disturbance operating conditions in the model. Also, efforts might be taken to further automate the process of setting the pre-disturbance operating conditions.

- Currently, disturbance events were mostly discovered through disturbance reports. These reports however, are only written for short circuit events. PhasorPoint provides tools to raise alarms when a disturbance occurs in the power system. This can be a valuable source of information for identifying disturbances that are suitable for model validation and calibration. At the moment however, PhasorPoint generates too many alarms, making it difficult to distinguish relevant events.
- With the inclusion of the entire grid of continental Europe in the TenneT Dynamic Model, both dynamic simulations and model validation are complicated tasks. As the TenneT Dynamic Model is mainly used for rotor angle stability and voltage stability studies, which are generally local phenomena, the question arises whether the inclusion of the European grid is of any benefit to the dynamic studies. Similar simulation results might be achieved with a more simplified power grid at the borders of the Dutch power grid. This would make the model easier to handle, and simulations run more quickly.
- Additional PMUs are required in the Dutch power grid in order to properly perform model validation. If strategically placed, Hybrid Dynamic Simulation can be performed in more locations. As Figure A.2 in Appendix A shows, many generating units in the Netherlands are connected to EHV busses that are part of a ring network. This means that it would require at least 4 PMUs to isolate that substation from the rest of the power grid. Generally speaking, it would then require less PMUs to measure the generating units directly.

A

Overview of the Dutch High Voltage grid

Figure A.1: Map of the Dutch power grid, retrieved from tennet.eu.

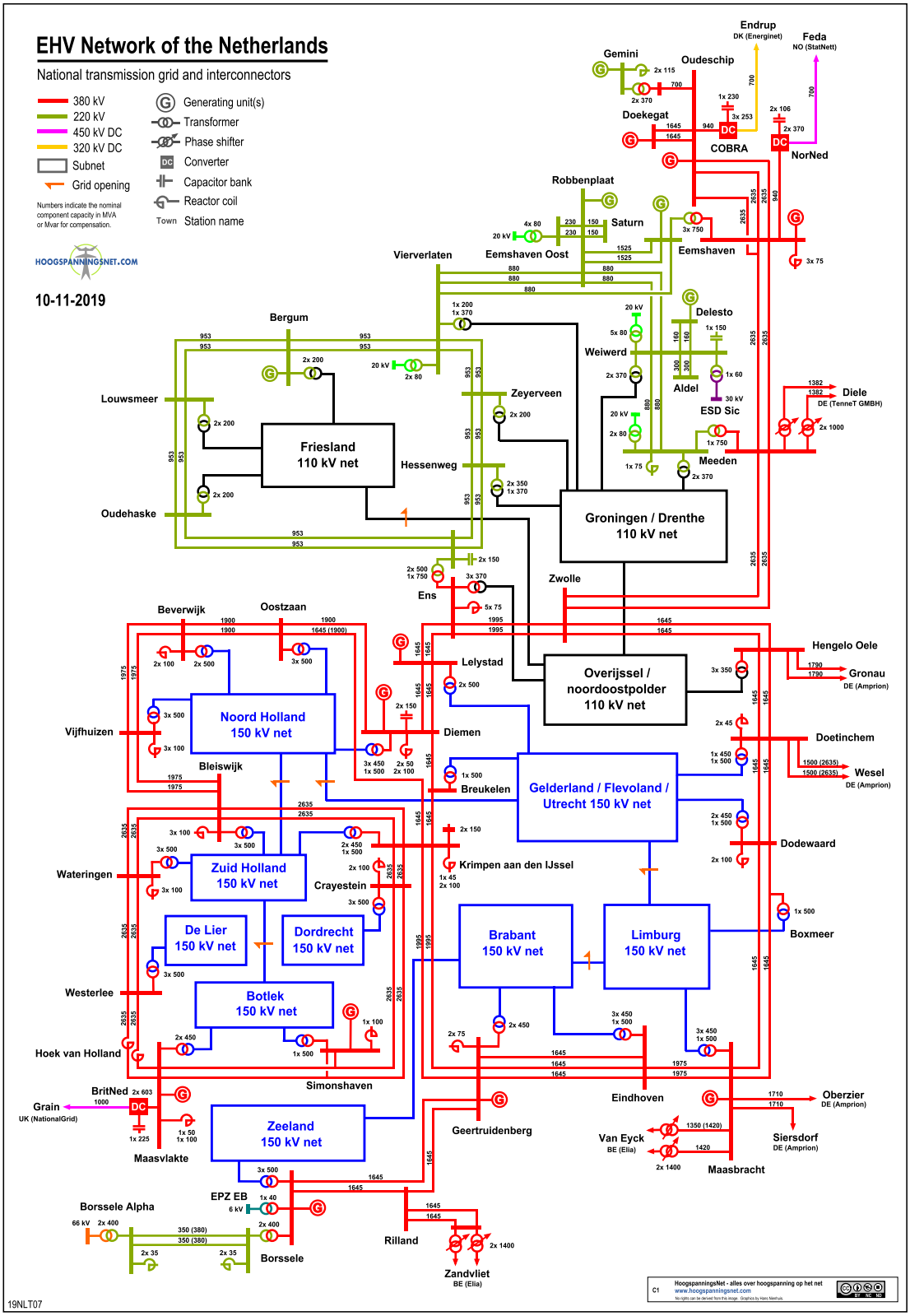

Figure A.2: Schematic of the Dutch Extra High Voltage grid, retrieved from hoogspanningsnet.com.

B

Single Machine Infinite Bus test system

Figure B.1 shows a single-line diagram of the Single Machine Infinite Bus test system. Various test simulations were run using this basic test system, containing a synchronous generator connected to an infinite bus through a transformer and two transmission lines. The tables below contain details about the model parameters. During the simulation, the synchronous generator was operating at an active power dispatch of 350 MW.

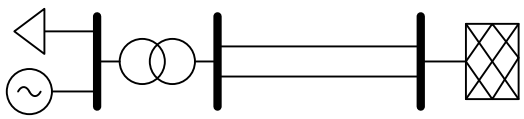

Figure B.1: Diagram of the Single Machine Infinite Bus test system.

Table B.1: Machine transformer parameters

Parameter	Value	Unit
Rated power	555	MVA
Rated voltage HV-side	380	kV
Rated voltage LV-side	21	kV
Resistance R_1	0	pu
Reactance X_1	0.028829	pu
Short-circuit voltage uk0	3	%
Short-circuit voltage uk0r	0	%

Table B.2: Line parameters

Parameter	Value	Unit
Rated voltage	380	kV
Rated current	1	kA
Line length	50	km
AC-Resistance $R_{1,2}$	0.1058	Ω/km
Reactance $X_{1,2}$	1.058	Ω/km
AC-Resistance R_0	0.4232	Ω/km
Reactance X_0	3.174	Ω/km

Table B.3: Parameters for generator dynamic model GENROU (PowerFactory model: Standard)

Parameter description	Symbol	Value	Unit
Rated apparent power	$MBASE$	524	MVA
d-axis open circuit transient time constant	T'_{d0}	6.3903	s
d-axis open circuit sub-transient time constant	T''_{d0}	0.0376	s
q-axis open circuit transient time constant	T'_{q0}	1.9975	s
q-axis open circuit sub-transient time constant	T''_{q0}	0.2345	s
Inertia	H	7.53	$MW.s/MVA$
Speed damping	D	40	pu
d-axis synchronous reactance	X_d	2.417	pu
q-axis synchronous reactance	X_q	2.296	pu
d-axis transient reactance	X'_d	0.278	pu
q-axis transient reactance	X'_q	0.746	pu
sub-transient reactance	$X''_d = X''_q$	0.222	pu
Leakage reactance	X_l	0.174	pu
Saturation factor at 1.0 pu voltage	$S(1.0)$	0.2273	-
Saturation factor at 1.2 pu voltage	$S(1.2)$	0.6981	-

Table B.4: Parameters for excitation system dynamic model ESST1A

Parameter description	Symbol	Value	Unit
Measurement delay	T_R	0.012	s
Maximum voltage regulator input limit	$V_{I,max}$	999	pu
Minimum voltage regulator input limit	$V_{I,min}$	-999	pu
Voltage regulator time constant	T_C	1	s
Voltage regulator time constant	T_B	6.378	s
Voltage regulator time constant	T_{C1}	0	s
Voltage regulator time constant	T_{B1}	0	s
Voltage regulator gain	K_A	400	pu
Voltage regulator time constant	T_A	0	s
Maximum voltage regulator output	$V_{A,max}$	6.2951	pu
Minimum voltage regulator output	$V_{A,min}$	-5.0361	pu
Maximum voltage regulator output	$V_{R,max}$	6.2951	pu
Minimum voltage regulator output	$V_{R,min}$	-5.0361	pu
Rectifier loading factor	K_C	0	pu
Excitation system stabiliser gain	K_F	0	pu
Excitation system stabiliser time constant	T_F	1	s
Exciter output current limiter gain	K_{LR}	0	pu
Exciter output current limiter reference	I_{LR}	0	pu

Table B.5: Parameters for turbine governor dynamic model GGOV1

Parameter description	Symbol	Value	Unit
Permanent Droop	R	0.1	pu
Electrical Power Transducer time constant	T_{pelec}	1	s
Maximum Speed Error Signal	$maxerr$	0.05	pu
Minimum Speed Error signal	$minerr$	-0.05	pu
Governor Proportional gain	$K_{p,gov}$	20	pu
Governor Integral Gain	$K_{i,gov}$	2	pu
Governor Derivative Gain	$K_{d,gov}$	0	pu
Governor Derivative Controller Time Constant	$T_{d,gov}$	1	s
Maximum Valve Position Limit	V_{max}	1	pu
Minimum Valve Position Limit	V_{min}	0	pu
Actuator Time Constant	T_{act}	0.5	s
Turbine Gain	K_{turb}	1	pu
No Load Fuel Flow	W_{fnl}	0.01	pu
Turbine Lag Time Constant	T_b	10	s
Turbine Lead Time Constant	T_c	3	s
Diesel Engine Transport Time Constant	T_{eng}	0	s
Load Limiter Time Constant	$T_{f,load}$	1	s
Load Limiter Proportional Gain	$K_{p,load}$	0.5	pu
Load Limiter Integral Gain	$K_{i,load,}$	0.2	pu
Load Limiter Reference Value	$L_{d,ref}$	1	pu
Mechanical Damping Coefficient	D_m	0	pu
Maximum Valve Opening Rate	R_{open}	0.1	pu/s
Maximum Valve Closing Rate	R_{close}	-1	pu/s
Power Controller Reset Gain	$K_{i,mw}$	0	pu
Acceleration Limiter Setpoint	A_{set}	0.1	pu/s
Acceleration Limiter Gain	K_a	1	pu/s
Acceleration Limiter Time Constant	T_a	0.1	s
Turbine Rated Power	T_{rate}	457	MW
Speed Governor Deadband	db	0	pu
Temperature Detection Lead Time Constant	T_{sa}	1	s
Temperature Detection Lag Time Constant	T_{sb}	10	s
Maximum Rate of Load Limit Increase	R_{up}	99	pu/s
Maximum Rate of Load Limit Decrease	R_{down}	-99	pu/s
Governor Droop Feedback Signal Selector	R_{select}	1	–
Switch for Fuel Source Characteristic	Flag	0	–

Table B.6: Parameters for stabiliser dynamic model PSS2A

Parameter description	Symbol	Value	Unit
1st Washout 1th Time Constant	T_{w1}	0.6	s
1st Washout 2th Time Constant	T_{w2}	4	s
1st Signal Transducer Time Constant	T_6	0	s
2nd Washout 1th Time Constant	T_{w3}	0.6	s
2nd Washout 2th Time Constant	T_{w4}	4	s
2nd Signal Transducer Time Constant	T_7	0	s
2nd Signal Transducer Factor	K_{s2}	-0.00004	pu
Washouts Coupling Factor	K_{s3}	1000	pu
Ramp Tracking Filter Deriv. Time Constant	T_8	1.7175	s
Ramp Tracking Filter Delay Time Constant	T_9	1.9505	s
PSS Gain	K_{s1}	15.5086	pu
1st Lead-Lag Derivative Time Constant	T_{s1}	0.0014	s
1st Lead-Lag Delay Time Constant	T_{s2}	0.0492	s
2nd Lead-Lag Derivative Time Constant	T_{s3}	1.7175	s
2nd Lead-Lag Delay Time Constant	T_{s4}	1.9505	s
Controller Minimum Output	$V_{st,min}$	-0.1	pu
Controller Maximum Output	$V_{st,max}$	0.1	pu
Derivator Factor	K_d	0.01	pu
1st Input Selector	I_{c1}	1	–
2nd Input Selector	I_{c2}	3	–
Ramp Tracking Filter	M	1	–
Ramp Tracking Filter	N	1	–
PSS base selector	IPB	1	–

C

2 Area 4 Generators test system

Figure C.1 shows a single-line diagram of the 2 Area 4 Generators test system. Various test simulations were run using this basic test system. The system is based on the 2 Area 4 Generator system as described in [21] in example 12.6. The system contains 4 synchronous generators interconnected by two long transmission lines. The tables below contain details about the model parameters.

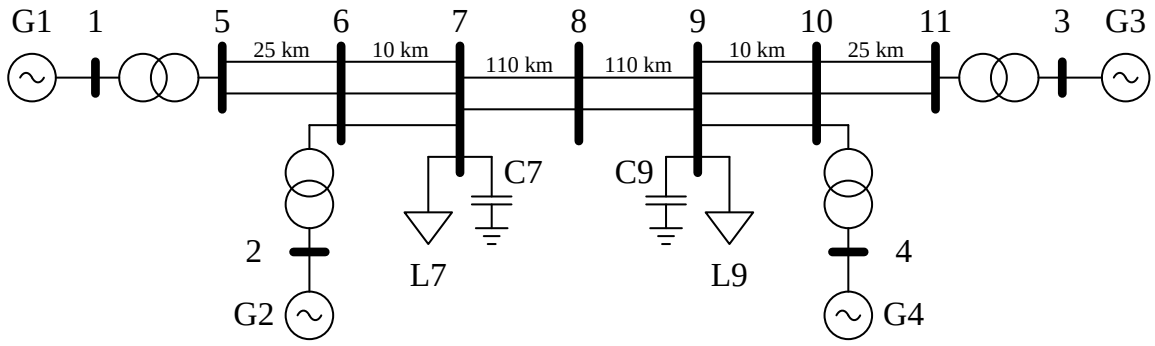

Figure C.1: Diagram of the 2 area 4 generator test system.

Table C.1: Power dispatch

Parameter	G1	G2	G3 (swing)	G4	L7	L9	C7	C9	Unit
Rated power	900	900	900	900	-	-	500	350	MVA
Active power	700	700	716	700	967	1767	-	-	MW
Reactive power	103	34	170	186	100	100	−521	−334	$Mvar$

Table C.2: Machine transformer parameters

Parameter	Value	Unit
Rated power	900	MVA
Rated voltage HV-side	230	kV
Rated voltage LV-side	20	kV
Reactance x1	0.15	pu
Resistance r1	0	pu
Short-circuit voltage uk0	3	%
Short-circuit voltage uk0r	0	%

Table C.3: Line parameters

Parameter	Lines 5-6 / 10-11	Lines 6-7 / 9-10	Lines 7-8 / 8-9	Unit
Rated voltage	230	230	230	kV
Rated current	1	1	1	kA
Line length	25	10	110	km
AC-Resistance $R_{1,2}$	0.1058	0.1587	0.0529	Ω/km
Reactance $X_{1,2}$	1.058	1.587	0.529	Ω/km
AC-Resistance R_0	0.4232	0.6384	0.2116	Ω/km
Reactance X_0	3.174	4.761	1.587	Ω/km

Table C.4: Parameters for generator dynamic model GENROU (PowerFactory model: Standard)

Parameter description	Symbol	Gen 1 + 2	Gen 3 + 4	Unit
Rated apparent power	$MBASE$	900	900	MVA
d-axis open circuit transient time constant	T'_{d0}	8	8	s
d-axis open circuit sub-transient time constant	T''_{d0}	0.03	0.03	s
q-axis open circuit transient time constant	T'_{q0}	0.4	0.4	s
q-axis open circuit sub-transient time constant	T''_{q0}	0.05	0.05	s
Inertia	H	6.5	6.175	$MW.s/MVA$
Speed damping	D	0	0	pu
d-axis synchronous reactance	X_d	1.8	1.8	pu
q-axis synchronous reactance	X_q	1.7	1.7	pu
d-axis transient reactance	X'_d	0.3	0.3	pu
q-axis transient reactance	X'_q	0.55	0.55	pu
sub-transient reactance	$X''_d = X''_q$	0.25	0.25	pu
Leakage reactance	X_l	0.172	0.172	pu
Saturation factor at 1.0 pu voltage	$S(1.0)$	0.0392	0.0392	-
Saturation factor at 1.2 pu voltage	$S(1.2)$	0.2672	0.2672	-

Table C.5: Parameters for excitation system dynamic model SEXS

Parameter description	Symbol	Value	Unit
Filter Derivative Time Constant	T_a	0.3	s
Filter Delay Time	T_b	10	s
Controller Gain	K	100	pu
Exciter Time Constant	T_e	0.05	s
Controller Minimum Output	E_{min}	0	pu
Controller Maximum Output	E_{max}	4	pu

Table C.6: Parameters for turbine governor dynamic model TGOV1

Parameter description	Symbol	Value	Unit
Controller Droop	R	0.3579	pu
Governor Time Constant	T_1	0.5	s
Maximum Gate Limit	V_{max}	1	pu
Minimum Gate Limit	V_{min}	0	pu
Turbine Derivative Time Constant	T_2	6	pu
Turbine Delay Time Constant	T_3	14	pu
Frictional Losses Factor	D_T	0	pu
Turbine power coefficient	A_t	1	pu

Table C.7: Parameters for stabiliser dynamic model PSS2A

Parameter description	Symbol	Value	Unit
1st Washout 1th Time Constant	T_{w1}	2	s
1st Washout 2th Time Constant	T_{w2}	2	s
1st Signal Transducer Time Constant	T_6	0	s
2nd Washout 1th Time Constant	T_{w3}	2	s
2nd Washout 2th Time Constant	T_{w4}	0	s
2nd Signal Transducer Time Constant	T_7	2	s
2nd Signal Transducer Factor	K_{s2}	0.1564	pu
Washouts Coupling Factor	K_{s3}	1	pu
Ramp Tracking Filter Deriv. Time Constant	T_8	0.5	s
Ramp Tracking Filter Delay Time Constant	T_9	0.1	s
PSS Gain	K_{s1}	5	pu
1st Lead-Lag Derivative Time Constant	T_{s1}	0.25	s
1st Lead-Lag Delay Time Constant	T_{s2}	0.03	s
2nd Lead-Lag Derivative Time Constant	T_{s3}	0.15	s
2nd Lead-Lag Delay Time Constant	T_{s4}	0.015	s
Controller Minimum Output	$V_{st,min}$	-0.1	pu
Controller Maximum Output	$V_{st,max}$	0.1	pu
Derivator Factor	K_d	0.01	pu
1st Input Selector	I_{c1}	1	$-$
2nd Input Selector	I_{c2}	3	$-$
Ramp Tracking Filter	M	0	$-$
Ramp Tracking Filter	N	0	$-$
PSS base selector	IPB	1	$-$

Bibliography

[1] IEC/IEEE 60255-118-1:2018. Measuring relays and protection equipment - part 118-1: Synchrophasor for power systems - measurements. Standard, IEC/IEEE, Dec 2018.

[2] J. Bos. EMS_SN_loading. Source code, 2019/03/13.

[3] Cigré Working Group C4.34. Application of phasor measurement units for monitoring power system dynamic performance. Technical report, Cigré, September 2017.

[4] R. A. C. T. de Groot. Modellen van het Nederlandse hoogspanningsnet en de omliggende landen ten bate van stabiliteitsstudies aan het 220 en 380 kV net. Technical report, DNV KEMA Energy & Sustainability, June 2015.

[5] I. C. Decker, A. S. e Silva, R. J. G. da Silva, M. N. Agostini, N. Martins, and F. B. Prioste. System Wide Model Validation of the Brazilian Interconnected Power System. In *IEEE PES General Meeting*. IEEE, July 2010. ISBN 978-1-4244-6551-4. doi: 10.1109/PES.2010.5590023.

[6] ENTSO-E Sub-group System Protection and Dynamics. Documentation on controller tests in test grid configurations. Technical report, ENTSO-E, November 2013.

[7] J. Grainger and W. D. Stevenson Jr. *Power System Analysis*. McGraw-Hill Education, first edition, 1994. ISBN 978-0070612938.

[8] E. Grebe, J. Kabouris, S. López Barba, W. Sattinger, and W. Winter. Low frequency oscillations in the interconnected system of Continental Europe. In *IEEE PES General Meeting*. IEEE, July 2010. ISBN 978-1-4244-6551-4. doi: 10.1109/PES.2010.5589932.

[9] J. E. Gómez and I. C. Decker. A novel model validation methodology using synchrophasor measurements. *Electric Power Systems Research*, 119:207–217, 2015. ISSN 0378-7796. doi: 10.1016/j.epsr.2014.09.024.

[10] A. A. Hajnoroozi, F. Aminifar, and H. Ayoubzadeh. Generating Unit Model Validation and Calibration Through Synchrophasor Measurements. *IEEE Transactions on Smart Grid*, 6(1):441–449, Jan 2015. ISSN 1949-3061. doi: 10.1109/TSG.2014.2322821.

[11] J. Heyberger and L. Vanfretti. Requirements for validation of Phasor Time domain simulations. Technical report, iTesla, November 2012.

[12] R. Huang, R. Diao, Y. Li, J. Sanchez-Gasca, Z. Huang, B. Thomas, P. Etingov, S. Kincic, S. Wang, R. Fan, G. Matthews, D. Kosterev, S. Yang, and J. Zhao. Calibrating Parameters of Power System Stability Models Using Advanced Ensemble Kalman Filter. *IEEE Transactions on Power Systems*, 33(3):2895–2905, May 2018. ISSN 1558-0679. doi: 10.1109/TPWRS.2017.2760163.

[13] Z. Huang, R. T. Guttromson, and J. F. Hauer. Large-scale hybrid dynamic simulation employing field measurements. In *IEEE Power Engineering Society General Meeting, 2004.*, volume 2, pages 1570–1576. IEEE, June 2004. doi: 10.1109/PES.2004.1373135.

[14] Z. Huang, T. Nguyen, D. Kosterev, and R. Guttromson. Model Validation of Power System Components Using Hybrid Dynamic Simulation. In *2005/2006 IEEE/PES Transmission and Distribution Conference and Exhibition*, pages 153–160. IEEE, May 2006. doi: 10.1109/TDC.2006.1668475.

[15] IEEE Task Force on Blackout Experience, Mitigation, and Role of New Technologies. Blackout Experiences and Lessons, Best Practices for System Dynamic Performance, and the Role of New Technologies. Technical report, IEEE, May 2007.

[16] IEEE Task Force on Generator Model Validation Testing of the Power System Stability Subcommittee. Guidelines for Generator Stability Model Validation Testing. In *2006 IEEE Power Engineering Society General Meeting*, June 2006. ISBN 1-4244-0493-2. doi: 10.1109/PES.2006.1709483.

[17] IEEE/CIGRE Joint Task Force on Stability Terms and Definitions. Definition and classification of power system stability. *IEEE Transactions on Power Systems*, 19(2):1387–1401, May 2004. ISSN 1558-0679. doi: 10.1109/TPWRS.2004.825981.

[18] D. Kopse, U. Rudez, and R. Mihalic. Applying a wide-area measurement system to validate the dynamic model of a part of european power system. *Electric Power Systems Research*, 119:1–10, 2015. ISSN 0378-7796. doi: 10.1016/j.epsr.2014.09.024.

[19] D. Kosterev. Hydro turbine-governor model validation in pacific northwest. *IEEE Transactions on Power Systems*, 19(2):1144–1149, May 2004. ISSN 1558-0679. doi: 10.1109/TPWRS.2003.821464.

[20] V. Kumar, M. Nagendran, V. Pandey, C. Kumar, and S. Chitturi. Improvements in synchronous generator parameter tuning using pmu data. In *2018 20th National Power Systems Conference (NPSC)*. IEEE, December 2018. ISBN 978-1-5386-6159-8. doi: 10.1109/NPSC.2018.8771818.

[21] P. Kundur, N. J. Balu, and M. G. Lauby. *Power System Stability And Control*. McGraw-Hill, Inc., first edition, 1994. ISBN 0-07-035958-X.

[22] Y. Lu, S. Kincic, H. Zhang, and K. Tomsovic. Validation of real-time system model in western interconnection. In *2017 IEEE Power Energy Society General Meeting*. IEEE, July 2017. ISBN 978-1-5386-2212-4. doi: 10.1109/PESGM.2017.8274340.

[23] J. Machowski, J. W. Bialek, and J. R. Bumby. *Power System Dynamics: Stability and Control*. John Wiley & Sons, Ltd, second edition, 2008. ISBN 978-0-470-72558-0. doi: 10.1201/9781420009248.

[24] MOD-033-1. Steady-State and Dynamic System Model Validation. Standard, NERC, July 2017.

[25] N. Nayak, H. Chen, W. Schmus, and R. Quint. Generator parameter validation and calibration process based on PMU data. In *2016 IEEE/PES Transmission and Distribution Conference and Exposition (T&D)*. IEEE, May 2016. ISBN 978-1-5090-2157-4. doi: 10.1109/TDC.2016.7519886.

[26] P. Pourbeik. Automated Parameter Derivation for Power Plant Models Based on Staged Tests. In *2009 IEEE/PES Power Systems Conference and Exposition*. IEEE, March 2009. ISBN 978-1-4244-3811-2. doi: 10.1109/PSCE.2009.4839940.

[27] P. Pourbeik. Approaches to Validation of Power System Models for System Planning Studies. In *IEEE PES General Meeting*. IEEE, July 2010. ISBN 978-1-4244-6551-4. doi: 10.1109/PES.2010.5589723.

[28] P. Pourbeik, C. Pink, and R. Bisbee. Power Plant Model Validation for Achieving Reliability Standard Requirements Based on Recorded On-Line Disturbance Data. In *2011 IEEE/PES Power Systems Conference and Exposition*. IEEE, March 2011. ISBN 978-1-61284-788-7. doi: 10.1109/PSCE.2011.5772520.

[29] W. Qiu, T. He, B. Choi, and Y. Mao. PJM static and dynamic model validation efforts and experiences for MOD-033. In *2017 IEEE Power Energy Society General Meeting*. IEEE, July 2017. ISBN 978-1-5386-2212-4. doi: 10.1109/PESGM.2017.8273949.

[30] A. Semerow, S. Höhn, M. Luther, W. Sattinger, H. Abildgaard, A. D. Garcia, and G. Giannuzzi. Dynamic Study Model for the Interconnected Power System of Continental Europe in Different Simulation Tools. In *2015 IEEE Eindhoven PowerTech*. IEEE, June 2015. doi: 10.1109/PTC.2015.7232578.

[31] K. S. Shetye, W. Jang, and T. J. Overbye. System Dynamic Model Validation using Real-Time Models and PMU Data. In *2018 Clemson University Power Systems Conference (PSC)*. IEEE, Sep. 2018. ISBN 978-1-7281-0316-7. doi: 10.1109/PSC.2018.8664078.

[32] *PSS®E 34.2 Program Operation Manual*. Siemens Power Technologies International, April 2017.

[33] *PSS®E 34.4 Model Library*. Siemens Power Technologies International, April 2018.

[34] UCTE Subgroup: Network models and forecast tools. UCTE data exchance format for load flow and three phase short circuit studies (UCTE-DEF). Standard, UCTE, May 2007.

[35] C. A. van Altenborg. Modelling Regional Power Grids for Large-Disturbance Stability Studies. Master's thesis, Delft University of Technology, 2017.

[36] WSCC Control Work Group and WSCC Modeling Validation Work Group. Test Guidelines for Synchronous Unit Dynamic Testing and Model Validation. Guideline, WECC (formerly WSCC), February 1997.

[37] V. Zimmer, I. C. Decker, and A. S. e Silva. A robust approach for the identification of synchronous machine parameters and dynamic states based on pmu data. *Electric Power Systems Research*, 165:167–178, December 2018. ISSN 0378-7796. doi: 10.1016/j.epsr.2018.09.008.